OPTIMUM POWER POINT TRACKING TECHNIQUES FOR GRID-CONNECTED PHOTOVOLTAIC SYSTEMS

A Thesis submitted to the

UPES

For the Award of

Doctor of Philosophy

in

Electronics and Communication Engineering

By

Sakshi Sharma

SEPTEMBER 2025

Supervisor

Dr. Piyush Kuchhal

Co-Supervisor

Dr. Vibhu Jately



Department of Electrical and Electronics Engineering

School of Engineering

UPES

Dehradun- 248007: Uttarakhand, INDIA

OPTIMUM POWER POINT TRACKING TECHNIQUES FOR GRID-CONNECTED PHOTOVOLTAIC SYSTEMS

A Thesis submitted to the

UPES

For the Award of

Doctor of Philosophy

in

Electronics and Communication Engineering

By

Sakshi Sharma

SAP-ID: 500095531

SEPTEMBER 2025

Supervisor

Dr. Piyush Kuchhal

Professor

Electrical Cluster, SOE,UPES

Co-Supervisor

Dr. Vibhu Jately

Associate Professor

Electrical Cluster, SOE,UPES



Department of Electrical and Electronics Engineering

School of Engineering

UPES

Dehradun- 248007: Uttarakhand, INDIA

DECLARATION

I declare that the thesis entitled **"*Optimum Power Point Tracking Techniques for Grid-Connected Photovoltaic Systems*"** has been prepared by me under the guidance of **Dr. Piyush Kuchhal,** Professor School of Advanced Engineering, UPES, Dehradun and co-supervision of **Dr. Vibhu Jately,** Associate Professor, School of Advanced Engineering, UPES, Dehradun. No part of this thesis has formed the basis for the award of any degree or fellowship previously.



Sakshi Sharma

Electrical Cluster

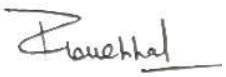
UPES

Dehradun-248007, Uttarakhand

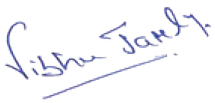
Date: 21st Sep 2025

CERTIFICATE

This is to certify that the thesis titled **"Optimum Power Point Tracking Techniques for Grid-Connected Photovoltaic Systems"** submitted by **Sakshi Sharma** (SAP ID: 500095531) in Partial completion of the requirements for the award of the Degree of Doctor of Philosophy (Engineering) is carried out by him under our joint supervision and guidance. It is certified that this thesis has not been submitted anywhere else for the award of any other diploma or degree of this or any other University.



Signature of Supervisor
Name of Supervisor: Dr. Piyush Kuchhal
Department: Electrical Cluster
Designation: Professor
School of Advanced Engineering, UPES, Dehradun, INDIA
Date: 21 Sept 2025



Signature of Co-supervisor
Name of Supervisor: Dr. Vibhu Jately
Department: Electrical Cluster
Designation: Associate Professor
School of Advanced Engineering, UPES, Dehradun, INDIA
Date: 21 Sept 2025

ABSTRACT

Harvesting the optimal power from the photovoltaic systems (PV) relies mainly on the maximum power point tracking (MPPT) employed. While the Perturb and Observe (P&O) method is commonly utilized for tracking the optimal power output (MPP) from a system, it can struggle to adapt quickly to sudden shifts in sunlight (irradiance). This instability leads to wasted power generation. Drift is when the optimal operating point deviates from the optimal power point. These deviations become more prominent due to intermittent environmental conditions, so amendments in the P&O algorithm are needed to improve the system's overall performance. Incorporating drift avoidance strategies into P&O algorithms is crucial to tackle this issue. To address the drift issue in MPP tracking, this work presents a fast dual perturbation-based P&O method that relies on repeated measurements and has a high convergence speed and an advanced adaptive voltage perturbation-based MPPT technique by integrating perturbation based on voltage steps into the conventional algorithm. The method dynamically regulates the step-size to the rate of irradiance change, yielding a fast and true MPPT.

In addition, a drift-free MPPT method and a multisampling MPPT algorithm are compared in this study, along with adaptive versions of P&O, incremental resistance (INR), and incremental conductance (INC). Among all these, the drift-free P&O method shows better tracking efficiency of 94.75% but response time is comparatively high (0.048s). The proposed algorithm was rigorously analysed under step increase and decrease in irradiance and on standard EN50530 irradiance profile. Simulations under varying solar irradiance profiles, such as rapid changes, show significant improvements in speed of tracking, accuracy with reduced fluctuations around the true MPP. The proposed algorithm recorded 98.55% tracking efficiency and time of response of 12ms compared to other MPPT algorithms. The proposed method improves solar energy system efficiency and dependability by producing steadier and

predictable power production for real-time applications in regions with frequent irradiance fluctuations.

Moreover, this work focuses on experimental validation of proposed dual perturbation based MPPT algorithm in comparison with existing P&O, adaptive P&O, and drift-free P&O based MPPT algorithms. The goal is to track MPPT properly and test the unique algorithm's ability to track MPP quickly. The effectiveness of the MPPT algorithms is assessed at the input of the boost converter to validate this. Since the objective is to develop a fast drift-free MPPT algorithm the efficiency of the proposed MPPT algorithm is evaluated at the DC-DC boost converter input. This ensures that the efficiency of the MPPT algorithm does not include the losses occurring within the boost converter. The hardware validation of dual perturbation based MPPT algorithm is performed and compared with existing P&O, adaptive P&O, and drift-free P&O based MPPT algorithms. Among all, the drift-free P&O shows the response time of 0.22 seconds and steady-state oscillations of 3.15% at 270W/m^2 and 2.99% at 480W/m^2. While 95.75% tracking efficiency is achieved for the same. The proposed dual perturbation-based P&O MPPT algorithm shows the response time of 0.10 s and steady-state oscillations of 2.02% at 270W/m^2 and 1.80% at 480W/m^2 and 98.05% maximum tracking efficiency is achieved. This much of tracking efficiency and response aims that the proposed algorithm is showing the good performance and able to track MPP efficiently. The work can be carried forward further for PV inverters.

Considering photovoltaic (PV) power plants are sporadic, the threat of grid failure is increased as their penetration into the electrical system rapidly increases. An extensive literature review suggests that the flexible power point tracking (FPPT) method might solve this issue. This method allows for real-time adjustments to tracking parameters, ensuring a more accurate alignment with dynamic conditions. As a result, researchers anticipate improved outcomes in various applications where precision is critical. These algorithms control the amount of power that the PV system produces up to a specific point, rather than constantly checking the MPP. The proposed work carries out a detailed comparative study of various constant power generations control strategies. The

control strategies are categorized in terms of current, voltage and power-based tracking abilities. A comparative comparison of several reported CPG/FPPT approaches is conducted. Several key performance indices were used in this analysis, including a variety of control approaches, illumination patterns, and fluctuations in irradiations, operating locations, tracking speeds, steady-state power swings, partial shading, rigidity, integrity, and tracking efficiency. Model-based control surpasses all other FPPT approaches in terms of maximum tracking efficiency of 98.57% and minimal steady-state power oscillations.

PV systems are mainly used in two ways either standalone or grid-tied photovoltaic systems. MPPT is best way to extract true maximum power from PV systems and transmit it to the grid but at the time of voltage or frequency deviation maximum power transfer leads to grid failure. Therefore, it is necessary to seek out an alternative approach to confirm the stability of the grid. Present work focused on the non-drifting flexible power point tracking algorithm for grid-integrated PV systems. The proposed algorithm is designed and implemented using two control strategies namely current and voltage control strategy. On the left side of the trail current control strategy is adopted while voltage control strategy is used on the right side of the power Vs voltage (P-V) curve. The proposed algorithm is tested under 1000W/m^2 and 500W/m^2 irradiance, and under variable irradiation conditions. The results show that the proposed algorithm has obtained the tracking efficiency of 99.87% and response time of 3ms. The reported technique can be further implemented in PV inverters.

ACKNOWLEDGEMENT

First and foremost, I want to thank Goddess Adi Shakti for bestowing upon me the wonderful chance to convey my gratitude to the many distinguished individuals who have embraced me with their love and encouragement throughout my doctoral studies. Beginning in the verdant and verdant UPES campus in Dehradun, the journey to this paradise begins along a basin in the Himalayas. I am driven to succeed by the enchanting and heavenly current that runs through my spirit. My naturalistic caretakers have set out on a mission to contribute little to human civilization. Start your journey to paradise at UPES in Dehradun, a beautiful and lush campus in the heart of the Himalayas. You'll be hemmed in on all sides by the rivers Asan and Song, which flow west and east, respectively, and are tributaries of the Yamuna and Ganga, respectively. I am driven to succeed by the enchanting and heavenly current that runs through my spirit. My naturalistic caretakers have set out on a mission to contribute little to human civilization. I am deeply grateful to Dr. Piyush Kuchhal and Dr. Vibhu Jately for the chance they granted me to work under their supervision. Thanks to their insightful criticism, professional advice, and intellectual supervision, I have grown professionally and personally. They never stopped encouraging me to be my best self. They helped me grow intellectually to the point where I am now. Dr. Rupendra Kumar Pachauri was an incredible source of positivity and strength for me during this journey, and I am truly grateful to him. Also, I would like to thank the committee members Dr. Rupendra Kumar Pachauri, Dr. Devendra Saini and Dr. Abhinav Sharma for their support and feedback. The faculty and staff at UPES, Dehradun's Electrical Cluster, have my deepest gratitude. Their availability of the essential lab space, equipment, and personnel, together with their aid in overcoming obstacles, greatly facilitated my research endeavor. On a more terrestrial level, I owe a great obligation to my parents and extended family, the worth of whom I will forever be grateful. For the indescribable blessings, love, care, and support bestowed upon me by my parents and in-laws, Mr. C. L. Sharma, Mrs. Shyama Sharma and Mrs. Sarita Devi, I am eternally grateful. Additional people I'd want to thank for being there

for me in times of need are my brother Shubham Sharma, my husband Pankaj Verma, and my friends Kaushal Kumar, Divya Arora, Supriya Sharma and Vatsala Anand. Thanks to everyone around me who is also on a quest for knowledge, this effort has progressed to this point. Amid the crisis, I was able to keep going thanks to their unwavering support and encouragement.



Sakshi Sharma

TABLE OF CONTENT

Declaration *(iii)*

Certificate *(iv)*

Abstract *(v)*

Acknowledgement *(viii)*

Table of Contents *(x)*

List of Figures *(xiv)*

List of Tables *(xxii)*

Abbreviations *(xxiv)*

Nomenclature *(xxvii)*

CHAPTER 1: Introduction **1-14**

1.1 Photovoltaic systems 1

1.2 Types of PV systems 4

1.3 Background 6

1.4 Motivation 8

1.5 Research Problem 10

1.6 Research Gaps 13

1.7 Objectives 14

1.8 Structure of Thesis 14

CHAPTER 2: Literature Review **15-31**

2.1 Maximum power point tracking 15

2.2 Flexible power point tracking 23

2.3 Summary 27

CHAPTER 3: Adopted Methodology and Discussion **32-37**

3.1 Adopted Methodology 32

3.2 Tools and models 35

3.3 Summary 37

CHAPTER 4: Design and Analysis of Maximum Power Point Tracking Algorithms 38-96

4.1 Introduction 38

4.2 PV Modelling and Analysis 41

4.2.1 Modelling of DC-DC Boost Converter 43

4.3 Maximum Power Point Techniques 46

4.3.1 Conventional P&O MPPT Algorithm 46

4.3.2 Conventional INC MPPT Algorithm 48

4.3.3 Conventional INR MPPT Algorithm 50

4.3.4 Adaptive P&O MPPT Algorithm 50

4.3.5 Adaptive INC MPPT Algorithm 52

4.3.6 Adaptive INR MPPT Algorithm 53

4.3.7 Drift-free P&O MPPT Algorithm 54

4.3.8 Multisampling P&O MPPT Algorithm 55

4.4 Proposed MPPT Algorithm 56

4.4.1 Adaptive Voltage perturbation based MPPT Algorithm 56

4.4.2 Dual perturbation based MPPT Algorithm 58

4.5 Results and Discussion 62

4.5.1 Step Increase-in Irradiance 62

4.5.2 Step Decrease-in Irradiance 72

4.5.3 EN50530 Standard Irradiance Profile 81

4.6 Summary 95

CHAPTER 5: Design and Analysis of Flexible Power Point Tracking Algorithms 97-128

5.1 Introduction 97

5.2 System Description and Mathematical Modelling 101

5.2.1 Mathematical Model of grid-connected PV system 103

5.3 FPPT Techniques 109

5.4 Proposed Algorithm 111

5.5 Results and Discussion 114

5.5.1 Irradiance- 1000 W/m^2 115

5.5.2 Irradiance- 500 W/m^2 117

5.5.3 Step Increase-in Irradiance Pattern 119

5.5.4 Step Decrease-in Irradiance Pattern 121

5.5.5 Comparative Analysis 123

5.6 Summary 126

CHAPTER 6: Hardware Implementation of Dual Perturbation based MPPT Algorithms 129-151

6.1 Introduction 129

6.2 MPPT PID Controller 130

6.2.1 Boost Section and Output 130

6.2.2 1R2120 MOSFET Gate Driver IC 131

6.2.3 MCU Section 132

6.2.4 Solar Voltage Sensing 133

6.2.5 Output Voltage Sensing 134

6.2.6 Power Section 134

6.2.7 Universal Asynchronous Receiver-Transmitter (UART) 135

6.2.8 Switches 135

6.2.9 LED'S 136

6.2.10 I2C 136

6.3 Results and Discussion 138

6.3.1 Irradiance – 270 W/m^2 140

6.3.2 Irradiance – 480 W/m^2 142

6.3.3 Step Increase-in Irradiance Pattern 144

6.3.4 Step Decrease-in Irradiance Pattern 146

6.3.5 Comparative Analysis 148

6.3.6 Statistical Analysis 150

6.4 Summary 151

CHAPTER 7: Conclusion and Future Scope **152-156**

REFERENCES **157-171**

List of Publication **172**

LIST OF FIGURES

Figure No. **Page No.**

Fig.1.1 Utilization of solar energy in photovoltaics 1

Fig.1.2 Flowchart of utilization of solar energy in photovoltaics 2

Fig.1.3 Animated view utilization of solar energy in photovoltaics for huge production by using devices like PV cell, model, panel and array. 2

Fig.1.4 Realistic view of production of electricity by using devices like PV cell, model/panel and array to make PV farms. 3

Fig.1.5 Fundamental steps of solar cell/module operation 3

Fig.1.6 Fundamental steps of solar cell/module operation under illumination 4

Fig.1.7 Schematic View of Standalone PV systems 5

Fig.1.8 Schematic view of grid connected PV systems 6

Fig.1.9 a) I-V curve and b): P-V curve of PV systems 7

Fig.1.10 Basic MPPT module of the PV panels 7

Fig.1.11 PV generation and consumption requirements 8

Fig.1.12 Total electricity generation in India from various resources 9

Fig.1.13 Total electricity consumption India in various sectors 9

Fig.1.14 Power balance of consumption and generation 9

Fig.1.15 Grid-connected PV penetration trends in global states of renewable generation 10

Fig.1.16 Generation with aspect to standalone and grid-connected PV system 10

Fig.1.17 (a) Drift from point 1 (b) Drift in case of rapid increase in insolation for existing P&O MPPT drift conditions 11

Fig.1.18 Flexible power point tracking (FPPT) 12

Fig.1.19 PV Power with FPPT under changing irradiance (a) increased (b) decreased 12

Fig.3.1 Flowchart of research methodology 33

Fig.3.2 Flowchart representation of adopted methodology to achieve 1st objective 34

Fig.3.3 Flowchart of adopted methodology to achieve 2nd objective 34

Fig.3.4 Graphical representation of adopted research methodology to achieve 3rd objective 34

Fig.3.5 Simulation model of MPPT algorithms 36

Fig.3.6 Simulation model of FPPT algorithms 36

Fig.3.7 Simulation model of FPPT algorithms 36

Fig.4.1 (a) I-V curve (b) P-V curve on various irradiance levels under STC 43

Fig.4.2 Equivalent circuit of MPPT assisted PV system 44

Fig.4.3 Schematic diagram: MPPT integrated PV system 45

Fig.4.4 Flowchart: Conventional P&O MPPT algorithm 47

Fig.4.5 Flowchart: Conventional INC MPPT algorithm 48

Fig.4.6 Flowchart: Conventional INR MPPT algorithm 49

Fig.4.7 Flowchart: Adaptive P&O MPPT algorithm 51

Fig.4.8 Flowchart: Adaptive INC MPPT algorithm 52

Fig.4.9 Flowchart: Adaptive INR MPPT algorithm 53

Fig.4.10 Flowchart: Drift-free P&O MPPT algorithm 54

Fig.4.11 Flowchart: Multisampling MPPT algorithm 55

Fig.4.12 I-V and P-V curves with shaded region under STC 56

Fig.4.13 Flowchart: Proposed adaptive voltage perturbation-based MPPT algorithm 58

Fig.4.14 Schematic diagram of the proposed MPPT technique 61

Fig.4.15 Flowchart: proposed dual perturbation based MPPT technique 61

Fig.4.16 Step increase in irradiance profile 62

Fig.4.17 Voltage response for a) P&O, b) Adaptive P&O, c) INC, d) Adaptive INC, e) INR, f) Adaptive INR, g) drift-free P&O, h) multisampling P&O, i) proposed an adaptive voltage perturbation-based (j) proposed dual perturbation based MPPT algorithms 63

Fig.4.18 Current response for a) P&O, b) Adaptive P&O, c) INC, d) Adaptive INC, e) INR & f) Adaptive INR, g) drift-free P&O, h) multisampling P&O, i) proposed an adaptive voltage perturbation-based (j) proposed dual perturbation based MPPT algorithms 65

Fig.4.19 Power response for a) P&O, b) Adaptive P&O, c) INC, d) Adaptive INC, e) INR, f) Adaptive INR, g) drift-free P&O, h) multisampling P&O, i) proposed an adaptive voltage perturbation-based (j) proposed dual perturbation based MPPT algorithms 67

Fig.4.20 Response time for various algorithms at step increase-in profile 69

Fig.4.21 Steady-state oscillations for various algorithms at step increase-in profile 69

Fig.4.22 Tracking Efficiency for various algorithms at step increase-in profile 70

Fig.4.23 Step decrease in irradiance profile 72

Fig.4.24 Voltage response for a) P&O, b) Adaptive P&O, c) INC, d) Adaptive INC, e) INR, f) Adaptive INR, g) drift-free P&O, h) multisampling P&O, i) proposed an adaptive voltage perturbation-based (j) proposed dual perturbation based MPPT algorithms 73

Fig.4.25 Current response for a) P&O, b) Adaptive P&O, c) INC, d) Adaptive INC, e) INR & f) Adaptive INR, g) drift-free P&O, h) multisampling P&O, i) proposed an adaptive voltage perturbation-based (j) proposed dual perturbation based MPPT algorithms 75

Fig.4.26 Power response for a) P&O, b) Adaptive P&O, c) INC, d) Adaptive INC, e) INR, f) Adaptive INR, g) drift-free P&O, h) multisampling P&O, i) proposed an adaptive voltage perturbation-based (j) proposed dual perturbation based MPPT algorithms 77

Fig.4.27 Response time for various algorithms at step decrease-in profile 78

Fig.4.28 Steady-state oscillations for various algorithms at step decrease-in profile 79

Fig.4.29 Tracking Efficiency for various algorithms at step decrease-in profile 79

Fig.4.30 Irradiance pattern of EN50530 82

Fig.4.31 Voltage response for a) P&O, b) Adaptive P&O, c) INC, d) Adaptive INC, e) INR, f) Adaptive INR, g) drift-free P&O, h) multisampling P&O, i) proposed an adaptive voltage perturbation-based (j) proposed dual perturbation based MPPT algorithms 83

Fig.4.32 Current response for a) P&O, b) Adaptive P&O, c) INC, d) Adaptive INC, e) INR & f) Adaptive INR, g) drift-free P&O, h) multisampling P&O, i)

proposed an adaptive voltage perturbation-based (j) proposed dual perturbation based MPPT algorithms 85

Fig.4.33 Power response for a) P&O, b) Adaptive P&O, c) INC, d) Adaptive INC, e) INR, f) Adaptive INR, g) drift-free P&O, h) multisampling P&O, i) proposed an adaptive voltage perturbation-based (j) proposed dual perturbation based MPPT algorithms 88

Fig.4.34 Comparative behaviour of conventional, adaptive and proposed MPPT techniques on the basis of radial diagram behaviour for (a) Tracking Speed, (b) Oscillations, (c) Stability, (d) Complexity, (e) Cost and (f) Tracking Efficiency 91

Fig.4.35 Response time of various algorithms 92

Fig.4.36 Tracking Efficiency of various algorithms 92

Fig.5.1 Schematic Diagram of the FPPT algorithm 108

Fig.5.2 P-V curve for constant power generation (CPG) 109

Fig.5.3 Control structure of Current based FPPT method 110

Fig.5.4 Control structure of Power based FPPT method 111

Fig.5.5 Current vs Voltage (I-V) and Power vs Voltage (P-V) curve at maximum power point (MPP) and flexible power point (FPP) 112

Fig.5.6 Flowchart of proposed FPPT algorithm 113

Fig.5.7 Schematic Diagram of the FPPT algorithm 113

Fig.5.8 Flowchart of proposed MPPT algorithm 114

Fig.5.9 Three-phase grid voltage 115

Fig.5.10 a) Voltage, b) current and c) power vs time curve for current based FPPT algorithm, 10. d) Voltage, e) current and f) power vs time curve for power

based FPPT algorithm, 10. g) Voltage, h) current and i) power vs time curve for proposed FPPT algorithm at 1000 W/m^2. 116

Fig.5.11 a) Voltage, b) current and c) power vs time curve for current based FPPT algorithm, 11. d) Voltage, e) current and f) power vs time curve for power based FPPT algorithm, 11. g) Voltage, h) current and i) power vs time curve for proposed FPPT algorithm at 500 W/m^2. 118

Fig.5.12 Step increase-in irradiance pattern 119

Fig.5.13 a) Voltage, b) current and c) power vs time curve for current based FPPT algorithm, 13. d) Voltage, e) current and f) power vs time curve for power based FPPT algorithm, 13. g) Voltage, h) current and i) power vs time curve for proposed FPPT algorithm. 120

Fig.5.14 Step decrease-in irradiance pattern 121

Fig.5.15 a) Voltage, b) current and c) power vs time curve for current based FPPT algorithm, 15. d) Voltage, e) current and f) power vs time curve for power based FPPT algorithm, 15. g) Voltage, h) current and i) power vs time curve for proposed FPPT algorithm 122

Fig.5.16 Radial response behaviour for comparative study 123

Fig.5.17 Response time graph for various algorithms 124

Fig.5.18 Steady-state oscillations graph for various algorithms 124

Fig.5.19 Tracking efficiency graph for various algorithms 124

Fig.6.1 Schematic diagram of boost converter and output 131

Fig.6.2 Schematic diagram of MOSFET gate driver IC (1R2110) 132

Fig.6.3 Schematic diagram of MCU Section 133

Fig.6.4 Schematic diagram of Output Voltage Sensor 134

Fig.6.5 Schematic diagram of Power Section 135

Fig.6.6 Schematic diagram of UART 135

Fig.6.7 Schematic diagram of Switches 136

Fig.6.8 Schematic diagram of LEDs 136

Fig.6.9 Schematic diagram of I2C 137

Fig.6.10 Realistic view of Hardware Prototype 140

Fig.6.11 Voltage response for a) P&O, b) Adaptive P&O, c) drift-free P&O and d) proposed dual perturbation based MPPT algorithms 141

Fig.6.12 Current response for a) P&O, b) Adaptive P&O, c) drift-free P&O and d) proposed dual perturbation based MPPT algorithms 141

Fig.6.13 Power response for a) P&O, b) Adaptive P&O, c) drift-free P&O and d) proposed dual perturbation based MPPT algorithms 142

Fig.6.14 Voltage response for a) P&O, b) Adaptive P&O, c) drift-free P&O and d) proposed dual perturbation based MPPT algorithms 143

Fig.6.15 Current response for a) P&O, b) Adaptive P&O, c) drift-free P&O and d) proposed dual perturbation based MPPT algorithms 143

Fig.6.16 Power response for a) P&O, b) Adaptive P&O, c) drift-free P&O and d) proposed dual perturbation based MPPT algorithms 144

Fig.6.17 Voltage response for a) P&O, b) Adaptive P&O, c) drift-free P&O and d) proposed dual perturbation based MPPT algorithms 145

Fig.6.18 Current response for a) P&O, b) Adaptive P&O, c) drift-free P&O and d) proposed dual perturbation based MPPT algorithms 145

Fig.6.19 Power response for a) P&O, b) Adaptive P&O, c) drift-free P&O and d) proposed dual perturbation based MPPT algorithms 146

Fig.6.20 Voltage response for a) P&O, b) Adaptive P&O, c) drift-free P&O and d) proposed dual perturbation based MPPT algorithms 147

Fig.6.21 Current response for a) P&O, b) Adaptive P&O, c) drift-free P&O and d) proposed dual perturbation based MPPT algorithms 147

Fig.6.22 Power response for a) P&O, b) Adaptive P&O, c) drift-free P&O and d) proposed dual perturbation based MPPT algorithms 148

Fig.6.23 Response time of MPPT algorithms 148

Fig.6.24 Steady-state oscillations of MPPT algorithms 149

Fig.6.23 Tracking efficiency of MPPT algorithms 149

LIST OF TABLES

Table No.	Page No.
Table 2.1 Literature review of existing MPPT approaches	19
Table 2.2 Literature review of existing CPG/FPPT approaches	28
Table 4.1 Specifications of PV module	46
Table 4.2 Specifications of Boost Converter	46
Table 4.3 Table of taxonomy based on comparative analysis for step increase-in irradiance profile	71
Table 4.4 Performance parameters of algorithms at step increase-in irradiance profile	72
Table 4.5 Table of taxonomy based on comparative analysis for step decrease-in irradiance profile	80
Table 4.6 Performance parameters of algorithms step decrease-in irradiance profile	81
Table 4.7 Table of taxonomy based on comparative analysis for EN50530 irradiance profile	94
Table 4.8 Performance parameters of algorithms at EN50530 irradiance profile	93
Table 5.1 Specifications of PV module	109
Table 5.2 Specifications of Boost Converter	109
Table 5.3 Performance Parameters of Algorithms 1000W/m	117
Table 5.4 Performance Parameters of Algorithms for 500W/m2	117
Table 5.5 Performance Parameters for Step increase-in pattern	119

Table 5.6 Performance Parameters for Step increase-in pattern 121

Table 5.7 Table of taxonomy based on comparative analysis 125

Table 5.8 Performance Parameters of Algorithms 126

Table 6.1 Specifications of PV module 137

Table 6.2 Specifications of Boost Converter 138

Table 6.3 Specifications of PID Controller 138

Table 6.4 Performance parameters of algorithms 150

Table 6.5 Descriptive Statistics 150

Table 6.6 Test Statistics 151

ABBREVIATIONS

ANFIS	:	Adaptive Fuzzy Neuro Interface
ANN	:	Artificial Neural Network
APF	:	Active Power Filter
ARO	:	Artificial Rabbit Optimization
BESS	:	Battery Energy Storage System
COA	:	Coati Optimization Algorithm
CPD	:	Customed Power Devices
CPG	:	Constant Power Generation
DPFC	:	Distributed Power Flow Controller
EANFIS	:	Evolutionary Adaptive Neuro Fuzzy Inference Scheme
ESOGI	:	Enhanced Second Order Generalised Integrator
FLL	:	Frequency Lock Loop
FPA	:	Flower Pollination Algorithm
FPP	:	Flexible Power Point
FSSO	:	Flying Squirrel Search Optimization
G	:	Irradiation
GMPP	:	Global Maximum Power Point
GMPPT	:	Global maximum power point Tracking
HIL	:	Hardware In Loop

HRES	:	Hybrid Renewable Energy System
I-V	:	Current- Voltage
IC	:	Incremental conductance
IWO	:	Invasive Weed Optimization
LMPP	:	Local maximum power point
LMS	:	Least Mean Square
LS	:	Least Square
MP	:	Maximum Power Point Tracking
MPP	:	Maximum Power Point
MPPT	:	Maximum Power Tracking
MROGI	:	Modified Reduced Order Generalised Integrator
P–V	:	Power- Voltage
PPGSs	:	Power Generating Schemes
PQ	:	Power Quality
PS	:	Partial shading
PSO	:	Particle swarm optimization
PV	:	Photovoltaic
P&O	:	Perturb and observe
SHAF	:	Shunt Active Power Filter
SHAPF	:	Shunt Hybrid Active Power Filter

SOFC	:	Solid Oxide Fuel Cell
T	:	Temperature
UPQC	:	Unified Power Quality Conditioner

NOMENCLATURE

I_{ph}	:	Photo current
I_d	:	Diode current
I_s	:	Shunt current
I_{pv}	:	Current across PV
V_{pv}	:	Voltage across PV
V_{dc}	:	DC voltage of solar panel
V_g	:	Grid voltage
V_{abc}	:	Three phase voltage
V_{ref}	:	Reference voltage
ΔD	:	Step size
ΔD_{max}	:	Upper bound of step size
φ	:	Phase
q	:	Charge of electron
K	:	Boltzmann constant
ΔT	:	Change in temperature
G_{STC}	:	Irradiation at STC
I_{sat}	:	Saturation current

V_{oc}	:	Open circuit voltage
P_i^t	:	Instantaneous position of particle
Y_i^t	:	Velocity of particle
d_i^{t+1}	:	Updated duty cycle
d_i^t	:	Instantaneous duty cycle
G_{best}	:	Best position
P_{best}	:	Best position of the particle
U_i^{t+1}	:	Solution vector
G_*	:	Global solution
$L(\lambda)$	:	Levy factor
Rb_i	:	Position of individual rabbits
N_{rb}	:	Rabbit position
C_{in}	:	Input capacitance
C_{out}	:	Output capacitance
f_{sw}	:	Switching Frequency
L	:	Inductor
R_{load}	:	Load Resistance

$P(n)$	:	Instantaneous Power
$E_r(n)$	:	Instantaneous Error
$\delta E_r(n)$	:	Change on Error
X	:	Population Matrix
K_p	:	Proportional Gain of PID
K_i	:	Integral Gain of PID

CHAPTER 1

INTRODUCTION

In this chapter, the thesis topic is introduced briefly. The chapter is comprised of total eight sections. The introduction provides a high-level overview of solar energy and its applications. Next, it will go over the different kinds of PV systems. Then, in the parts that follow, it will cover the background and the rationale behind them. The following three sections elaborate on the research problem, as well as the research gaps and aims. The structure of the thesis makes up the final section.

1.1 Photovoltaic Systems

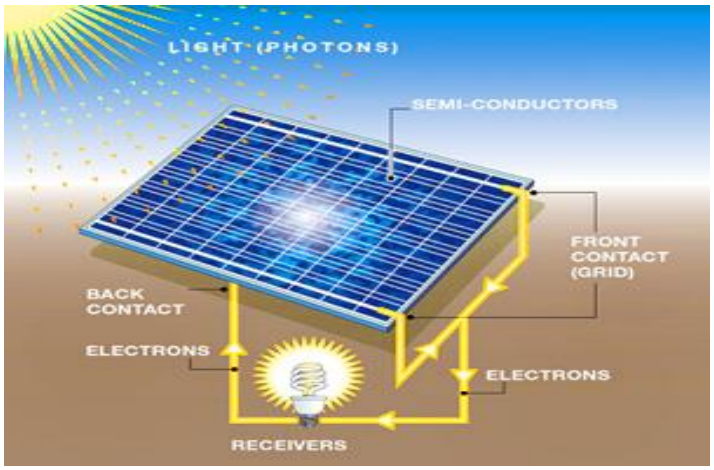


Fig. 1.1. Utilization of solar energy in Photovoltaics

Due to its availability, lack of pollution, and contemporary production methods, solar power has become one of the most popular energy sources (Leridon, 2020; Lewis, 2016). It is one of the fastest growing energy production methods currently (Lewis, 2016; Parlevliet & Moheimani, 2014). The sun's rays and heat may be harnessed in a variety of ways, including photovoltaics (PV) and concentrated solar power (CSP) (Lewis, 2016; Parlevliet & Moheimani, 2014; Qiu et al., 2018). Photovoltaics is one of the most promising technologies to utilize solar energy in an adequate way for commercial purpose (Husain et

al., 2018; Nayak et al., 2019). A device that transforms solar energy into electrical energy is called a PV cell or solar cell (Honsberg & Bowden, 2019; Nayak et al., 2019; Tyukhov, n.d.). Photovoltaics' use of solar energy is shown in Fig. 1.1.

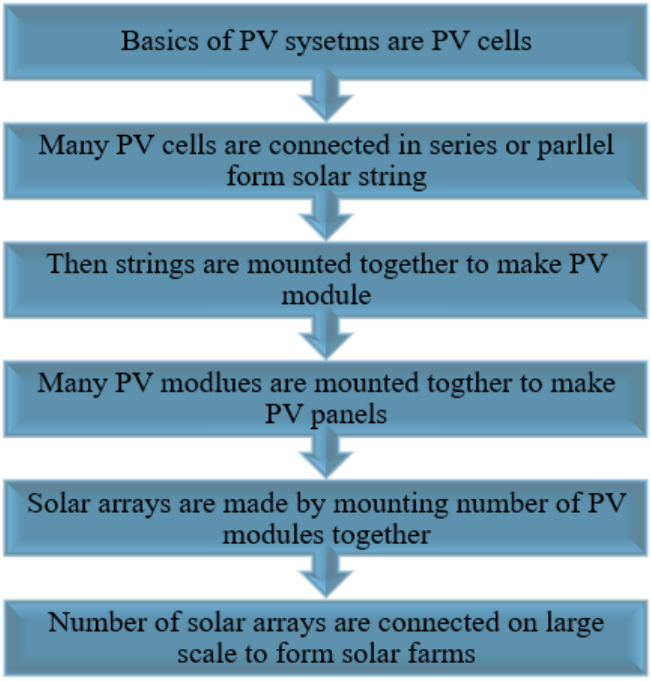


Fig. 1.2. Flowchart of utilization of solar energy in photovoltaics.(Nayak et al., 2019)

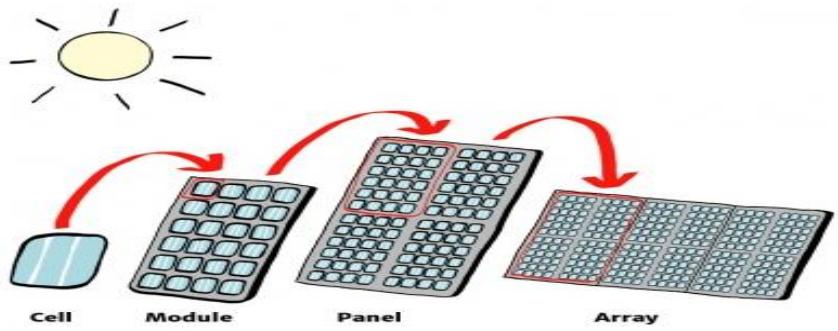


Fig. 1.3. Animated view utilization of solar energy in photovoltaics for huge production by using devices like PV cell, model, panel and array. (Nayak et al., 2019)

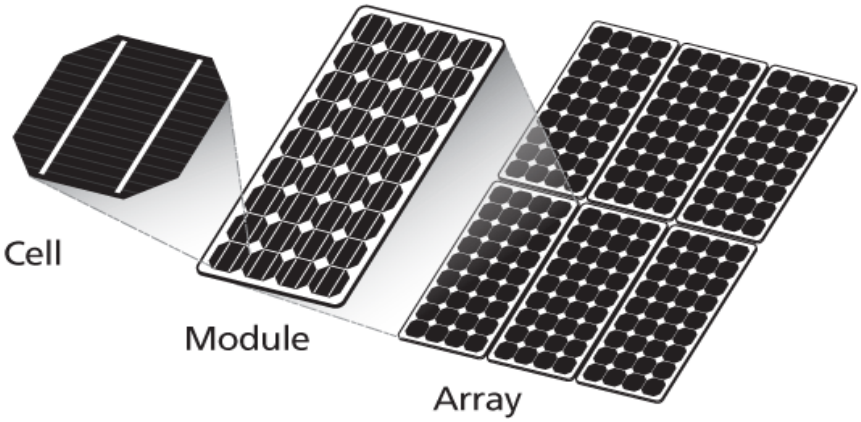


Fig. 1.4. Realistic view utilization of solar energy in photovoltaics for mass production of electricity by using devices like PV cell, model/panel and array to make PV farms. (Nayak et al., 2019)

The fundamental component underlying PV systems is a PV cell. A solar PV module is made up of several solar cells assembled into one structure to capture solar energy to produce commercial power. A solar array is then created by connecting several solar panels. In the last many solar arrays are setup together to form a solar farm for huge electricity production (Tyukhov, n.d.). The flowchart perspective of PV cells is presented in Fig. 1.2. Similarly, the animated view and realistic view for the same is depicted in Fig. 1.3 and 1.4 respectively.

Working of PV systems includes three key steps as depicted in Fig. 1.5:

- Generation
- Separation
- Collection



Fig. 1.5. Fundamental steps of solar cell/module operation.

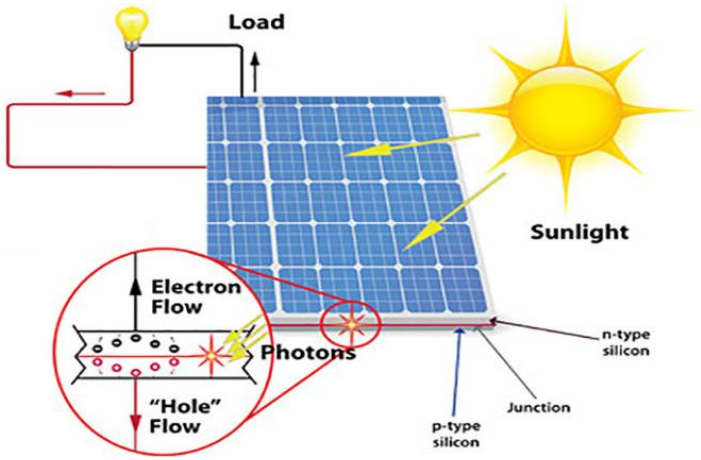


Fig. 1.6. Fundamental steps of solar cell/module operation under illumination. (Nayak et al., 2019)

When light is absorbed in form of photons, the electron-hole pair gets generated. This process is called generation of charge carriers as shown in Fig. 1.6. After generation, electrons will start moving towards n-type and hole will start moving towards p-type. This process is called separation of charge carriers. Through Fig. 1.6 the carrier dynamics of the generated carriers can be understood. Further the generated carriers will contribute to light generated current to generate power from the solar cell. This process is called collection of charge carriers.

1.2 Types of PV systems

PV systems can be broadly classified into two types: grid-connected and standalone systems:

- **Standalone PV systems**

In these systems the solar panels are not directly connected to grid but utilized to charge the battery banks. These types of systems are used for the home or small industrial supply by making use of batteries. The power is generated on small scale level and used at household level. In this method generally PV panels are installed at rooftops, the generated electricity is stored

in battery banks. Inverters help in the generated power's control and stabilization by the charge controllers. The battery banks and inverters are connected to the distribution board so as to utilize the electricity for common household appliances like fans, water heating and lights etc. (Hashimoto et al., 2017; Honsberg & Bowden, 2019; Husain et al., 2018). Fig. 1.7 represents the schematic of standalone PV systems.

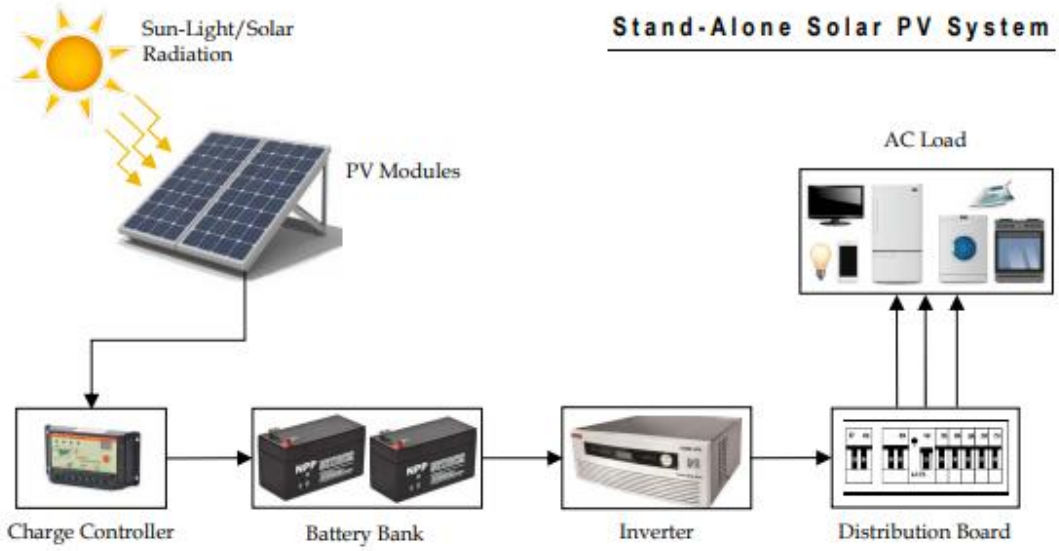


Fig. 1.7. Schematic View of Standalone PV systems.(Hashimoto et al., 2017)

- Advantages of Standalone systems:
  i. Good option for non-grid connected areas
  ii. Self-sufficient for meeting the energy demands
  iii. Not affect by grid failure
- Challenges of Standalone systems:
  i. More Expensive
  ii. High maintenance
  iii. Difficult to replace batteries

- **Grid Connected PV systems**

Large PV systems are always connected to grid. The power is generated on large scale level in the solar farms. The generated power from the solar farms

is fed to the grid and then distributed to common people or to the industries. Grid is a network that is used for the electricity distribution purpose (Albarracin & Alonso, 2013; Hashimoto et al., 2017; V. Sharma et al., 2019). Fig. 1.8 is showing the schematic view of PV-grid system.

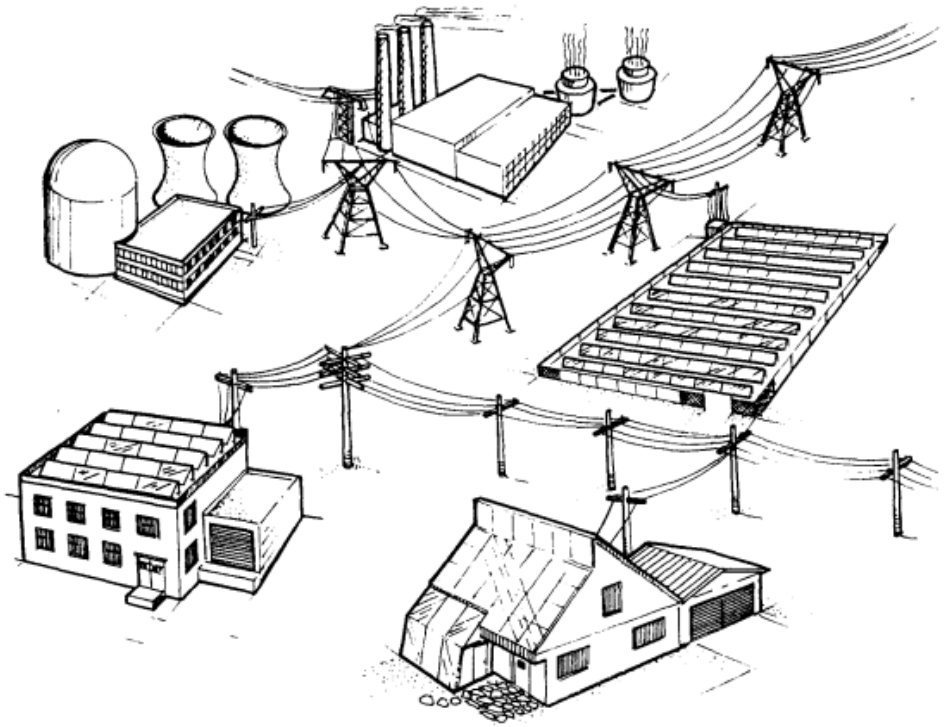


Fig. 1.8. Schematic view of grid linked PV systems. (Hashimoto et al., 2017)

- Advantages of Grid linked systems:
  i. Cheaper than the standalone system.
  ii. Provides the advantage of net metering
- Challenges of Grid connected systems:
  i. Doesn't provide the facility to store the power supply
  ii. Consumers need to pay fees charged by utility companies.

1.3 Background

In many countries PV systems are the main source of power supply nowadays. However, the power generated by PV panels comes with certain

challenges. The primary concern is maximizing power extraction from the PV panels for commercial use. Fig. 1.9 illustrates the current density-voltage curve and P-V curve of photovoltaic cells.

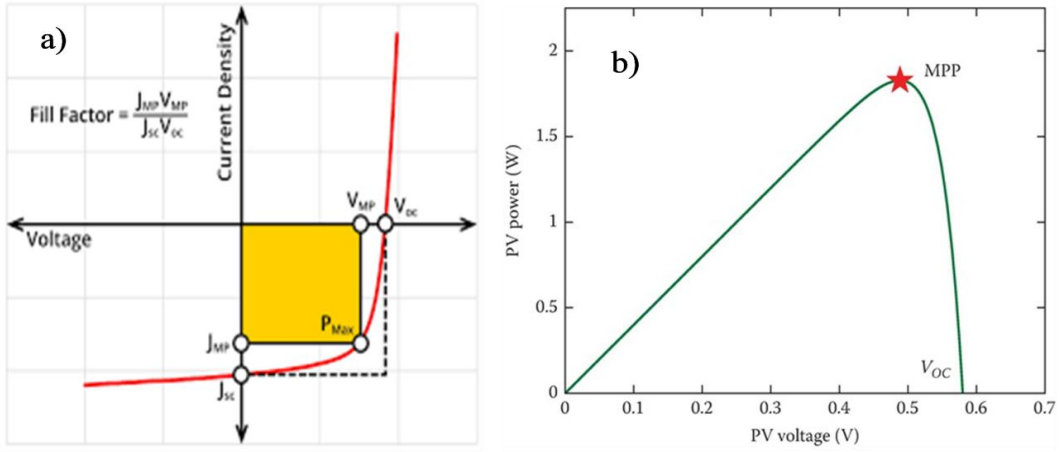


Fig. 1.9. (a) I-V curve and (b): P-V curve of PV systems

The main challenge lies in tracking the Maximum Power Point (MPP) to extract the optimal power from the PV panel. Fig. 1.10 illustrates the basic MPPT module for PV panels (Albarracin & Alonso, 2013; V. Sharma et al., 2019).

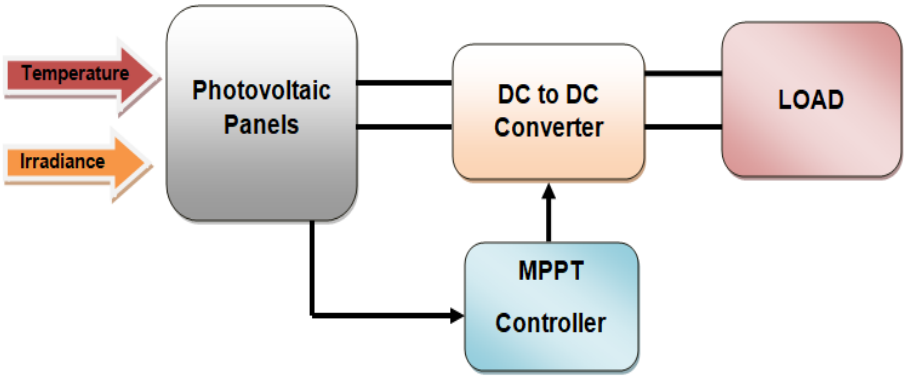


Fig. 1.10. Basic MPPT module of the PV panels

1.4 Motivation

The imperative to make the transition towards sources of sustainable energy is essential considering humanity's rising energy demands. One of the best technologies for using solar energy is solar panels or modules. PV power can be generation utilized in two ways i.e., standalone as well as grid as shown in Fig. 1.11.

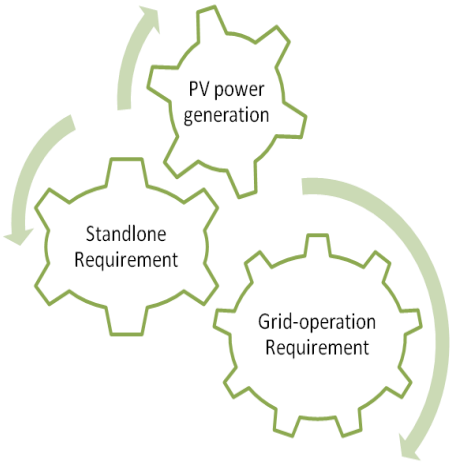


Fig. 1.11. PV generation and consumption requirements.

Photovoltaic (PV) systems generate power, but to effectively utilize this energy—as illustrated in Fig. 1.12 and Fig. 1.13—it is crucial to track the Maximum Power Point (MPP) to meet the growing energy demand. Figure 1.14 demonstrates the balance between power generation and consumption. Among various energy harvesting technologies, solar PV systems stand out for their efficiency and prominence, as shown in Fig. 1.15. In grid-connected PV systems, power is fed directly to the utility grid (Fig. 1.16), with the main goal of maximizing power extraction using MPPT while minimizing transmission losses. However, under normal operating conditions, to enhance the overall efficacy of MPPT is employed in the PV systems. Operating at MPPT is not always feasible due to limited flexibility during grid intermittency, making FPPT essential for fast and efficient power extraction under dynamic conditions

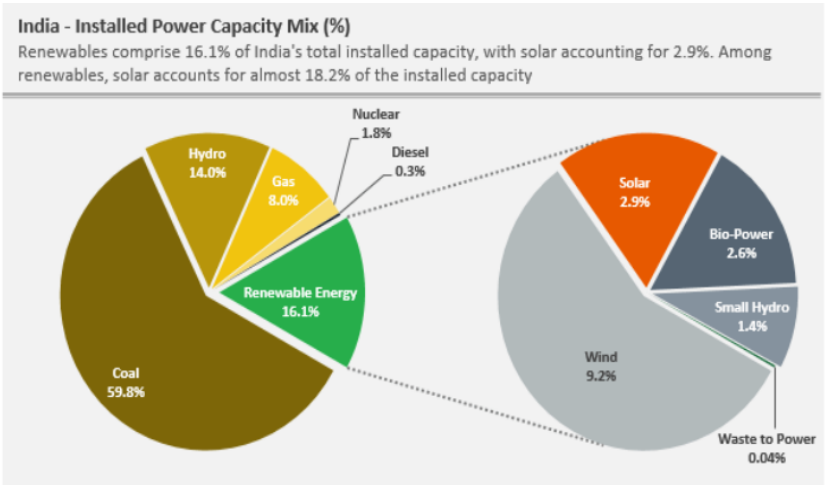


Fig. 1.12. Total electricity generation in India from various resources (Freis et al., 2016).

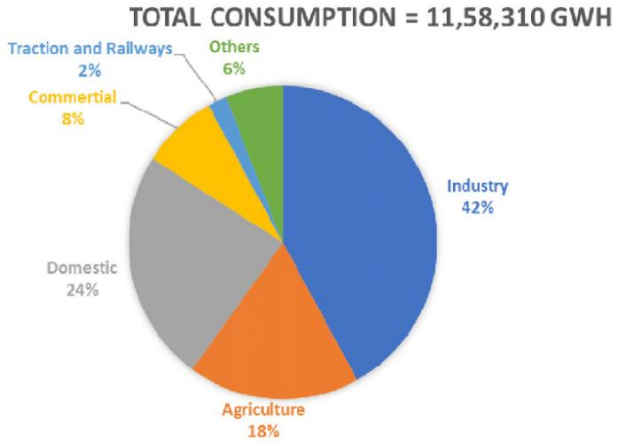


Fig. 1.13. Total electricity consumption India in various sectors (Freis et al., 2016).

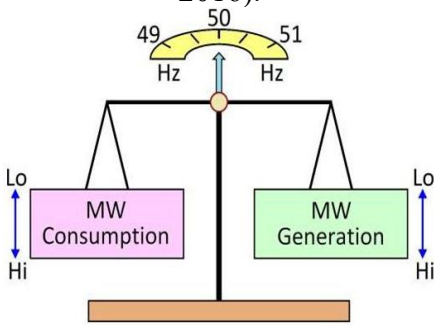


Fig. 1.14. Power balance of consumption and generation (Sharma et al., 2019).

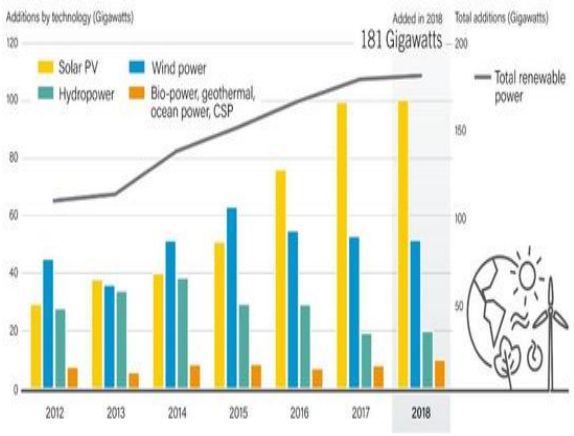


Fig. 1.15. Grid-connected PV penetration trends in global states of renewable generation (Sharma et al., 2019).

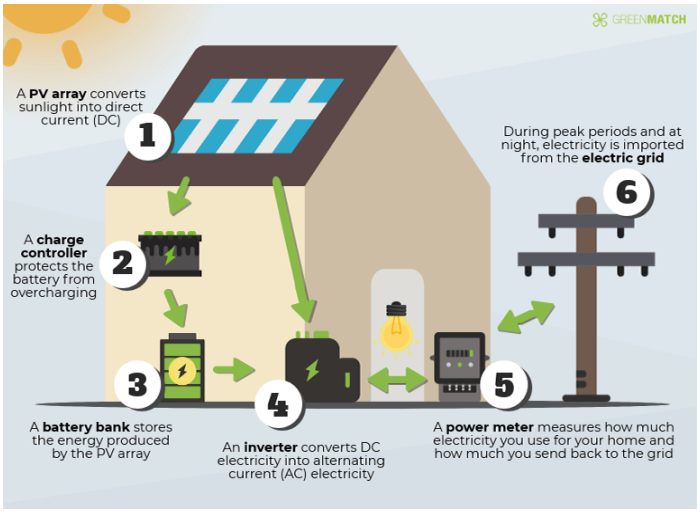
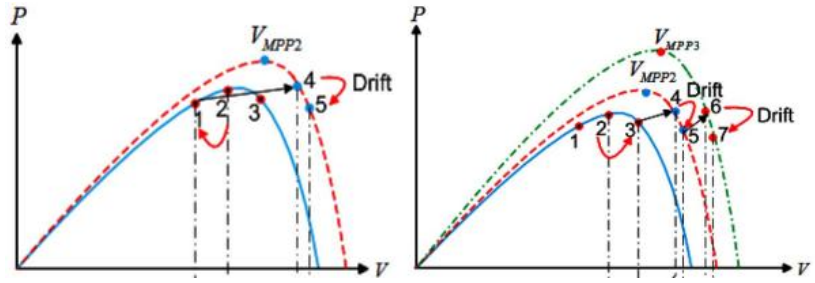


Fig. 1.16. Generation with aspect to standalone and grid-connected PV systems (Albarracín & Alonso, 2013)

1.5 Research Problem

This work is mainly focused on extracting the maximum power being generated from the PV systems. Conventionally P&O, INC, INR algorithms are used for the implementation of MPPT based controllers. But still traditional MPPT algorithms are prone to some challenges like less tracking efficiency, low convergence speed and drift phenomena. Among all, drift phenomena is one of the major challenges in MPPT algorithms as shown in Fig. 1.16. The rise in insolation causes the drift problem, and it gets worse when the insolation

increases rapidly, which usually happens on overcast days. In Fig. 1.16, drift can occur from three steady-state locations; the perturbation time (Ta) interval relies on the point of change in insolation. The drift problem is caused by the ambiguity in detecting whether the power gain (dP > 0) is due to disturbance or insolation. Assume Fig. 1.17. Traditional P&O MPPT drift study (a) Drift from point (1), (b) Rapid insolation increase drift. From the Fig. 1.17 (a) it is observed that there is a substantial increase in the insolation when the system is operated at point 1; as a result, the operating point is shifted to a new point (4) during the same kTa perturbation interval on the isolation curve. Now at point (4), as dP = P4(kTa) − P2((k − 1) Ta) > 0 and dV = V4(kTa) − V2((k − 1) Ta) > 0, the duty cycle is reduced, thereby moving to point (5) away from the MPP known as drift. Similarly, at points (2) and (3), where insolation increases, the conventional P&O algorithm faces drift issues due to its inability to accurately respond to rapid changes.



(a) (b)

Fig 1.17. (a) Drift from point 1. (b) Drift in case of rapid irradiation increment for existing P&O MPPT drift conditions (Killi & Samanta, 2015)

MPPT algorithms are prone to drift phenomena. Also, it creates a challenge to shift from MPP to CPP (constant power point) when any kind of fault or disturbance occur at the grid side of grid-connected PV systems. Also, because solar power is intermittent, MPPT makes grid management more difficult and doesn't give any flexibility to help the system out. Since FPPT aids in grid stabilization and provides flexibility to supply grid support, it is necessary to transition to it. When any kind of fault occur in the grid the MPP

point gets shifted to FPP point and power curtailment is performed to support grid.

Under normal conditions, PV systems typically operate using MPPT; however, during grid disturbances or fluctuating irradiance, operation under FPPT becomes necessary for faster response as shown in Fig 1.18. There can be both cases either the power can increase also as represented in Fig. 1.19 a) or the power can decrease as represented in Fig 1.19 b). In the both the cases we need to make MPPT shift to FPPT.

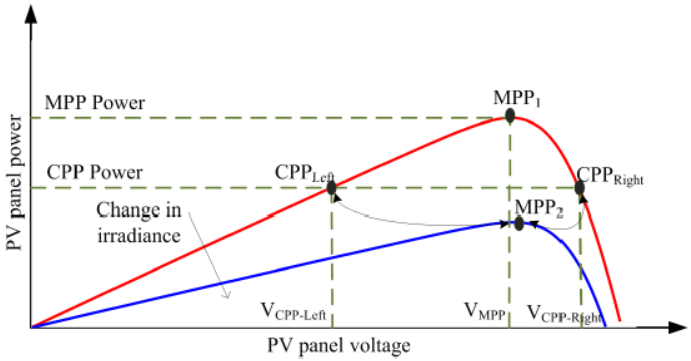


Fig. 1.18. Flexible power point tracking (FPPT).

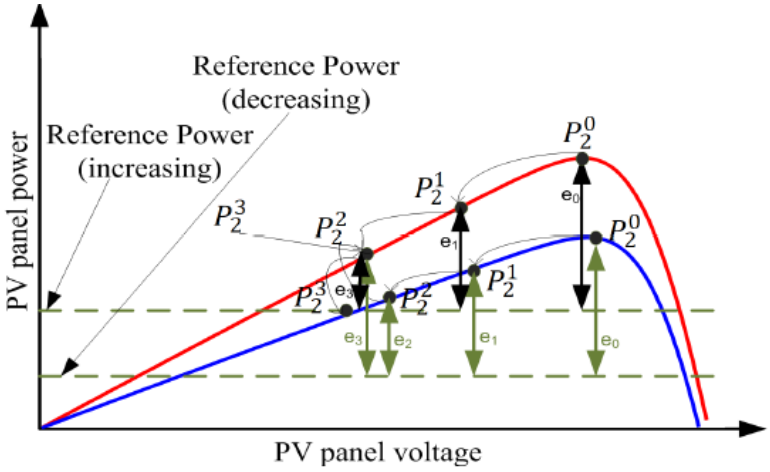


Fig. 1.19. PV Power with FPPT under changing irradiance (a) increased (b) decreased

1.6 Research Gaps

The following areas of unanswered questions have been highlighted by the literature review:

- MPPT algorithms are prone to drift phenomena thus resulting in loss of power which considerably impacts the PV system efficiency.
- It is quite challenging to determine the scaling factor values for wide irradiance range.
- The optimization of perturbation step-size is not investigated under rapid changes in irradiance.
- The lack of flexibility in MPPT makes grid assistance difficult to provide, and the intermittency of solar energy generation further complicates grid operation. In order to improve the grid's dynamic stability, active power curtailment, also known as the FPPT algorithm, is crucial.
- FPPT algorithms in the present literature have investigated the power point tracking performance under constant irradiance. Therefore, the algorithm’s performance should be thoroughly evaluated under varying irradiance and temperature conditions and remain unaffected by changes in the power threshold value.
- FPPT developed so far are sluggish to track the optimum power point.
- An adaptive step-size based FPPT algorithm should be formulated for enhancing the speed of convergence of the algorithm.
- FPPT algorithm performance should be further improved based on the optimizing the operating boundary between transient and steady state.
- FPPT should accurately track the optimum power point irrespective of increasing or decreasing power reference value.

1.7 Objectives

- Formulation and implementation of a drift-free MPPT algorithm under varying irradiance conditions.
- Design and simulation of an improved drift-free FPPT algorithm under sudden change in irradiance levels.
- Experimental validation of MPPT and FPPT algorithms to track the optimum power during realistic irradiance varying test conditions.

1.8 Structure of Thesis

The thesis is organized as mentioned below:

- **Chapter 2: Literature Review:** provides the literature review related to MPPT and FPPT algorithms.
- **Chapter 3: Adopted Methodology and Discussion:** presents the adopted methodology to achieve the objectives stated above.
- **Chapter 4: Formulation and implementation of a novel drift-free MPPT algorithm under varying irradiance conditions (Objective 1):** explains the simulation and implementation of various MPPT algorithms and proposed MPPT algorithm.
- **Chapter 5: Design and simulation of an improved drift-free FPPT algorithm under sudden change in irradiance levels (Objective 2):** discussed about the design and implementation of existing FPPT algorithms and proposed FPPT algorithm.
- **Chapter 6: Experimental validation of MPPT and FPPT algorithms to track the optimum power during realistic irradiance varying test conditions (Objective 3):** provides the detailed discussion about the hardware implementation and validation of proposed MPPT algorithm using experimental prototype.
- **Chapter 7: Conclusion and Future Scopes:** explains the conclusion and future scopes of the thesis in detail.

CHAPTER 2

LITERATURE REVIEW

This chapter reviews the various existing approaches of MPPT and FPPT/CPG techniques and presents them in a tabular form. MPPT approaches discussed in detail are illustrated in table 2.1. Further, FPPT/CPG approaches are also discussed and shown in table 2.2.

2.1. Maximum power point tracking

This subsection delivers a detailed description of MPPT methodologies that have been reported in the literature so far.

Authors have performed the simulation and experimental analysis of INC based MPPT algorithms. The results are analysed by using variable step size-based INC and INR algorithms for MPPT. The algorithm is analyzed on MATLAB/Simulink as well as experimental testbench and it shows the maximum tracking efficiency of 91.3%. The algorithm still needs to be investigated under rapid change in irradiance conditions (Mei et al., 2010).

In this work simulation-based studies have carried out by using perturb and observe algorithm. The analysis is performed on MATLAB/Simulink platform. The PV characteristics are analysed for PV array and achieve 92.1% tracking efficiency. But still, algorithm is not tested for rapidly changing irradiance conditions (Sholapur et al., 2014).

The authors have introduced modified P & O algorithm to avoid drift phenomena as compared to the basic P&O algorithm. The algorithm can avoid drift but not that much accurately while achieving the tracking efficiency of 93.5%. But algorithm is not supportive for drift avoidance at rapid change in irradiance conditions (Killi & Samanta, 2015).

In this work dual tracking based MPPT control algorithm is suggested to maximize the PV system's output power. The Simulink platform is used to do the analysis. But it does not provide any grid support (Jately & Arora, 2017).

A improved drift-free P&O algorithm is proposed to maximize electricity from PV systems with a higher efficiency. The adopted strategy makes algorithm complex which leads to increase in steady-state oscillation also. Moreover, it is not able to avoid drift phenomena and lacking in supporting grid (Pilakkat & Kanthalakshmi, 2018).

In this work a drift-free P&O MPPT controller approach with higher efficiency. The authors have used a current senor less experimental setup to reduce the power losses. The algorithm is not able to avoid drift under changing irradiance and environmental conditions (Li et al., 2019).

An efficient P&O algorithm is proposed providing the highest tracking efficiency of 96.8% by proposing an efficient and updated P&O algorithm with a drift mitigation feature under varying irradiation conditions. But it makes challenge to operate under abrupt environmental conditions (V. Kumar & Singh, 2020).

In this work different types of P&O algorithms are analyzed for avoiding drift under fluctuating irradiance. The work is mainly focused to avoidance of drift occurred while tracking MPPT under changing irradiance (Riquelme-Dominguez & Martinez, 2020).

Authors have proposed a fuzzy current-sensor less MPPT algorithm to reduce power losses. The authors have achieved the maximum tracking efficiency of 97.5%. But drift avoidance still creates an issue. Also, the algorithm is not able to track MPPT accurately under changing irradiance or environmental conditions (Saremi et al., 2020).

Authors has conducted a comparative analysis of MPPT algorithms utilizing the EN50530 dynamic evaluation technique in 2020, and the suggested MPPT algorithm achieved a tracking efficiency of 95.5%. When drift occurs, the algorithm has trouble tracking MPP (Li et al., 2020).

Moreover, load protection system is assessed on power optimizer by using adaptive step-size to avoid drift. The authors have successfully obtained 97.3% tracking efficiency, but steady-state oscillations are comparatively high (Manjunath et al., 2021).

A S&S MPPT based algorithm is designed and simulated to monitor PV systems' maximum power output for efficiency gains in which 98.2% tracking efficiency is achieved. But, the algorithm cannot avoid drift (Kavya & Jayalalitha, 2021).

A fine and coarse MPPT control-based algorithm with improved tracking efficiency is proposed and designed. The proposed algorithm achieved 98.5% tracking efficiency, but it is sluggish in nature and steady-state oscillations are also high (Kavya & Jayalalitha, 2022).

The authors have performed simulation and experimental studies of a manhattan metric-based P&O MPPT algorithm for PV systems. This method makes the algorithm complex and power losses also increased. The authors have obtained 96.7% tracking efficiency, but steady state oscillations are increased. The algorithm is not bale operate accurately under changing irradiance or environmental conditions. (Kesilmiş, 2022).

The work suggests a changeable step size-based P&O MPPT algorithm, achieving an overall efficiency of 95.05%. However, this performance came at the cost of increased convergence time, and the algorithm experienced higher power dissipation during rapid changes in irradiance (Saberi et al., 2023).

In this work a drift-avoided P&O algorithm is presented which requiring fewer sensors while maintaining an overall efficiency of 98.01%. The reduction in the number of sensors led to decreased steady-state oscillations and increased response time. Despite these improvements, the algorithm remains susceptible to instability under dynamic changes in irradiance and variable load conditions. The algorithm is prone to drift and shows high steady-state oscillations under dynamic change in irradiance (Kumar Nayak et al., 2023).

The study is carried out to enhance the efficiency of a drift-free P&O-based MPPT by using a new optimization method, leading to a better performance. The algorithm shows the maximum tracking efficiency of 98.25%. The authors concentrated on preventing drift in the P&O algorithm but did not address the issues of steady-state oscillations and response time. Moreover, the algorithm becomes unstable when there are sudden irradiance and load resistance changes (Pathak et al., 2024).

Table 2.1. Literature review of existing MPPT approaches

References	Algorithm (s)	Type of Study	Summary
(Mei et al., 2010a)	INC and INR based MPPT algorithms	Simulation and Experimental	• The results are analysed by using variable step size-based INC and INR algorithms for MPPT. • MPPT algorithm is not tested for rapidly changing irradiance conditions.
(Sholapur et al., 2014)	P&O	Simulation	The PV characteristics are analysed for PV array. MPPT algorithm is not tested for rapidly changing irradiance conditions.
(Killi & Samanta, 2015)	Improved P&O algorithm	Experimental	To prevent drift, a modified P&O MPPT algorithm is created. MPPT algorithm is not supportive for drift avoidance.
(Jately & Arora, 2017)	Dual tracking technique based MPPT control	Simulation	To maximize PV system power, dual tracking MPPT control is designed. No grid support is available in MPPT.
(Pilakkat & Kanthalakshmi, 2018)	Improved drift-free variable step-size P&O MPPT based control	Experimental	Suggested variable step-size based P&O drift-free MPPT control. MPPT offers no feature to provide grid support.

(Li et al., 2019)	Improved drift-free P&O algorithm for MPPT	Experimental	Proposed a drift-free current sensor less MPPT algorithm. MPPT offers no feature to provide grid support.
(V. Kumar & Singh, 2020)	Modified P&O for MPPT algorithm	Simulation	Proposed a drift-free P& O algorithm for MPPT tacking under change in irradiance. MPPT offers no feature to provide grid support.
(Riquelme-Dominguez & Martinez, 2020)	Comparison of different P&O variants for drift avoidance in MPPT	Simulation	Different types of P & O algorithms are compared for avoiding drift in the fluctuating irradiance. MPPTs offer no feature to provide grid support.
(Saremi et al., 2020)	Fuzzy current-sensor less MPPT algorithm-based control	Simulation	Dual-tracking MPPT control maximizes PV power. MPPT lacks grid support.

(Li et al., 2020)	MPPT algorithm comparison during the dynamic evaluation approach of EN50530	Experimental	A comparative analysis of various MPPT algorithms is conducted using EN50530 dynamic testing, noting that MPPT operates without grid support.
(Manjunath et al., 2021)	A drift-free P&O technique that utilizes adaptive duty cycle	Experimental	Variable step-size based drift-free P&O MPPT featuring power optimizer along with load management. Occurrence of drift may lead to a decrease in the efficiency of MPPT algorithm.
(Kavya & Jayalalitha, 2021)	A Novel Shift and Search (S&S) MPPT algorithm	Simulation	A novel S&S MPPT algorithm tracks maximum power in PV systems to optimize efficiency. MPPT offers no feature to provide grid support
(Kavya & Jayalalitha, 2022a)	An efficient algorithm for coarse and fine regulation	Simulation	To increase MPPT efficiency, a novel coarse and fine MPPT control methodology is introduced. MPPT algorithm efficiency may decrease due to drift.

(Kesilmiş, 2022)	MPPT regulation incorporates an improved P&O.	Simulation and Experimental	An algorithm for tracking photovoltaic systems' highest power point that is based on the Manhattan metric. Drift occurrence may lead to the decrease in the efficiency of MPPT algorithm.
(Saberi et al., 2023)	Variable step-size based P&O algorithm	Simulation	The variable-duty cycle P&O technique is adopted. However, quick irradiance changes diminished its great power.
(Kumar Nayak et al., 2023)	Drift-avoided P&O algorithm	Simulation with Experimental	A drift avoided P&O algorithm is designed and implemented. It avoids drift but struggle under rapid change in irradiance conditions.
(Pathak et al., 2024)	Drift-free P&O based MPPT algorithm	Simulation and Experimental	Proposed and build a drift-free P&O MPPT algorithm. The authors did not discuss steady-state deviation or response speed.

2.2. Flexible power point tracking

Recently, numerous studies have introduced FPPT control solutions by carefully altering hill-climbing algorithms to increase convergence speed and reduce stead-state power oscillations to track PV system CPP.

In (Mirhosseini et al., 2014), The authors addressed the fault-ride-through scenario for grid-integrated PV systems by proposing a DC-link energy-based FPPT controller, which was validated under standard test conditions (STC). However, its performance under rapidly changing irradiance conditions has not been analyzed.

In (Sangwongwanich et al., 2015), The authors proposed a fixed voltage step-based FPPT control method where the FPP is tracked using a constant voltage step size under standard test conditions (STC). The algorithm was tested under varying irradiance levels during reduced power mode and demonstrated fast response. Owing to its rapid performance, the proposed algorithm can be effectively applied in multi-string grid-integrated PV systems during voltage ride-through conditions.

In (Tafti et al., 2016), the authors proposed a FPPT algorithm by deploying advanced P&O based power control strategy to ensure fast and smooth transition between MPP and CPG when it is compared with conventional P&O technique. Additionally, the suggested approach works with single-stage PV systems, but PV voltage operating range is rather limited; so, some changes will be needed to make the algorithm run for stable operation.

In (Sangwongwanich, Yang, & Blaabjerg, 2017), the authors carried out a detailed investigation for constant power generation method for power reserve. The work proposed a cost-effective method for constant power generation under STC to ensure availability of power reserve during frequency-ride-through

period. However, the proposed method needs to be tested under rapidly changing irradiance conditions.

In (Tafti et al., 2017), the authors proposed a dual perturbation time step based FPPT control. Detailed investigations are carried out on two perturbation time steps for both MPPT and FPPT control algorithms. The suggested approach may track MPP's left or right point of operation. The method works for single- and two-stage photovoltaic power plants (PVPPs).

In (Sangwongwanich, Yang, Blaabjerg, & Sera, 2017), the authors proposed a delta power control (DPC) method to increase the stability of grid-connected PV systems. Although the PV power in this work is controlled on the left side of the PV curve, which increases efficiency, the scheme's complexity prevents it from being cost-effective.

In (Sangwongwanich, Yang, Blaabjerg, & Wang, 2017), the authors developed three CPG techniques using P&O algorithm. A two-stage grid-connected photovoltaic (GCPV) experimental test bench is used to assess these three techniques, which rely on power control (P-CPG) and a current controlling. These algorithms are compared based on parameters like steady-state performance, tracking error, stability and complexity. It has been realized that I-CPG is simple in structure, but it is prone to instability and P-CPG shows good steady-state response. But in CPG-P&O algorithms, the tracking error increases with rapid change in irradiance.

In (Tafti, Sangwongwanich, Yang, Konstantinou, et al., 2018), the authors performed experimental analysis by making use of dual step-size based FPPT control. The proposed method used two distinct step-sizes for efficient tracking during transient and steady-state. However, CPG performance can be enhanced by making use of adaptive voltage step-size calculations.

In (Tafti, Sangwongwanich, Yang, Pou, et al., 2018), The authors devised adaptive step-size FPPT control to track PV system MPP and FPP. The algorithm presented is complicated.

In (Tafti, Townsend, et al., 2018), the authors implemented a modified power-based FPPT algorithm, which could track CPP on both left and right side of MPP, i.e. multi-mode operation. The proposed algorithm has the capability to quickly track CPP, but it will not be applicable in case of rapid change in irradiance.

In (Narang et al., 2019), the authors investigated a dynamic voltage reference and MPC based FPPT control to address frequency and voltage ride through issues. Transient response under variations in frequency and voltage fluctuations is used to measure the algorithm's efficacy.

In (Yan et al., 2020), the authors proposed a dc-link voltage based FPPT control, where FPP is tracked using model predictive controller and is tested on battery load. The focus is to regulate the battery by considering lifetime, but algorithm is not explored much.

In (Gomez-Merchan et al., 2020), the authors introduced binary search based FPPT control, which mainly improves the speed of convergence by iteratively reducing the search space to half of its previous value. But algorithm is not tested under rapid change in irradiance or temperature.

In (Kumaresan et al., 2021), the authors introduced secant method based FPPT control, which tracks the FPP irrespective of increasing or decreasing power reference value under STC. The proposed method is fast and shows less steady-state oscillations, but it becomes unstable in environmental aspect.

An interactive suppression technique employing error signals was presented by Hou et al. (2021). To ensure consistent generation of power, the authors

developed the FPPT control method for photovoltaic (PV) systems. This method still lacks the capacity to quickly modify parameters, even though it performs better than the traditional Perturb and Observe (P&O) strategy.

In (A. Kumar & Kumar, 2021), the authors suggested a fuzzy logic control and least mean square (LMS) control for CPG under varying irradiance and constant temperature conditions. But the method is complex which makes it costly from application point of view.

A hill ascending approach based on FPPT management under PSC was developed by the authors in (Xie & Wu, 2022). However, it is ineffective at lowering steady-state oscillations.

In (Tafti et al., 2022), the authors proposed a GFPPT control under PSC. The primary goal is to attain CPP with greater efficiency under circumstances when irradiance changes quickly.

In (B. Zhang et al., 2022), the authors proposed a virtual synchronous generator (VSG) control strategy based FPPT algorithm. It can stabilize the grid during intermittency but has not been tested.

In (Ahmed et al., 2022), the authors presented dc-link model based MPPT/FPPT control, which has the capability to operate under changing irradiance. Researchers developed finite-set model predictive control (FS-MPC) to manage grid-connected PV system active and reactive power exchange. But parameters like steady-state oscillations, speed of convergence and tracking efficiency are not up to the mark.

In (Oufettoul et al., 2023) to overcome the effect of PSC, the authors have presented a hybrid hill climbing and particle swarm optimization (HC&PSO) for implementing the FPPT algorithm. It has also been validated and tested. But the method is prone to drift occurrence.

The authors of (Guanghua et al., 2024) suggested a control technique for active disturbance rejection FPPT that is based on errors for PV systems to generate constant power. Although the technology outperforms the traditional P&O approach, it still lacks quick parameter adjustment.

2.3. Summary

Based on the insights gained from the literature survey, it is evident that various MPPT and FPPT techniques have been proposed, each with distinct merits and limitations for grid-connected PV systems. The review highlights the need for an optimized approach that ensures fast tracking, minimal oscillations, and high efficiency under dynamic environmental conditions and flexible at the time of intermittency occurred in the grid. To address these research gaps, the present work develops a systematic methodology that focuses on the design, modelling, and implementation of an optimum MPPT and FPPT technique. The following chapter outlines the proposed methodology, including the system architecture, control strategies, and simulation framework adopted for performance evaluation.

Table 2.2. Literature review of existing CPG/FPPT approaches

References	FPPT Algorithm(s)	Type of Study	Summary
(Mirhosseini et al., 2014)	Dc-link energy based FPPT control	Simulation	FPPT is carried out under constant irradiance condition. FPP of operation is always chosen to the right side of P-V curve.
(Sangwongwanich et al., 2015)	Fast FPPT control	Experimental	Advanced power control strategy is deployed to ensure fast and smooth transition between MPP and CPG.
(Tafti et al., 2016)	Fixed voltage step based FPPT control	Simulation	FPP is tracked using constant voltage step-size under step-change in irradiance.
(Sangwongwanich, Yang, & Blaabjerg, 2017)	Constant power generation method for power reservation	Simulation	A cost-effective constant power generation method is proposed and realized for power reserve
(Tafti et al., 2017)	Dual perturbation time step based FPPT control	Experimental	Two perturbation time steps are selected for MPPT and FPPT operation.

(Sangwongwanich, Yang, Blaabjerg, & Sera, 2017)	Delta power control (DPC) strategy for CPG	Experimental	Delta power control (DPC) is suggested to stabilize PV systems.
(Sangwongwanich, Yang, Blaabjerg, & Wang, 2017)	Current based, power based and P&O based CPG control	Experimental	CPP is achieved by using three different CPG techniques based on current, power and P&O algorithm methods respectively.
(Tafti, Sangwongwanich, Yang, Konstantinou, et al., 2018)	Dual step-size based FPPT control	Experimental	Two distinct step-sizes are used for efficient tracking during transient and steady-state.
(Tafti, Townsend, et al., 2018)	Multi-mode power based FPPT algorithm	Experimental	Proposed a modified power based FPPT algorithm which can track CPP on both left and right side of MPP i.e. multi-mode operation.
(Tafti, Sangwongwanich, Yang, Pou, et al., 2018)	Adaptive duty cycle based FPPT control	Experimental	Tracking MPP and FPP uses an adaptive step-size.
(Narang et al., 2019)	Dynamic voltage reference and MPC based FPPT control	Experimental	Duty cycle for FPPT is obtained using inductor current reference value

(Yan et al., 2020)	dc-link voltage based FPPT control	Simulation	FPPT is tracked using model predictive controller when connected to a battery-based load.
(Gomez-Merchan et al., 2020)	Binary search based FPPT control	Experimental	Speed of convergence is improved by iteratively reducing the search space to half of its previous value.
(Kumaresan et al., 2021)	Secant method based FPPT control	Experimental	The proposed algorithm tracks the FPP irrespective of increasing or decreasing power reference value and under sudden variations of irradiance.
(A. Kumar & Kumar, 2021)	Fuzzy logic controller (FLC) based CPG	Simulation	Proposed a FLC based control to dc-dc boost converter to provide support to the grid-connected PV systems.
(Xie & Wu, 2022)	FPPT control under PSC	Simulation	Developed a hill climbing method based FPPT control under PSC.
(Tafti et al., 2022)	Novel global FPPT control under partial shading conditions	Experimental	Developed a GFPPT control and tested the same under partial shading conditions

(B. Zhang et al., 2022)	VSG control strategy based FPPT algorithm	Simulation	Developed a virtual synchronous generator (VSG) control strategy based FPPT algorithm.
(Ahmed et al., 2022)	Model based MPPT and FPPT control	Simulation and Experimental	Developed a dc-link model-based MPPT/FPPT control and FS-MPC algorithm to manage active and reactive power exchange in gird-connected PV systems.
(Oufettoul et al., 2023)	A hill climbing and particle swarm optimization (HC&PSO)	Simulation and Experimental	Non-uniform irradiation conditions are employed in the design and implementation of the suggested algorithm. It has also undergone testing and validation. However, the technique is prone to drift.
(Guanghua et al., 2024)	Active disturbance rejection FPPT control	Simulation	It a FPPT control that is based on errors for PV systems to generate constant power. Although the technology outperforms the traditional P&O approach, it still lacks quick parameter adjustment.

CHAPTER 3

ADOPTED METHODOLOGY AND DISCUSSION

This chapter represents the research methodology adopted to achieve the research objectives. Methodology is explained in detailed in two subsections namely adopted methodology and tools and models. In adopted methodology subsections, a detailed explanation of workflow is presented. While, in tools and models subsection, various steps about the tool are described.

3.1.Adopted Methodology

The research methodology to be adopted to perform the research work is mentioned below in bullet points as well as in flowchart form also in fig. 3.1. The algorithms are simulated using MATLAB/Simulink:

- Literature survey:
  - Comprehensive literature review was carried out in three distinct phases to identify and analyze the existing research gaps.
  - Problem definition is formulated based on the gaps analysed by performing literature survey.
  - From the problem definition the research objectives are formulated to cover the research gaps and synopsis is presented.
  - The objectives are mentioned in the following sub section.
- Objectives:
  1. Formulation and implementation of a novel drift-free MPPT algorithm under varying irradiance conditions.
  2. Design and simulation of an improved drift-free FPPT algorithm under sudden change in irradiance levels.
  3. Experimental validation of MPPT and FPPT algorithms to track the optimum power during realistic irradiance varying test conditions.

➢ Achievement of Objectives:

- Three objectives are framed by analysing research gaps and problem.
- To achieve the 1st objective, conventional and adaptive- P&O, INC, and INR MPPT techniques are simulated and implemented on MATLAB/Simulink.
- Further, an improved drift-free adaptive voltage perturbation and dual perturbation based MPPT algorithms are designed and developed on MATLAB/Simulink platform.
- To achieve 2nd objective, the evaluation parameters like current (I), voltage (V), power (P) and duty cycle (d) are considered for designing a novel FPPT algorithm. The FPPT algorithm is designed and tested on standard test conditions (STC), and under partial shadowing conditions.
- Further, deigned FPPT algorithm is implemented and tested under changing irradiance conditions and under partial shading conditions on MATLB/Simulink platform.
- To achieve 3rd objective, a proposed drift-free MPPT & FPPT algorithm is implemented and tested on experimental prototype. So, the designed drift-free MPPT algorithm is implemented and tested on hardware platform.

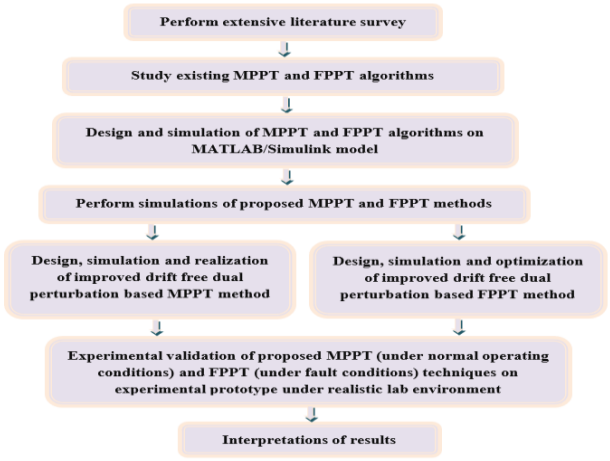


Fig 3.1. Flowchart of research methodology

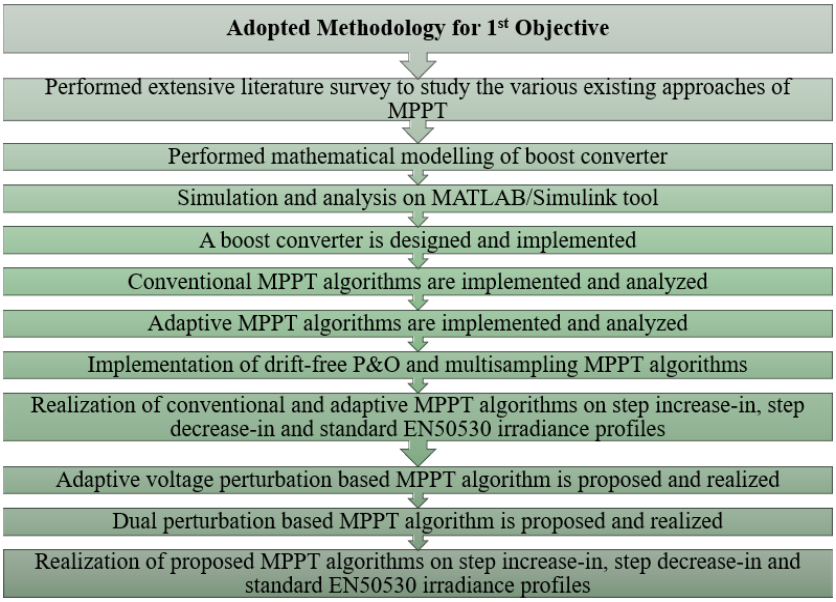


Fig 3.2. Flowchart representation of adopted methodology to achieve 1st objective

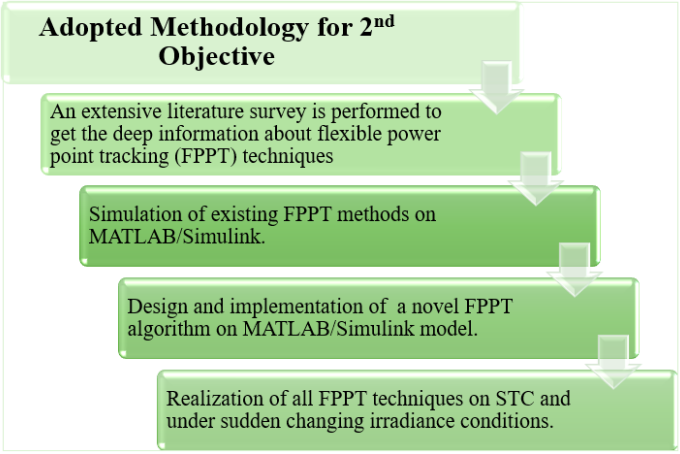


Fig 3.3. Flowchart of adopted methodology to achieve 2nd objective

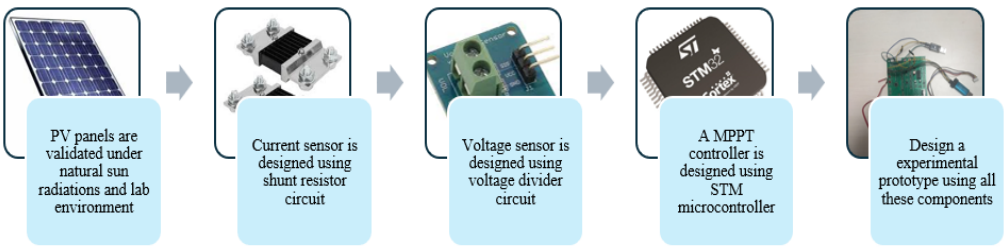


Fig 3.4. Graphical representation of adopted research methodology to achieve 3rd objective

3.2. Tools and Models

A fundamental tool for modeling, simulating, and evaluating complex systems, MATLAB/Simulink is utilized in this work. When it comes to modeling and simulating real-world processes and dynamic systems, the graphical programming environment MATLAB/Simulink is second to none. Because of its adaptability in building component blocks and simplicity of integration with mathematical functions, it was selected to simulate [certain system or process, for example, a control system or a renewable energy system] for this research. One advantage of using Simulink is the ability to build, test, and modify system components independently. This allowed for a more controlled and precise modeling of system behaviors.

The research followed a step-by-step approach. First, system parameters and constraints were defined based on theoretical analysis and literature review. Key variables were then incorporated into the Simulink model, with each subsystem represented through interconnected blocks, providing a visual and structural representation of the system. Different scenarios were simulated to observe the dynamic responses of each variable, and parameters were adjusted to optimize performance. Because of this iterative procedure, it was possible to explore intricate relationships inside the model and make real-time tweaks to obtain desired results.

Lastly, the simulation results were analysed, validated, and compared with theoretical predictions and experimental data (where applicable) to ensure model accuracy and reliability. The results from MATLAB/Simulink were further refined using MATLAB scripts for post-processing, including data visualization and statistical analysis, to interpret system behaviour under various conditions. Overall, the versatility and integration features of MATLAB/Simulink made it the perfect tool for this study, enabling the creation

of a solid, scalable model with dependable results to back up the findings and conclusions.

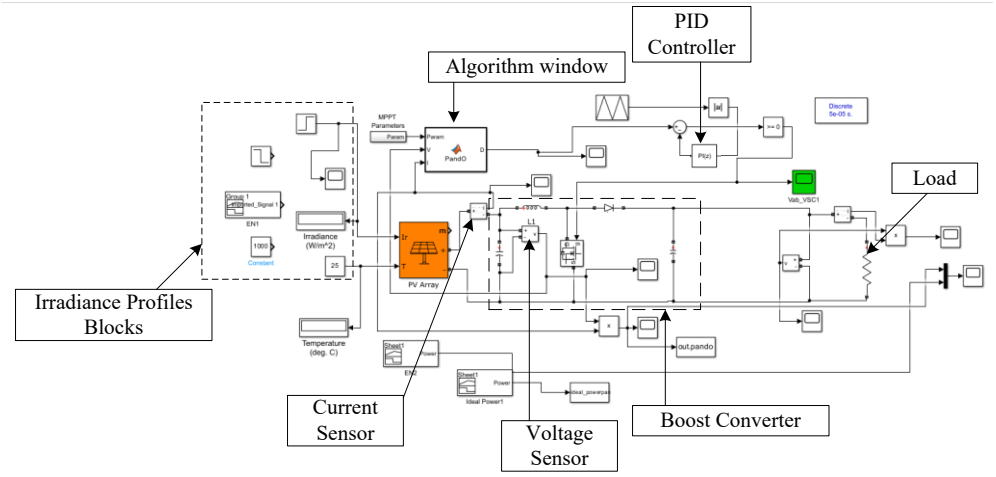


Fig 3.5. Simulation model of MPPT algorithms

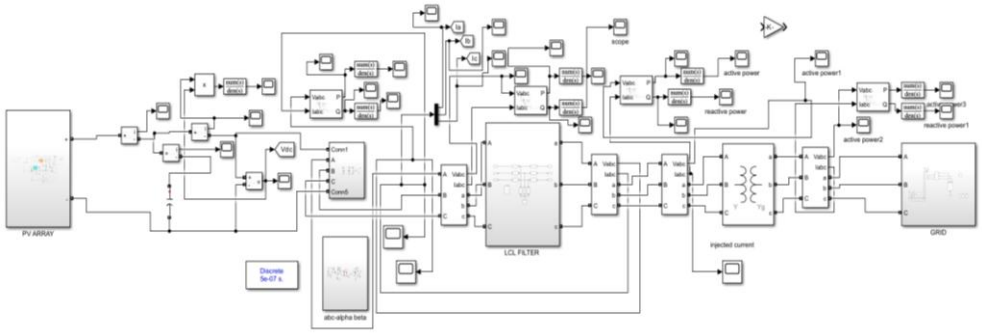


Fig 3.6. Simulation Circuit of Grid-connected PV systems

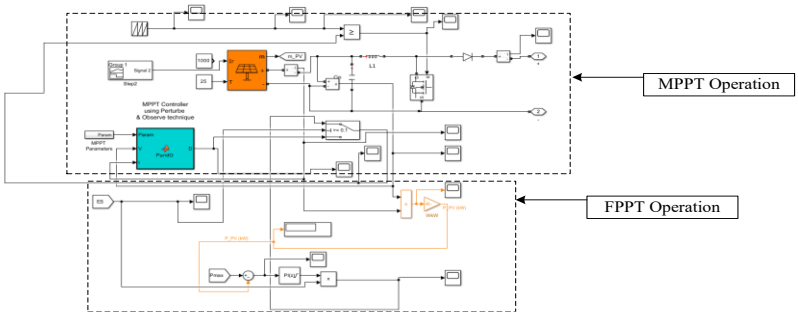


Fig 3.7. Simulation model of FPPT algorithms

3.3. Summary

The proposed methodology outlines the design and implementation of various MPPT and FPPT techniques for standalone and grid-connected PV systems, ensuring accurate modelling and simulation. The results derived from these techniques are presented with a focus on tracking efficiency, response time and steady-state oscillations and stability under varying environmental conditions. A detailed discussion follows, where the comparative performance of the methods is analysed to highlight their strengths, limitations, and suitability for grid integration. This flow establishes a clear link between the developed methodology, the obtained results for MPPT and FPPT techniques, and their implications in the coming chapters.

CHAPTER 4

DESIGN AND ANALYSIS OF MAXIMUM POWER POINT ALGORITHMS

In gird-connected PV systems, developed dc-link model-based MPPT/FPPT control and FS-MPC algorithm for active and reactive power exchange.

4.1. Introduction

The recent surge in interest in photovoltaic (PV) systems is largely attributable to their ease of installation and minimal maintenance needs. The effectiveness and performance of PV systems are now crucial considerations in optimizing their contribution to the energy mix as the globe moves toward sustainable energy sources (Talha et al., 2022). However, the performance of PV systems is highly sensitive to various environmental factors, particularly solar radiation, which can change rapidly due to weather conditions like clouds, shadows, or dust (Parlevliet & Moheimani, 2014). The consequence of high variation in irradiance results in a significant challenge to maintain the stable power output of PV systems (Chen et al., 2015). MPPT is used to keep PV systems at its MPP under different situations (Peng et al., 2017). Anatomically tweaking PV system operating point maximizes MPPT algorithm power. Among various MPPT techniques, P&O is utilized generally because of its straightforwardness and comfort of execution (Yadav et al., 2020).

However, traditional P&O methods often need some tweaking to maintain their accuracy and efficiency under rapidly changing irradiance conditions (Podder et al., 2019). Reason being fixed perturbation step size in conventional P&O algorithms may cause fluctuations near MPP, or in some cases, it may even cause the system to diverge from the MPP during rapid changes in irradiance (Mousa et al., 2021a). In order to tackle these issues,

adaptive perturbation-based MPPT algorithms have been suggested (Tawiah-Mensah et al., 2022). Adaptive approaches are designed to improve the precision of tracking and speed of response of the PV system by continuously changing the perturbation step size according to the rate of change in irradiance (Hashim et al., 2023a). The adaptive approach allows the system to respond more effectively to rapid changes in environmental conditions, thereby maintaining optimal performance and minimizing power loss (Büyük & İnci, 2023a). In (Lin & Liao, 2024), the authors focused on optimizing PV system performance using adaptive perturbation-based MPPT techniques in scenarios of rapidly changing irradiance. Minimizing tracking time and power oscillations is intended to increase the efficiency of MPPT algorithms (Motahhir et al., 2020).Various adaptive strategies, such as variable step size and fuzzy logic control, have been explored and compared with traditional fixed-step MPPT methods. In (Belkaid et al., 2017), the study analysed the trade-offs between tracking speed and stability, considering the impact on overall system efficiency.

In (Shaikh et al., 2023), the authors investigated the implementation challenges and potential solutions for adaptive perturbation-based MPPT techniques. In (Chellal et al., 2021a), Simulations and experimental validations show that conventional and adaptive approaches work under varying irradiation circumstances. Numerous iterations of the P&O algorithm have been extensively documented, each with unique approaches to enhance performance of the PV system (Escobar et al., 2017). In (Bhattacharyya et al., 2020), During operation, a drift-avoided P&O-based MPPT algorithm should swiftly monitor the MPP and minimize steady-state oscillations around it. However, this reduction in steady-state oscillations led to an increased response time for the proposed algorithm. In (Hua & Zhan, 2021), a hybrid P&O-based MPPT algorithm was introduced, characterized by zero steady-state oscillations and achieving a maximum tracking efficiency of 99.5%, with a transient response time of 14.5 seconds. The investigators, in (Kavya & Jayalalitha, 2022b),

present an updated P&O method designed for coarse and fine control, addressing the shortcomings of earlier versions by demonstrating convergence times up to 55% faster and significantly reduced oscillations compared to traditional and drift-free methods. Although this method uses a power-based control strategy, it becomes unstable in situations when the irradiance changes quickly.

In (Chellakhi et al., 2022), an enhanced P&O MPPT approach using variable step size is proposed, achieving low oscillations, 99.6% tracking efficiency, a 30 s response time, and minimal power loss. However, despite these improvements, the method needs help to reliably track the MPP when faced with sudden changes in irradiance and resistance. In (Kahani et al., 2022), a P&O-based MPPT algorithm was introduced to minimize oscillations near the MPP, achieving a tracking efficiency of 95.27%. The authors employed a variable step size to improve the algorithm's accuracy. However, the algorithm still struggles to track the MPP effectively during rapid changes in irradiance and load. In (Pathak et al., 2024), the efficiency of a drift-free P&O-based MPPT was enhanced using a new optimization method, leading to a better performance. The authors concentrated on preventing drift in the P&O algorithm but did not address the issues of steady-state oscillations and response time. Moreover, the algorithm becomes unstable when there are sudden irradiance and load resistance changes. In (Saberi et al., 2023), the authors have proposed a P&O MPPT algorithm utilizing a variable step size, achieving an overall efficiency of 95.05%. However, this performance came at the cost of increased convergence time, and the algorithm experienced higher power dissipation during rapid changes in irradiance. In (Kumar Nayak et al., 2023), a drift-avoided P&O algorithm was presented, requiring fewer sensors while maintaining an overall efficiency of 98.01%. The reduction in the number of sensors led to decreased steady-state oscillations and increased response time. Despite these improvements, the algorithm remains susceptible to instability

during rapid changes in irradiance and load. The algorithm is prone to drift and shows high steady-state oscillations under dynamic change in irradiance. Moreover, the existing MPPT algorithms are complex in nature and exhibit instability under rapid changes in environmental conditions (Alaas et al., 2023; X. Zhang et al., 2023). To overcome the challenges faced by traditional and adaptive hill-climbing based MPPT algorithms under dynamic irradiance conditions, this work presents an improved MPPT algorithm designed to mitigate drift. This algorithm not only has a high speed of convergence but also maintains stability even under dynamic change in irradiations. The algorithm tracks the MPP by using voltage as a perturbation parameter and operates only at the right-hand side of the power curve. The following are the key novelty features of the proposed research work.

Novelty Features

- Comprehensive analysis of existing MPPT algorithms has been conducted to identify their limitations under rapidly changing irradiance conditions.
- The proposed voltage based MPPT technique improves the accuracy and reliability of MPPT by overcoming the drift which ensures optimal power extraction from PV systems even when solar irradiance fluctuates.
- The proposed algorithm is rigorously tested and equated with other MPPT algorithms under different case scenarios. The performance of the proposed algorithm is analysed for the standard irradiance profile EN50530. Moreover, the proposed algorithm exhibits minimum drift in the highest slope region of EN50530 irradiance profile.

4.2.PV Modelling and Analysis

The mathematical modelling section elucidates the intricate relationships governing the behaviour of the PV system under dynamic irradiance changes. This mathematical model encompasses the intricate

relationships between the system's components, including the PV panels, boost converter, and load. To accurately predict system behavior and identify the optimal MPP operating point, factors such as electrical characteristics, temperature variations, and solar irradiance levels are considered. It then became the basis for designing and implementing the drift-free MPPT strategy, which lets the PV system's performance be precisely controlled and optimized even when the environment changes.

The below mentioned PV modeling mathematical equation is used to carry forward the discussed research work. Eq. (4.1) is used to evaluate PV current (I_{PV}) as,

$$I_{PV} = I_{ph} - I_d - I_{rsh} \qquad (4.1)$$

Further, the change in temperature of the PV cell is calculated by using Eq. (4.2) as,

$$\Delta T = T - T_{ref} \qquad (4.2)$$

The significant parameters of PV modules at a specific temperature and irradiance, such as open circuit voltage (V_{oc}), short circuit current (I_{sc}), threshold voltage (V_{th}), reverse saturation current of diode (I_0), series resistance (R_s) and photo-current correspondent to G (I_{ph}) are evaluated by Eq. (4.3) to Eq. (4.8), as shown below:

$$V_{oc} = \frac{V_{oc}}{\left(1+\left[\beta_{oc}\times\log\frac{G_{ref}}{G}\right]\times\left(\frac{T_{ref}}{T}\right)^{\gamma pmpp}\right)} \qquad (4.3)$$

$$I_{sc} = \left(\frac{G}{G_{STC}}\right) \times I_{sc} \times \left(1 + (\alpha_{sc} \times \Delta T)\right) \qquad (4.4)$$

$$V_{th} = \frac{(N_s \times k \times T)}{q} \qquad (4.5)$$

$$I_0 = \left(I_{sc} - \left(\frac{V_{oc}}{R_{sh}}\right)\right) \times e^{\left(\frac{-V_{oc}}{A \times V_{th}}\right)} \qquad (4.6)$$

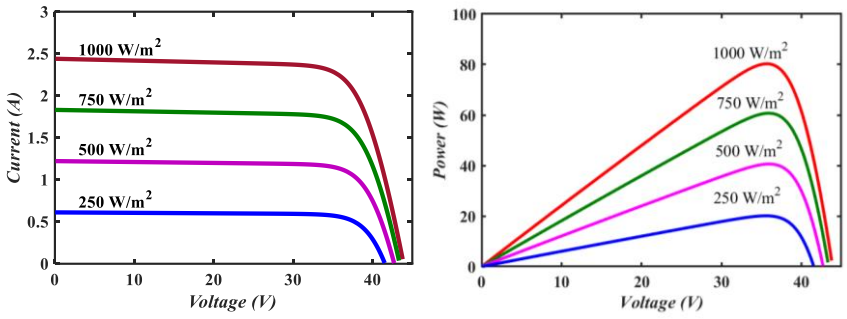
$$R_s = R_{so} - \left(\left(\frac{A \times V_{th}}{I_0} \right) \times e^{\left(\frac{-V_{oc}}{A \times V_{th}} \right)} \right) \qquad (4.7)$$

$$I_{ph} = \left(I_{sc} \times \left(1 + \left(\frac{R_3}{R_{sh}} \right) \right) \right) + \left(I_0 \times \left(e^{\left(\frac{-V_{oc}}{A \times V_{th}} \right)} - 1 \right) \right) \qquad (4.8)$$

Equations (4.3) to (4.8) are used to calculate the characteristic equation, as mentioned in Eq. (4.9), relating the PV system current (I_{PV}) voltage (V_{PV}) as,

$$I_{PV} = I_{ph} - I_{0p} \left(e^{\left(\frac{q \times (V_{PV} + R_S \times I_{PV})}{A \times N_S \times K \times T} \right)} - 1 \right) + \left(\frac{V_{PV} + R_S + I_{PV}}{R_{sh}} \right) \qquad (4.9)$$

The mathematical model helps evaluate I-V and P-V curves at variable irradiance and temperature. In Fig. 4.1(a)-(b), the I-V and P-V curves at different temperatures under fixed solar irradiation as 1000 W/m^2.



(a) (b)

Fig. 4.1. (a) I-V curve (b) P-V curve on various irradiance levels under STC

4.2.1. Modelling of DC-DC Boost Converter

A comprehensive analysis of DC-DC boost converter is presented in this subsection. An integral part of the system design, the boost converter allows for effective control and conversion of power. It is based on the maximum power transfer theory, which says that no loss occurs during power transfer from a source to a load when their respective internal resistances are equal.The boost converter keeps the PV system running at its MPP under different irradiance situations by adjusting the voltage levels to meet the needs of the load or energy

storage system. Because of this, the system is able to improve its performance and energy harvesting efficiency on a constant basis by drawing the most possible power from the solar panels. Moreover, the MPPT algorithm is built to withstand the dynamic environmental circumstances often found in real-world PV systems, due to the boost converter's capability to adjust to fluctuating input voltages and effectively supply power to the load. The developed boost converter and PV module utilized in this investigation are described in Tables 4.1 and 4.2. Fig. 4.2 shows PV equivalent circuit. The complete PV system setup used to implement the MPPT algorithm is shown in Fig. 4.3.

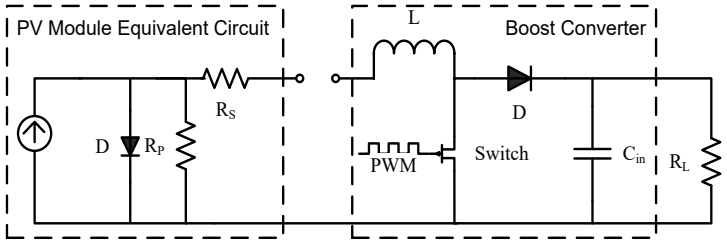


Fig. 4.2. Equivalent circuit of MPPT assisted PV system

Moreover, the mathematical modelling of the same is discussed below in detail. The given equations are used to design the boost converter as per the specified values of PV module system. Eq. (4.11) provides the relation between the PV input and output currents (I_{PV}, & I_0) of the boost converter. Eqs. (4.10)–(4.11) explain the relation of the input (R_{in}) and load resistance (R_{load}) in respect of duty cycle as,

$$V_0 = 1 - \frac{V_{PV}}{1-D} \tag{4.10}$$

$$I_{0p} = I_{PV} \times (1 - D) \tag{4.11}$$

$$R_{in} = R_{load} \times (1 - D)^2 \tag{4.12}$$

Here, $D = D_{mpp}$ and $R_{in} = R_{inmpp}$ at MPP. Eq. (4.12) is rewritten as Eqs. (4.13), (4.14), and (4.15), which show the boost converter's state equations throughout a switching cycle.

$$R_{inmpp} = R_{load} \times \left(1 - D_{mpp}\right)^2 \quad (4.13)$$

$$L\frac{dI_{PV}}{dt} = V_{PV} \times (1 - d)V_0 \quad (4.14)$$

$$C\frac{dV_0}{dt} = V_{PV} \times (1 - d)I_{PV} - \frac{V_0}{R} \quad (4.15)$$

Here, I_{PV}, V_{PV} and V_0 are input electrical performance parameters Such as current, input voltage.

$$G_{vd}(s) = \frac{\tilde{v}_{PV}}{\hat{d}} = \frac{cs + \frac{1}{R} - (1-d_0)I_{PV_0}}{LCs^2 + \frac{L}{R}s + (1-d_0)^2} \quad (4.16)$$

$$G_{id}(s) = \frac{\tilde{\imath}_{PV}}{\hat{d}} = \frac{V_{o_0}C\,s + \frac{V_{o_0}}{R} - (1-d_0)I_{PV_0}}{LCs^2 + \frac{L}{R}s + (1-d_0)^2} \quad (4.17)$$

In above mentioned Eqs, (4.16) and (4.17) $\tilde{v}_{PV}$, $\tilde{\imath}_{PV}$ and $\hat{d}$ are perturbations in I_{PV}, V_{PV}, d respectively.

Furthermore, Eqs. (4.18) & (4.19) Present the transfer functions of the PI control loops for current and voltage regulation.

$$G_v(s) = K_{pv} + \frac{K_{iv}}{s} \quad (4.18)$$

$$G_c(s) = K_{pc} + \frac{K_{ic}}{s} \quad (4.19)$$

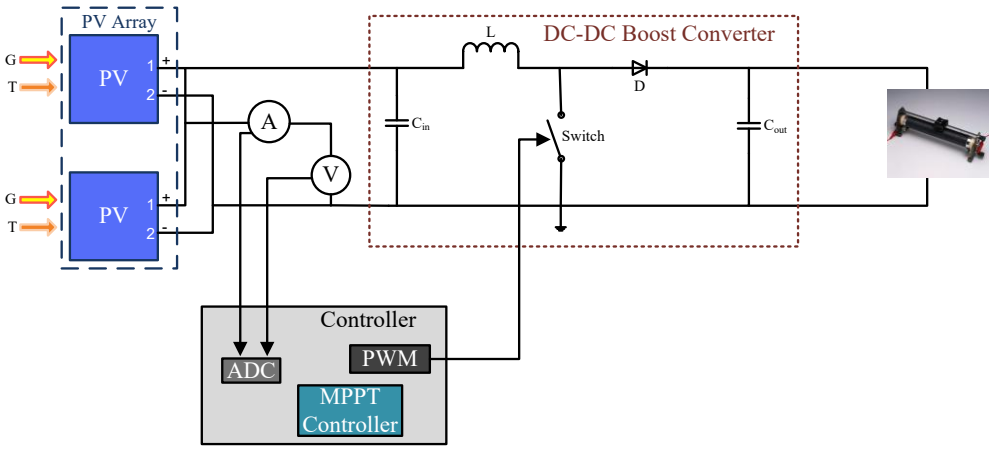


Fig. 4.3. Schematic diagram of MPPT integrated PV system

Table 4.1. Specifications of PV module

PV Panel Parameters	Specifications
P_{max} (W)	40.14
N_s	36
V_{oc} (V)	21.90
I_{sc} (A)	2.45
V_{MPP} (V)	17.40
I_{MPP} (A)	2.30

Table 4.2. Specifications of Boost Converter

Components	Specifications
Capacitor C_{in} (μF)	99.95
Inductor L (mH)	15.39
Switch	IGBT
Diode D	MOS-FET
Capacitor C_{out} (mF)	30.26
Switching Frequency (kHz)	20

4.3.Maximum Power Point Tracking Techniques

This work mainly focuses on the comparative study of conventional, adaptive and proposed MPPT algorithms. Existing MPPT algorithms such as P&O, INC and INR are discussed in detail in this section (Alaas et al., 2023; Sarang et al., 2024). he MPPT algorithms are developed and simulated in the MATLAB/Simulink environment, and their performance is validated using a real-time system (RTS) controller. The detailed analysis of the above-mentioned methods is discussed in following three sub-sections.

4.3.1. Conventional P&O MPPT Algorithm

Popular MPPT algorithms include the traditional P&O method. The primary problems of the P&O algorithm include continuous steady-state oscillations and poor tracking, which might lead to going away from MPP during fast irradiance changes. P&O dynamic behavior is improved by variable step size and perturbation frequency (Alaas et al., 2023). The flowchart of the

same is depicted in Fig. 4.4. The traditional P&O method uses power control strategy for operation. To operate the algorithm, current (I) and voltage (V) are measured and using these measured values, power (P) is calculated. To evaluate the duty cycle (D), it detects changes in power (dP) by manipulating the operational change in voltage (dV). Eq. (4.20) is used to calculate the change in duty cycle (ΔD) where, D_{old} is the perturbation step of duty cycle.

$$D = D_{old} \mp \Delta D \qquad (4.20)$$

When the power goes up i.e. $(dP > 0)$, the perturbation keeps going in the same direction; when it goes down, the direction flips. In other words, when $dP > 0$ and $dV > 0$, D_{old} will decrease. Either, if $dP < 0$ and $dV > 0$, D_{old} will decrease else D_{old} will increase.

Although this method is straightforward and efficient, it may face difficulty with the ever-changing environmental circumstances, which could result in inefficiencies.

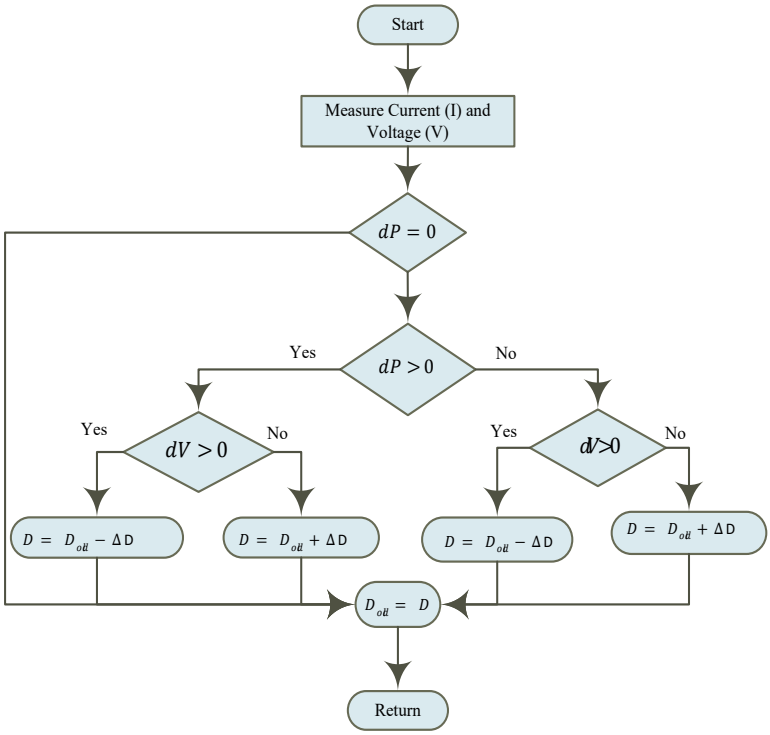


Fig. 4.4. Flowchart: Conventional P&O MPPT algorithm

4.3.2. Conventional INC MPPT Algorithm

Conventional incremental conductance (INC) (Alaas et al., 2023) can ascertain the distance to the MPP and locate the real operating point in relation to it. It surpasses the P&O since it can also cease perturbation upon reaching the MPP. INC outperforms P&O in tracking rapidly changing irradiance. To enhance tracking accuracy and dynamic performance in different environments, INC is suggested. Fig. 4.5 illustrates the corresponding flowchart.

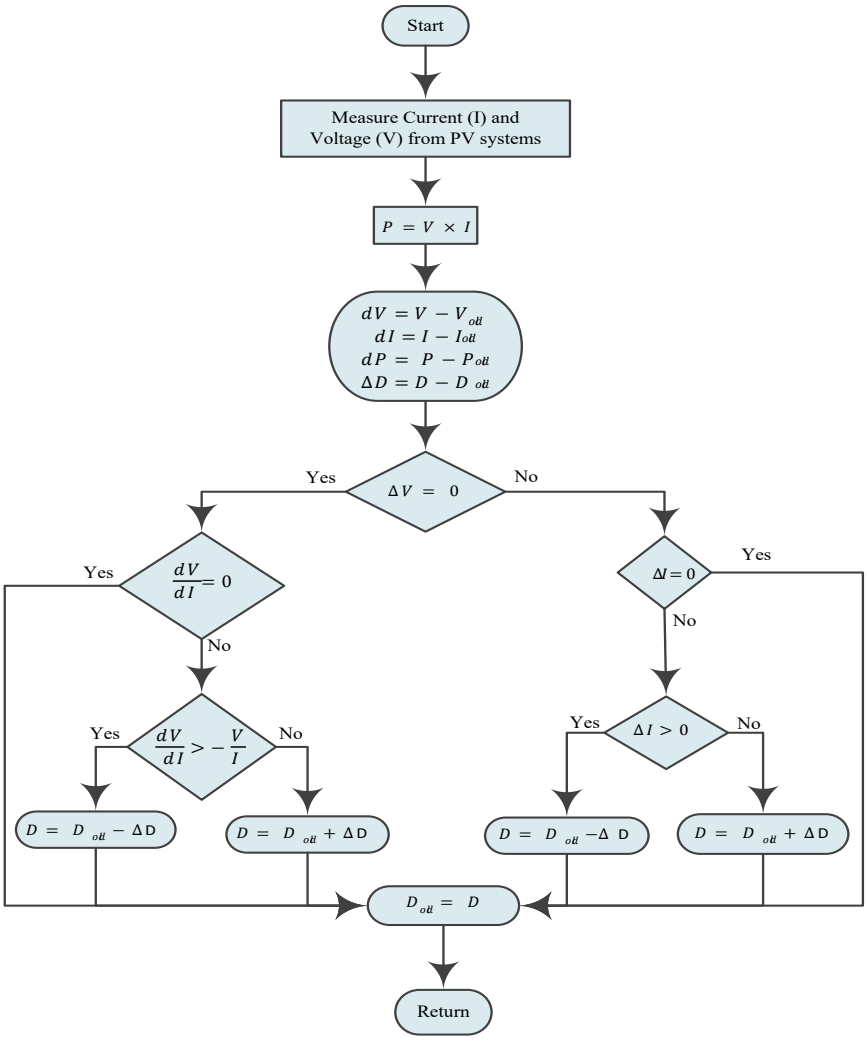


Fig. 4.5. Flowchart: Conventional INC MPPT algorithm

To obtain the optimal duty cycle (D), it compares the change in current over voltage $\left(\frac{dV}{dI}\right)$ to the instantaneous conductance $\left(\frac{V}{I}\right)$ and then makes perturbations based on the results. The duty cycle (D) will be optimized on the basis of $\frac{dV}{dI} > -\frac{V}{I}$, D will decrease else D will increase. Else if $1 + \frac{\Delta I}{\Delta V}$ <0, D will either drop or grow.

The algorithm outperforms the P&O technique, particularly in dynamic weather situations, by effectively tracking quick changes in irradiance. Its complexity, meanwhile, can make its implementation a bit hard.

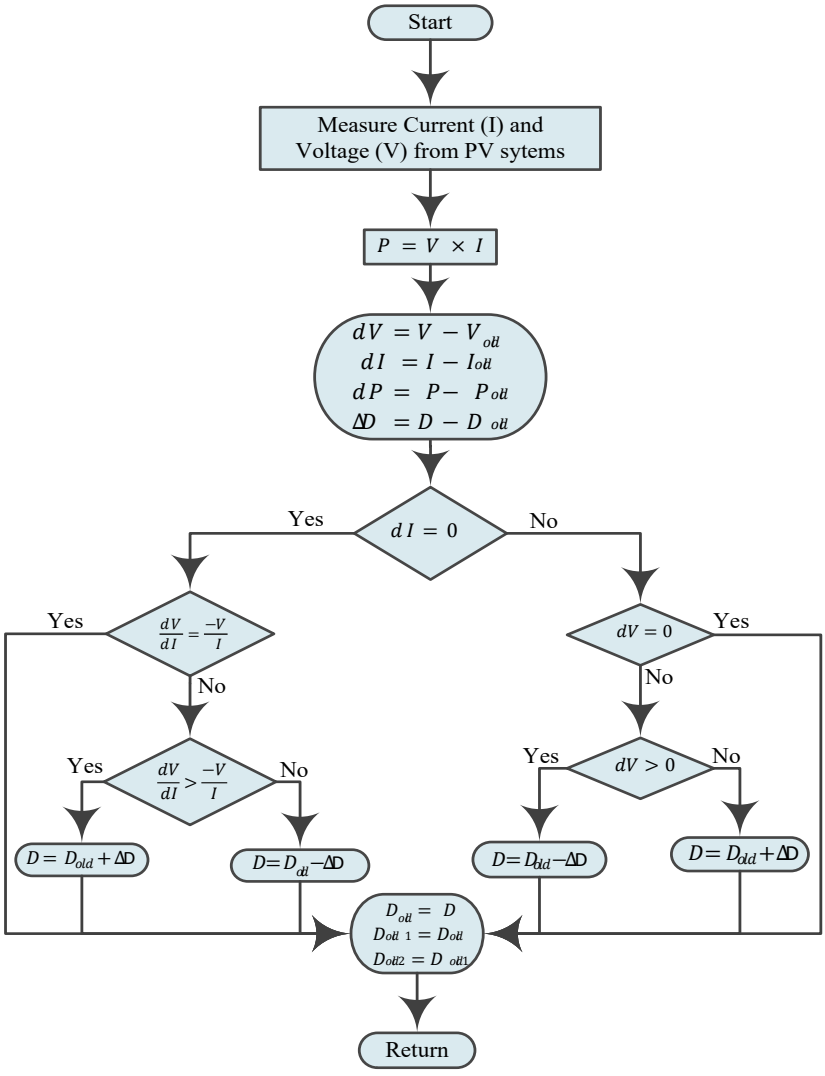


Fig. 4.6. Flowchart: Conventional INR MPPT algorithm

4.3.3. Conventional INR MPPT Algorithm

The conventional incremental resistance (INR) algorithm (Sarang et al., 2024) can track MPP and as compared with INC, the tracking accuracy could be better. The P&O method is the most used MPPT algorithm because of its simplicity and genericity. See Fig. 4.6 for the flowchart. This method works on current control strategy.

The duty cycle is optimized by using Eq. (4.21).

$$\frac{dV}{dI} = -\frac{V}{I} \tag{4.21}$$

Compare the derivative of current to voltage to discover the result. If Eq. (4.21) is greater than 0 then D will decrement else D will increment. To keep everything running well in all kinds of weather, the program tweaks the operating point until it hits maximum power. Because of its quick response to changes in irradiance, this approach is favoured.

Conventional MPPT algorithms have slow response and suffer from wrong tracking directions. So, advance adaptive versions of P&O, INC, and INR algorithms (Jately & Arora, 2017; Tella et al., 2024) have been designed and implemented to tackle these challenges. Adaptive versions of MPPT algorithms can track MPP speedily compared to conventional MPPT algorithms but are prone to drift issues. So, drift-free P&O algorithm is analysed to address this issue. This technique is discussed thoroughly in next sub-section (Killi & Samanta, 2015). Moreover, an adaptive voltage perturbation based MPPT technique is developed and realized in detail in below mentioned sub-section.

4.3.4. Adaptive P&O MPPT Algorithm

The adaptive P&O MPPT algorithm (Jately & Arora, 2017) adjusts the operating point by altering voltage and measuring power output. See Fig. 4.7 for the flowchart. The procedure stays the same when power (P) increases and

reverses when power lowers. The adaptive version automatically modifies perturbation step size based on system response to improve MPP tracking speed and accuracy. It constantly readjusts the operating point by adjusting the voltage and watching the power change (dP) that comes from it. It changes the perturbation size (ΔD), which improves efficiency and speeds convergence in different environmental situations compared to the classic version. As a result, the performance of PV system in enhanced.

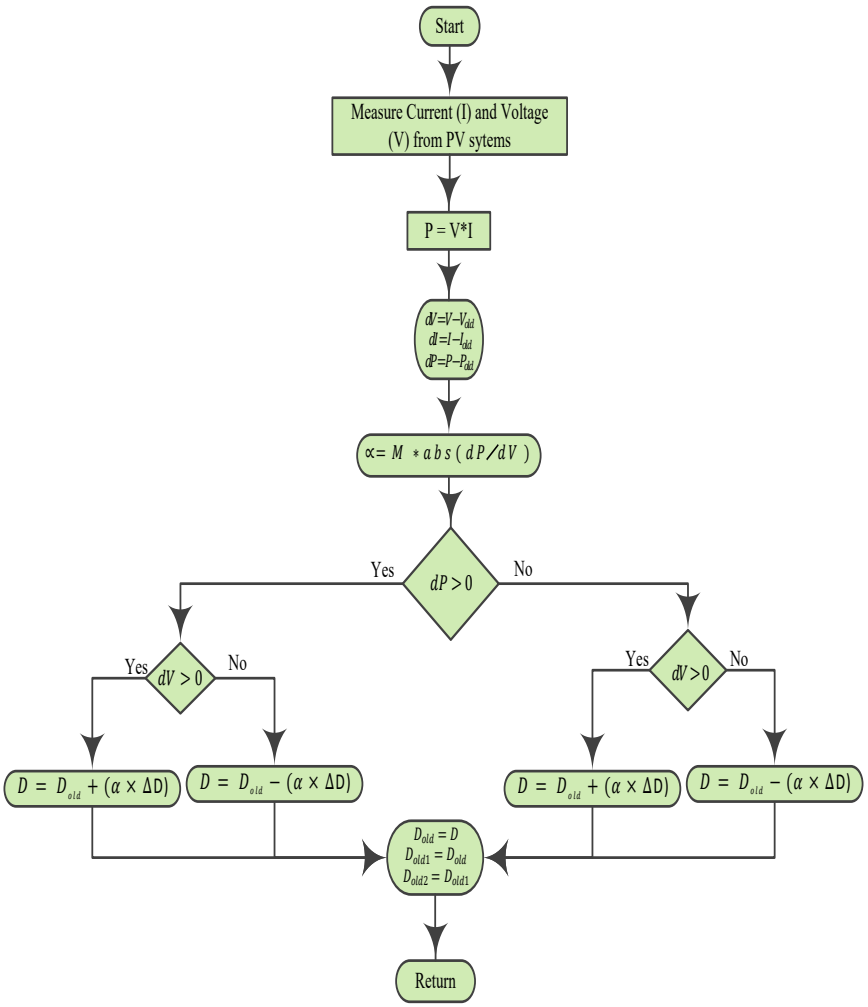


Fig. 4.**7.** Flowchart: Adaptive P&O MPPT algorithm

4.3.5. Adaptive INC MPPT Algorithm

An improved variant of INC technique, the Adaptive INC MPPT algorithm (Jately & Arora, 2017) maximizes energy harvesting in photovoltaic systems. It fine-tunes the operating point to maximize power extraction in response to changing external factors like temperature and irradiance. The flowchart of the same is illustrated in Fig. 4.8. The technique tracks faster and more accurately than INC approaches in real time. Because of its versatility, it works well in the face of ever-changing solar circumstances.

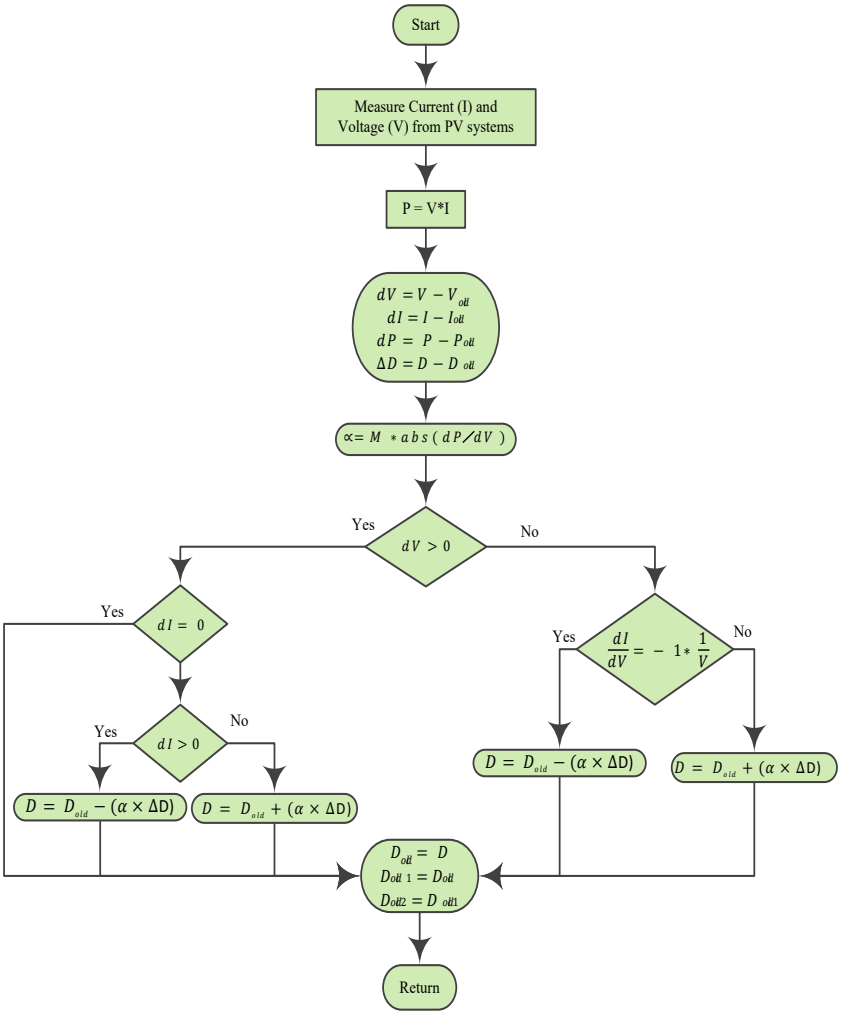


Fig. 4.8. Flowchart: Adaptive INC MPPT algorithm

4.3.6. Adaptive INR MPPT Algorithm

Adaptive version of INR MPPT algorithm (Tella et al., 2024) calculates the duty cycle (D) by dynamically adjusting ΔD (change in D by its perturbation D_{old}). It improves the system's capacity to swiftly and precisely track MPP by integrating incremental conductance with real-time response to changing environmental conditions. This results in enhanced performance and energy efficiency even when solar irradiance and temperature are changing at a rapid pace. When applied to solar energy systems, the algorithm works satisfactorily. The flowchart of the same is illustrated in Fig. 4.9.

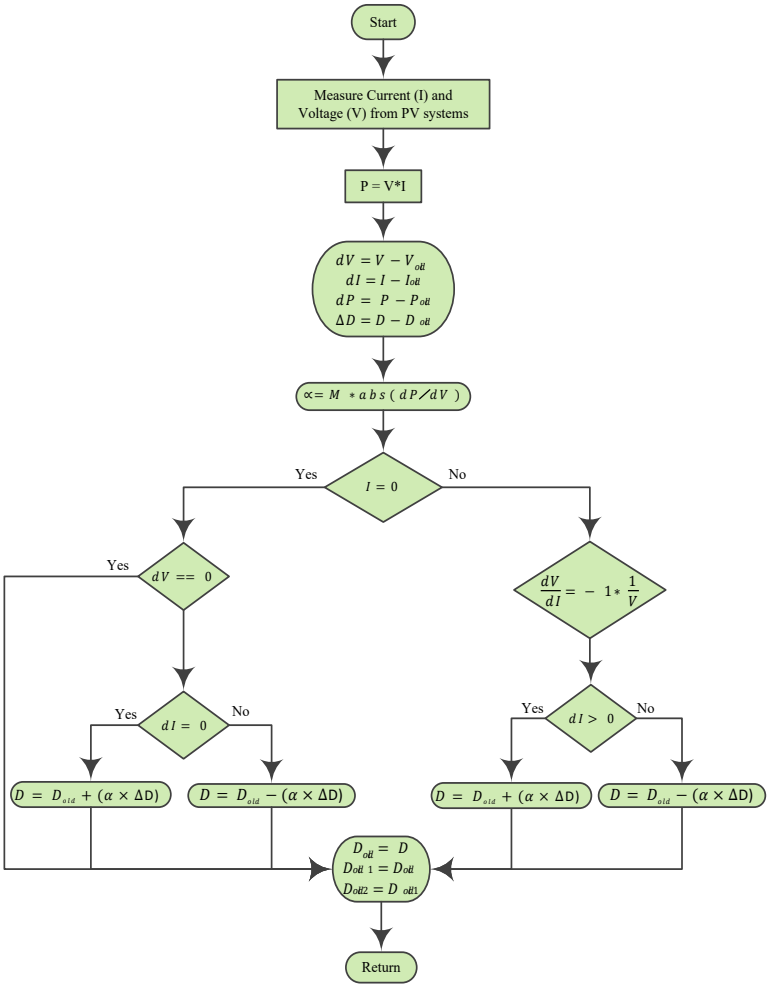


Fig. 4.9. Flowchart: Adaptive INR MPPT algorithm

4.3.7. Drift-free P&O MPPT Algorithm

The drift-free P&O method (Killi & Samanta, 2015) outperforms adaptive and traditional MPPT algorithms. It corrects for drifting away from the MPP induced by quick environmental changes, eliminating power oscillations at that point. As a result, solar energy conversion becomes more efficient and tracking becomes more precise. With its consistent and dependable performance, the algorithm performs well in dynamic settings.

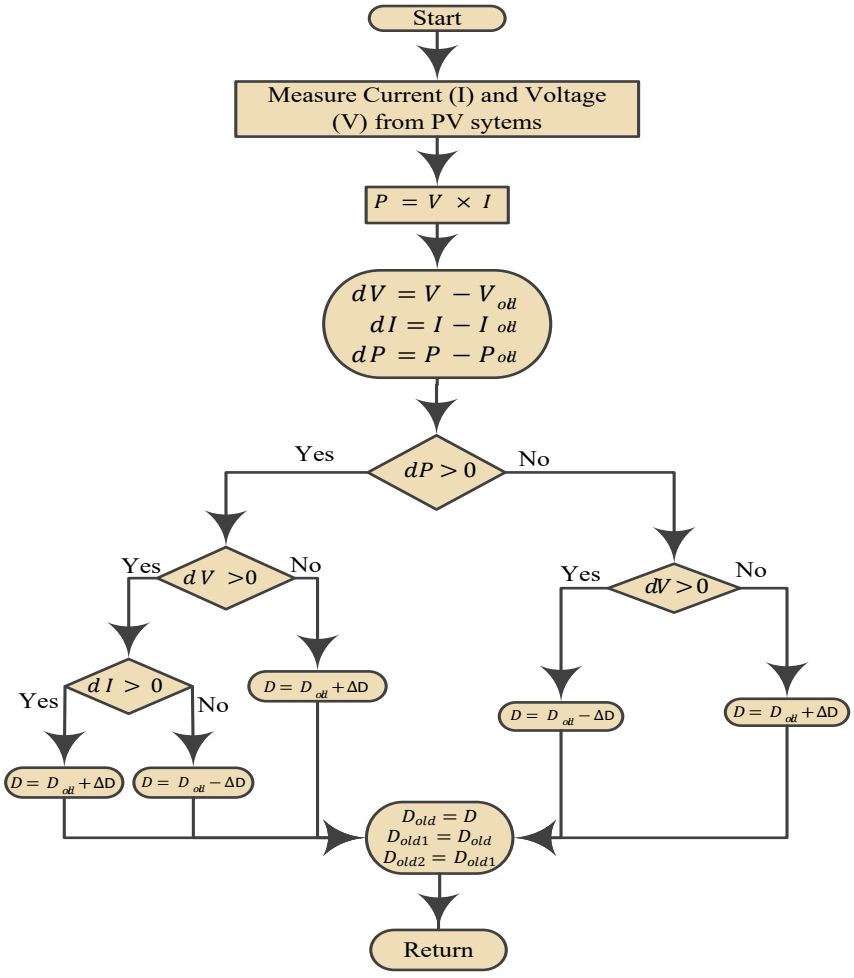


Fig. 4.10. Flowchart: Drift-free P&O MPPT algorithm

Fig. 4.10 displays the corresponding flowchart. It uses a power control approach as its foundation. Calculating the change in voltage (dV), change in current (dI), and change in power (dP) optimizes the duty cycle (D). The

mathematical conditions for it are: If dP > 0, dV > 0 and dI > 0 then D will increment by ΔD else D will decrement. D is evaluated by using multiple perturbations. This technique helps in avoiding drift and increase the speed of tracking, but response time is comparatively high.

4.3.8. Multisampling P&O MPPT Algorithm

This section explains the multisampling P&O based MPPT algorithm (Escobar et al., 2017). The algorithm works on the voltage perturbation control strategy.

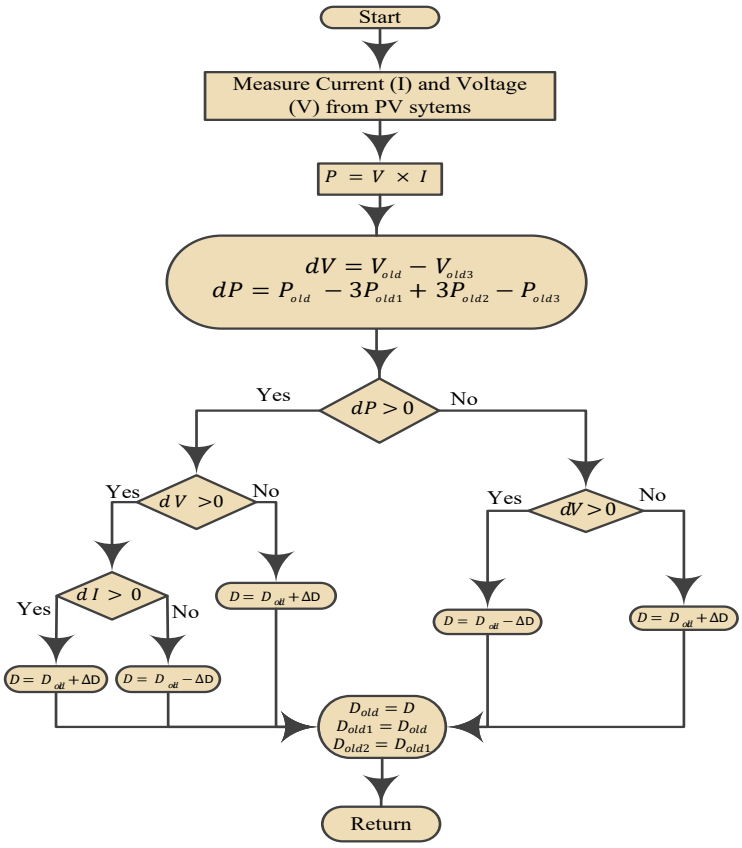


Fig. 4.11. Flowchart: Multisampling MPPT algorithm

The multisampling P&O MPPT algorithm flowchart is displayed in Fig. 4.11. This technique achieves reduced steady-state oscillations by using numerous iterations.

4.4.Proposed MPPT Algorithm

This section comprises of the details of proposed MPPT algorithms. Two algorithms have been proposed namely adaptive voltage perturbation-based and dual perturbation-based MPPT algorithms respectively. The detailed explanation is mentioned in below mentioned subsections.

4.4.1. Adaptive Voltage perturbation based MPPT Algorithm

This section describes the adaptive perturbation-based MPPT algorithm. The algorithm works on the voltage perturbation control strategy. Fig. 4.12 shows the current Vs voltage (I-V) and power vs voltage (P-V) response curves for the proposed MPPT algorithm.

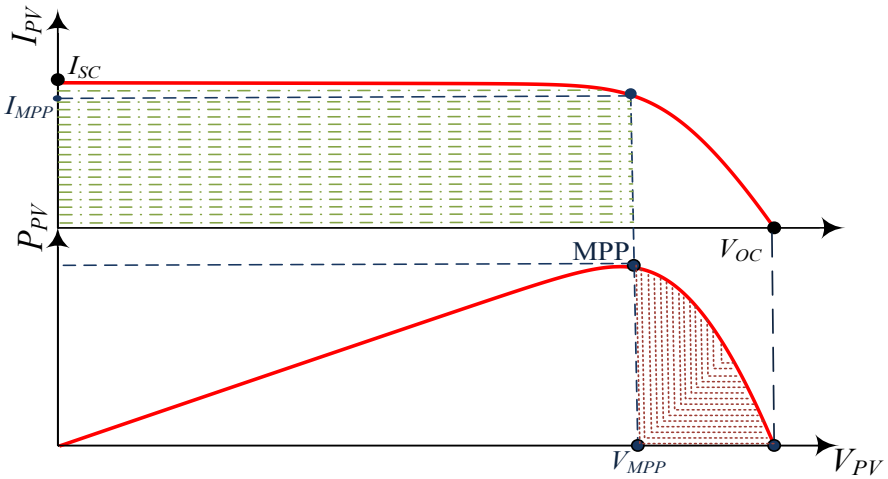


Fig. 4.12. I-V and P-V curves with shaded region under STC

The shaded region represents the area under the curve. It has been reflected that the green coloured-shaded area is larger than the red-coloured-shaded area. The operating region of the proposed algorithm will lie in a red coloured area (i.e. voltage perturbation-based algorithm), and either the slope $\left(\frac{dP}{dV} > 0\right)$ of the curve lies on the left or right side of the trail. This area will operate on voltage control strategy.

The hill-climbing method relies on a control mechanism based on voltage perturbations. The proposed method will always climb in the MPP direction at the left trail of the slope; either the MPP point lies on the left or right side of the P-V curve. Based on Eq. (4.22) & Eq. (4.23), the operating region is calculated as mentioned below:

$$V_{OC} \approx \frac{S}{S_{nom}} I_{SC}(S_{nom}, T_{nom})\, k_A \approx m_S \qquad (4.22)$$

where, $m = \frac{I_{SC}\,(S_{nom}, T_{nom})\, k_A}{S_{nom}}$,

$$V_{ref} = V_{PV}(k) + (\text{sign}\,(V_{PV}(k) - V_{PV}(k-1)) \times \text{sign}(\Delta P_{PV}) \times \Delta I(k) \quad (4.23)$$

Where $V_{PV}(k)$ is the next perturbation PV voltage and $V_{PV}(k-1)$ is an initial perturbation of PV voltage, ΔP_{PV} is the change in the PV power between two perturbation steps ($\Delta P_{PV} = P_{PV}(k) - P_{PV}(k-1)$) and $\Delta I(k)$ is the change in the current perturbation steps.

The flowchart for the suggested adaptive perturbation-based MPPT algorithm is displayed in Fig. 4.13. The performance parameters like voltage (V_{PV}), current (I_{PV}) and power (P_{PV}), as well as V_{OC} and J_{SC} are determined. Then, the area of operation is estimated to be the operating region. The operating limit is calculated based on the adaptive control mode; it will decide the operating region. This will ensure that the proposed algorithm will continuously operate on the left side of the P-V curve.

The proposed voltage perturbation-based hill climbing MPPT technique will start operating on the left trail of the P-V curve. Multiple voltage perturbations are utilized to track MPP speedily. If $dP > 0$, then $dV > 0$, so the voltage will increase by ΔV. Else, the voltage will decrease by ΔV. If $dP > 0$ is not true, then $dV > 0$, the voltage will increase. Otherwise, the voltage will decrease. This method is used to perturb voltage (V_{PV}) and track in right direction of PV trail while avoiding drift.

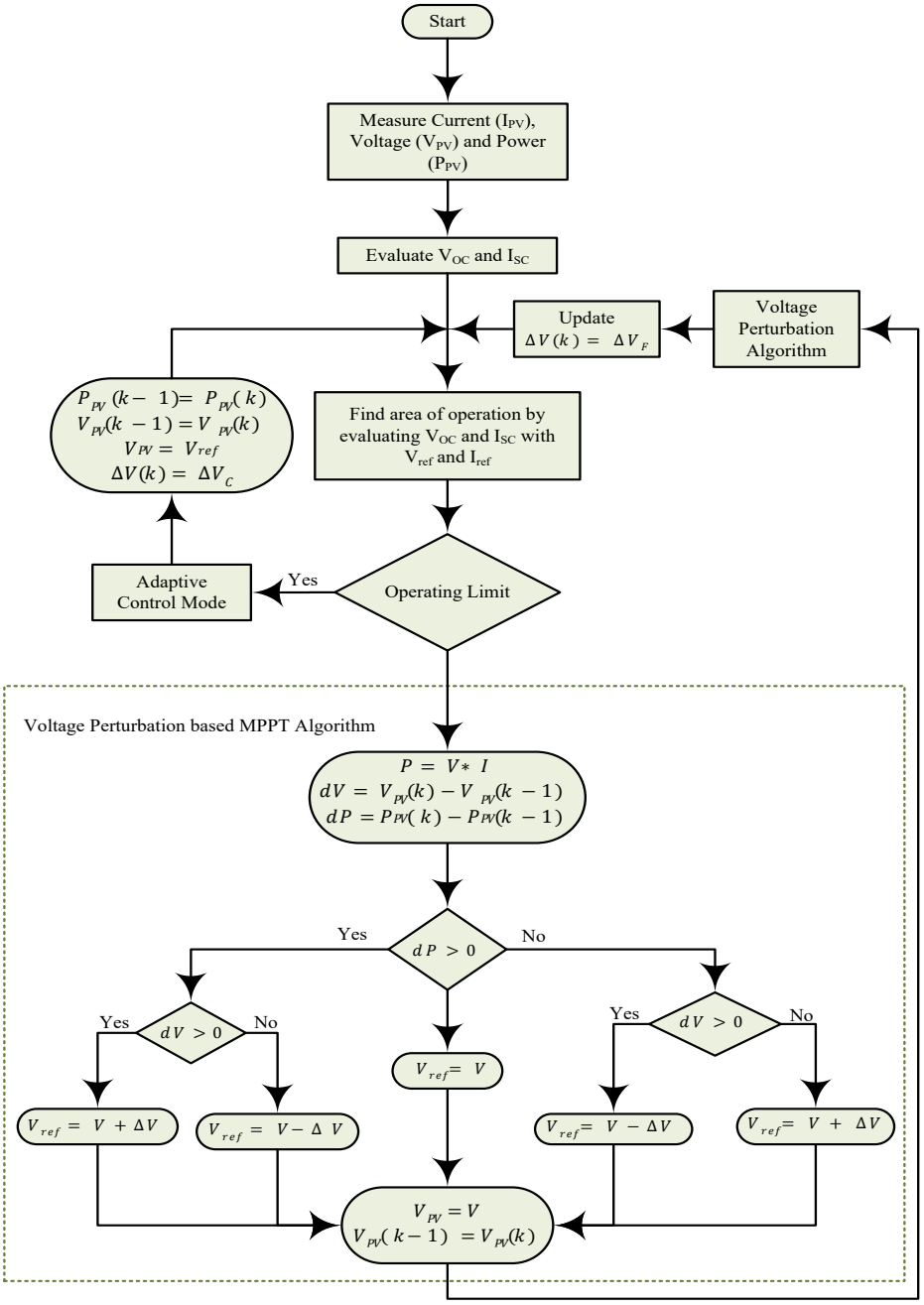


Fig. 4.13. Flowchart of Proposed adaptive voltage perturbation-based MPPT algorithm

4.4.2. Dual perturbation based MPPT Algorithm

A new method for quick MPPT is presented under the section on suggested algorithms to reduce drift in PV systems subjected to variations in

dynamic irradiance. The program quickly adjusts the operating point using complex control techniques and real-time data processing to ensure optimal power extraction. Adaptive perturbation approaches and dynamic tracking mechanisms are some of the design aspects of the algorithm, which are explained in detail. When compared to more conventional approaches, the results show that the algorithm significantly improves stability while decreasing oscillations. Discussions also include the algorithm's adaptability to different environments and its capacity to scale, which lays the groundwork for future developments in MPPT technology. The suggested method is an extension of the P&O algorithm in its most fundamental form. This algorithm's design makes use of a voltage and current control method.

A schematic diagram is presented in Fig. 4.14 which shows the workflow of the dual perturbation new method for proposed algorithm. If $\frac{dP}{dV} > 0$, then current based perturbation algorithm will operate and reference current (I_{ref}) will be evaluated from the same. Else voltage perturbation-based algorithm will operate to evaluate reference voltage (V_{ref}) out of this. On this calculation the algorithm will modify the voltage and current.

The proposed flowchart is shown in Fig. 4.15. To achieve precise computations, the suggested approach employs several perturbations. Because of this technique, the algorithm is both quick and simple.

Initially, the PV panel's current (I)and voltage (V) are monitored. The PV panels' maximum available power (P) is determined: $P = V \times I$. A multisampling iteration method is used to improve the accuracy of the proposed algorithm. The initial power (P_{old}) for the initial iteration is calculated as $P_{old} = V_{old} \times I_{old}$ where V_{old} and I_{old} is the voltage and current of initial iteration. For the next iteration, the power is named, and current and voltage values are V_{old1} and I_{old1}, respectively, determined by using$P_{old1} = V_{old1} \times I_{old1}$. In the final

iteration, the power is determined by using $P_{old2} = V_{old2} \times I_{old2}$, where the values of current, voltage and power are named as I_{old2}, V_{old2}, and P_{old2}, respectively. The change in voltage is taken as $dV = V - V_{old2}$, and $dI = I - I_{old2}$ is used to realize the change in current. While the change in power is evaluated using Eq. (4.24) as,

$$dP = P - 3 \times P_{old} + 3 \times P_{old1} - P_{old2} \qquad (4.24)$$

If the change in power and change is current, i.e., $\frac{dP}{dV} > 0$, then (the algorithm will operate on the left trail of the P-V curve) it will check either $dP > 0$. If this condition is satisfied, it calculates whether is $dV > 0$. If it's true, then reference the current (I_{ref}) will decrease; else, I_{ref} will increase. If $dV > 0$ is not true, then I_{ref} will increase and if this condition is true, then I_{ref} will decrease. When $\frac{dP}{dV} > 0$ is not true (the algorithm will operate on the right trail of the P-V curve), then it will again check whether $dP > 0$ is true or not. If this condition is true, it will be determined as per $dV > 0$. If this condition is true, then V_{ref} will increase; else, V_{ref} will decrease. ΔI and ΔV are initially taken as 15% and 30% for the proposed algorithm. The below-mentioned equations Eq. (4.25)- (4.26) are used to calculate the maximum step-size ΔI (perturbation step of current) and ΔV (perturbation step of voltage), respectively, where N_p and N_s are the number of modules connected in parallel and series, respectively. If $dP > 0$ is not true, it will be whether dV>0 is true. If this is true, then V_{ref} will increase and if this condition is false, then V_{ref} will decrease as,

$$\Delta I_{max} = \frac{\Delta I}{N_p} \qquad (4.25)$$

$$\Delta V_{max} = \frac{\Delta I}{N_p} \qquad (4.26)$$

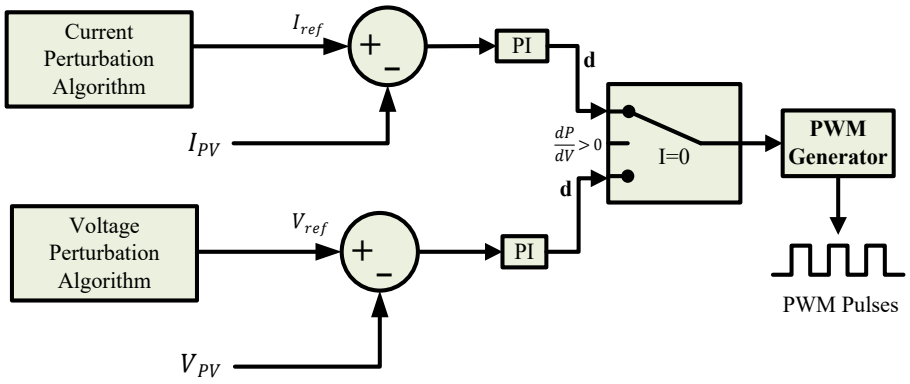


Fig. 4.14. Schematic diagram of the proposed MPPT technique

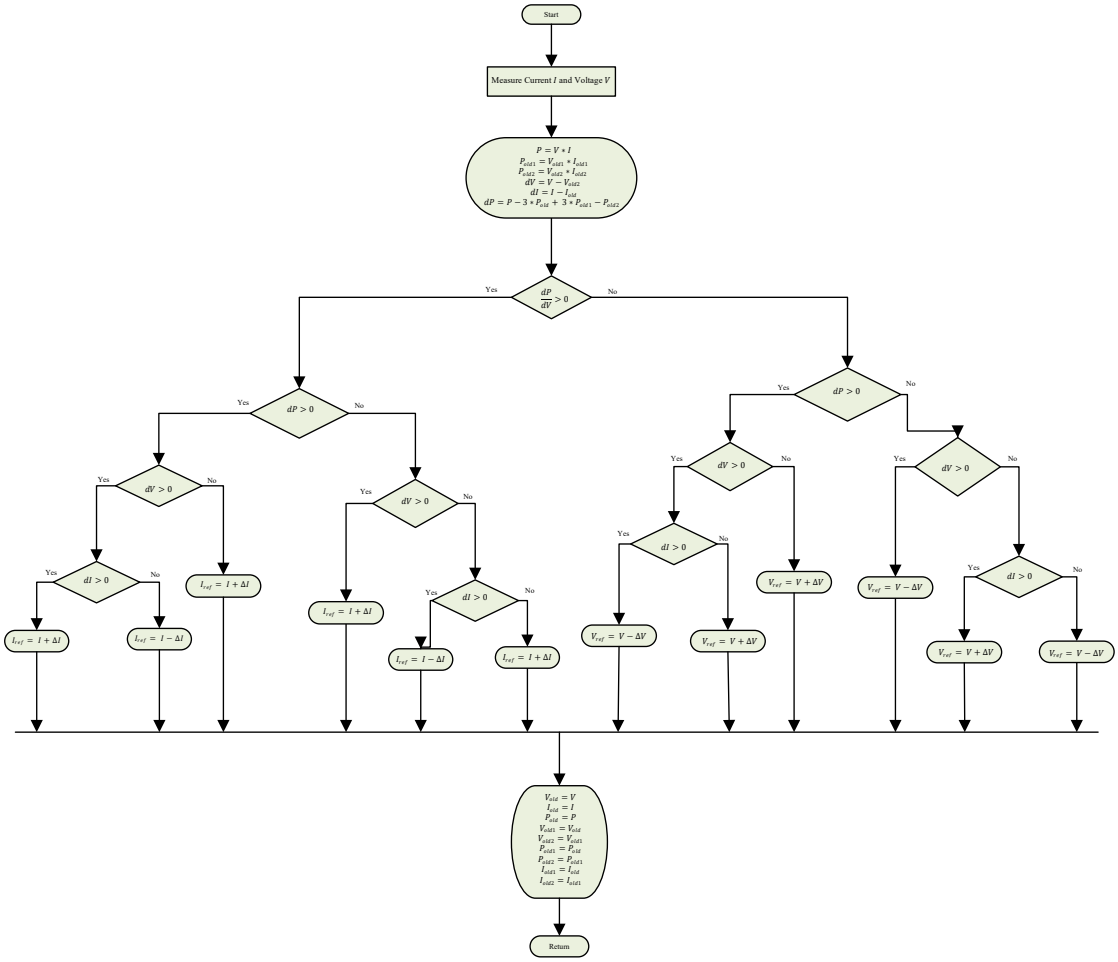


Fig. 4.15. Flowchart: proposed dual perturbation based MPPT technique

4.5.Result and Discussion

The algorithms are evaluated on step increase-in, step decrease-in and standard EN50530 irradiance profile. The detailed analysis is explained in three different subsections namely step increase-in, step decrease-in and EN50530 irradiance profile, respectively.

4.5.1. Step Increase-in Irradiance

A comparative analysis is conducted between state-of-the-art adaptive P&O, INC and INR, drift-free P&O, and multisampling MPPT algorithms and traditional P&O, INC, and INR MPPT algorithms. A voltage perturbation-based and dual-perturbation based MPPT algorithms are proposed and analysed. Fig. 4.16 shows step-increase irradiance assessments. The algorithms use PV parameters including voltage, current, and power.

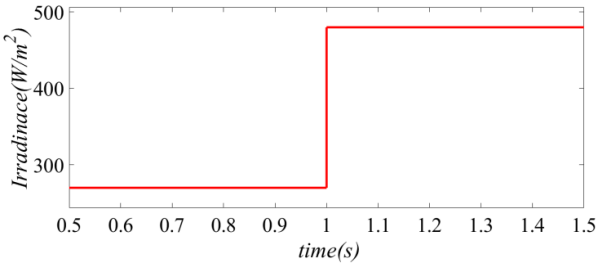


Fig. 4.16. Step increase in irradiance profile

A) Voltage Analysis

This section provides an algorithm-specific breakdown of voltage analysis. With respect to PV voltage, the proposed adaptive voltage perturbation-based and dual perturbation-based MPPT algorithms are implemented, in addition to conventional P&O, INC, and INR MPPT methods, a state-of-the-art adaptive P&O, INC, and INR method, a drift-free P&O and multisampling MPPT method as shown in Fig. 4.17.

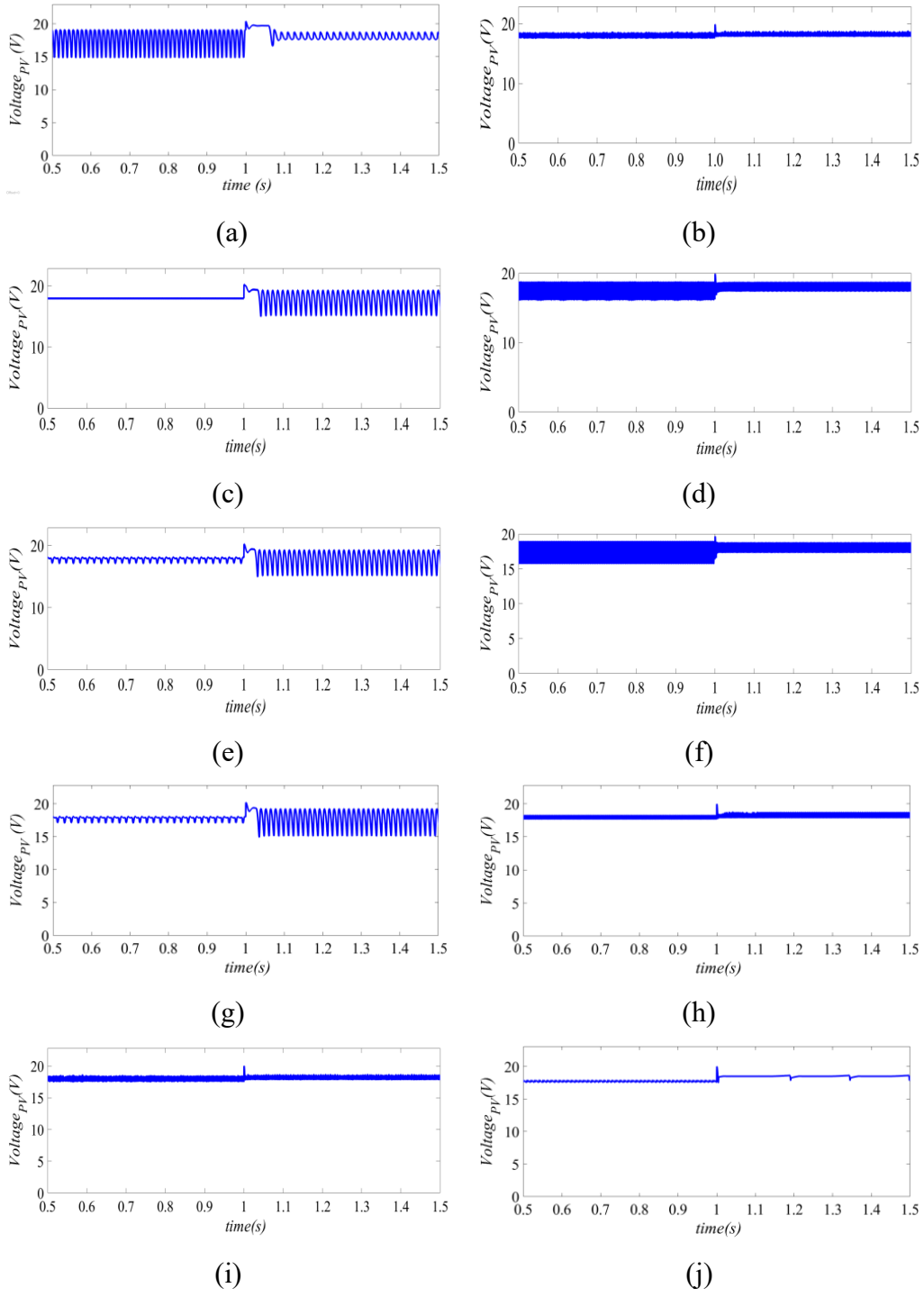


Fig. 4.17. Voltage response for a) P&O, b) Adaptive P&O, c) INC, d) Adaptive INC, e) INR, f) Adaptive INR, g) drift-free P&O, h) multisampling P&O, i) proposed an adaptive voltage perturbation-based (j) proposed dual perturbation based MPPT algorithms

Traditional P&O, INC, and INR methods' steady-state voltage responses are shown in Fig. 4.17 (a), (c) and (e). P&O algorithm surpasses other methods (0.030 s response time and 97.51% success rate), however it has relatively large stead-state oscillations (2.28% at low irradiance and 2.15% at high irradiance). Fig. 4.17 (b), (d), and (f) show the steady-state voltage responses of adaptive versions of the P&O, INC, and INR methods. Compared to other methods, adaptive P&O performs better, with a response time of only 0.028 s, a success rate of 97.35%, and low steady-state oscillations (2.12% at low irradiance and 2.02% at high irradiance, respectively). The voltage response of the drift-free P&O MPPT algorithm, as shown in Fig. 4.17 (g), demonstrates a maximum tracking efficiency of 96.95%, a response time of 0.022s, and low steady-state oscillations. The voltage response of multisampling MPPT algorithm is shown in Fig. 4.17 (h). In addition, Fig. 4.17 (i) shows an MPPT method that is based on adaptive voltage perturbation which shows low steady-state oscillations (i.e. 0.98% at 270W/m^2 and 1.01% at 480W/m^2), 0.012 s response time. An efficiency level of 98.95% in tracking is attained by the proposed approach. Fig. 4.17 (j) shows the dual perturbation based MPPT algorithm which shows the lowest steady-state oscillations (i.e. 0.93% at 270W/m^2 and 0.99% at 480W/m^2), 0.002 s response time and 99.01% tracking efficiency.

B) Current Analysis

In this subsection, the detailed explanation of current analysis corresponds to various algorithms. Conventional P&O, INC and INR MPPT techniques and a state-of-art adaptive P&O, INC and INR techniques, drift-free P&O and multisampling MPPT techniques along with the proposed adaptive voltage perturbation-based and dual perturbation-based MPPT algorithms, are realized in terms of PV current. The pictorial representation of the same is depicted in Fig. 4.18.

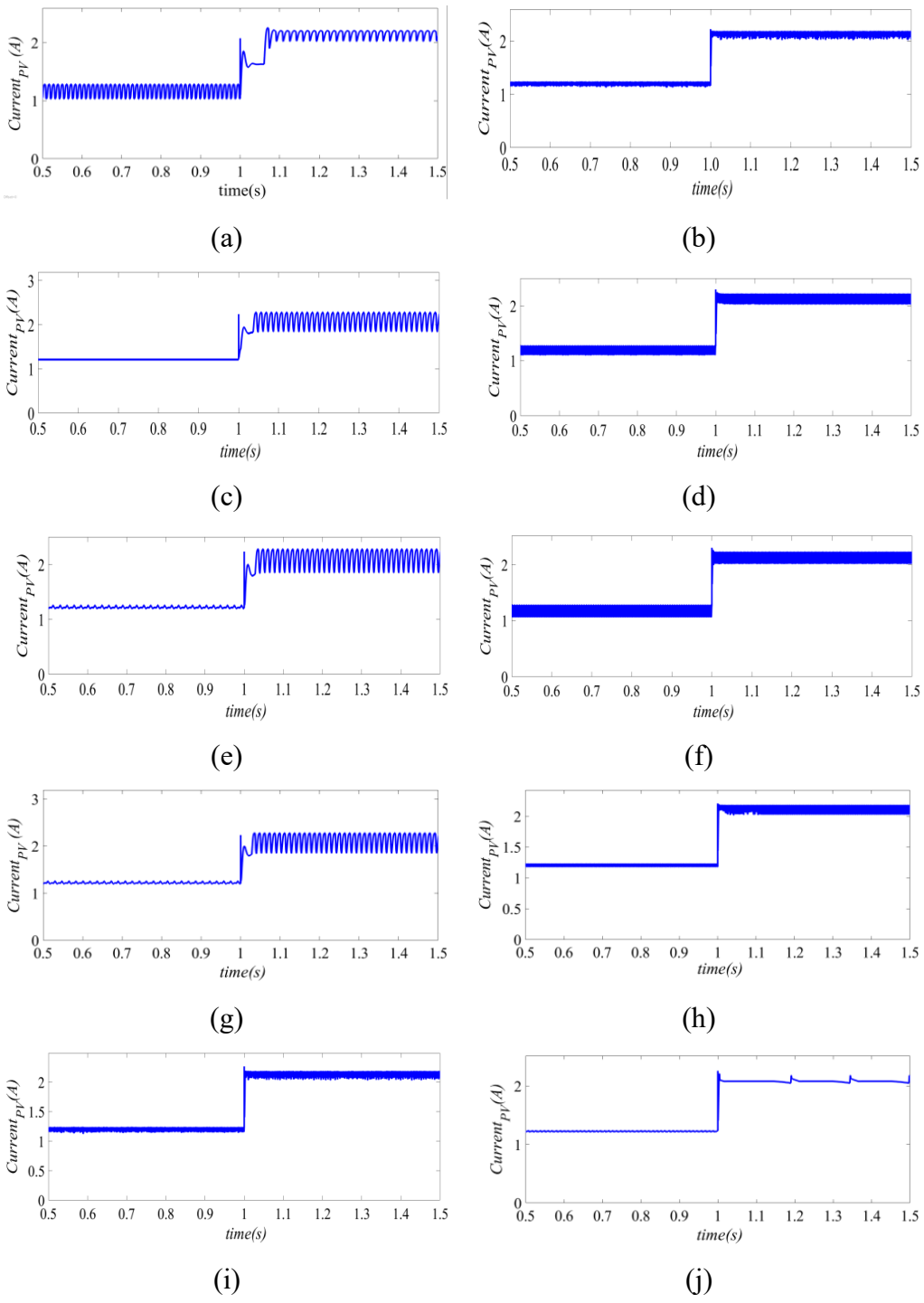


Fig. 4.18. Current response for a) P&O, b) Adaptive P&O, c) INC, d) Adaptive INC, e) INR & f) Adaptive INR, g) drift-free P&O, h) multisampling P&O, i) proposed an adaptive voltage perturbation-based (j) proposed dual perturbation based MPPT algorithms

The steady-state current response for conventional P&O, INC and INR techniques are depicted in Fig. 4.18 (a), (c) & (e). When compared to other techniques, P&O algorithm shows better performance (0.030 s response time and 97.51%) but steady-state oscillations are comparatively high (2.28% at low irradiance and 2.15% at high irradiance). Similarly, steady-state voltage response of adaptive versions of P&O, INC & INR techniques are illustrated in Fig. 4.18 (b), (d) & (f). The adaptive P&O technique shows better performance as compared to other techniques (0.028 s response time and 97.35% efficiency and low steady-state oscillations i.e., 2.12% at low irradiance and 2.02 at high irradiance). As seen in Fig. 4.18 (g), the drift-free P&O MPPT algorithm's voltage response exhibits low steady-state oscillations, a response time of 0.022s, and a maximum tracking efficiency of 96.95%. Fig. 4.18 (h) displays the multisampling MPPT algorithm's voltage response. In addition, Fig. 4.18 (i) shows an MPPT method that is based on adaptive voltage perturbation which shows low steady-state oscillations (i.e. 0.98% at 270W/m^2 and 1.01% at 480W/m^2), 0.012 s response time. An efficiency level of 98.95% in tracking is attained by the proposed approach. Fig. 4.18 (j) shows the dual perturbation based MPPT algorithm which shows the lowest steady-state oscillations (i.e. 0.93% at 270W/m^2 and 0.99% at 480W/m^2), 0.002 s response time and 99.01% tracking efficiency.

C) Power Analysis

Several algorithms are compared with a thorough description of power analysis in this sub-section. With respect to PV power, the suggested adaptive voltage perturbation-based MPPT algorithm is implemented, in addition to conventional P&O, INC, and INR MPPT methods, a state-of-the-art adaptive P&O, INC, and INR method, and a drift-free P&O MPPT method. Fig. 4.19 shows a visual representation of the same.

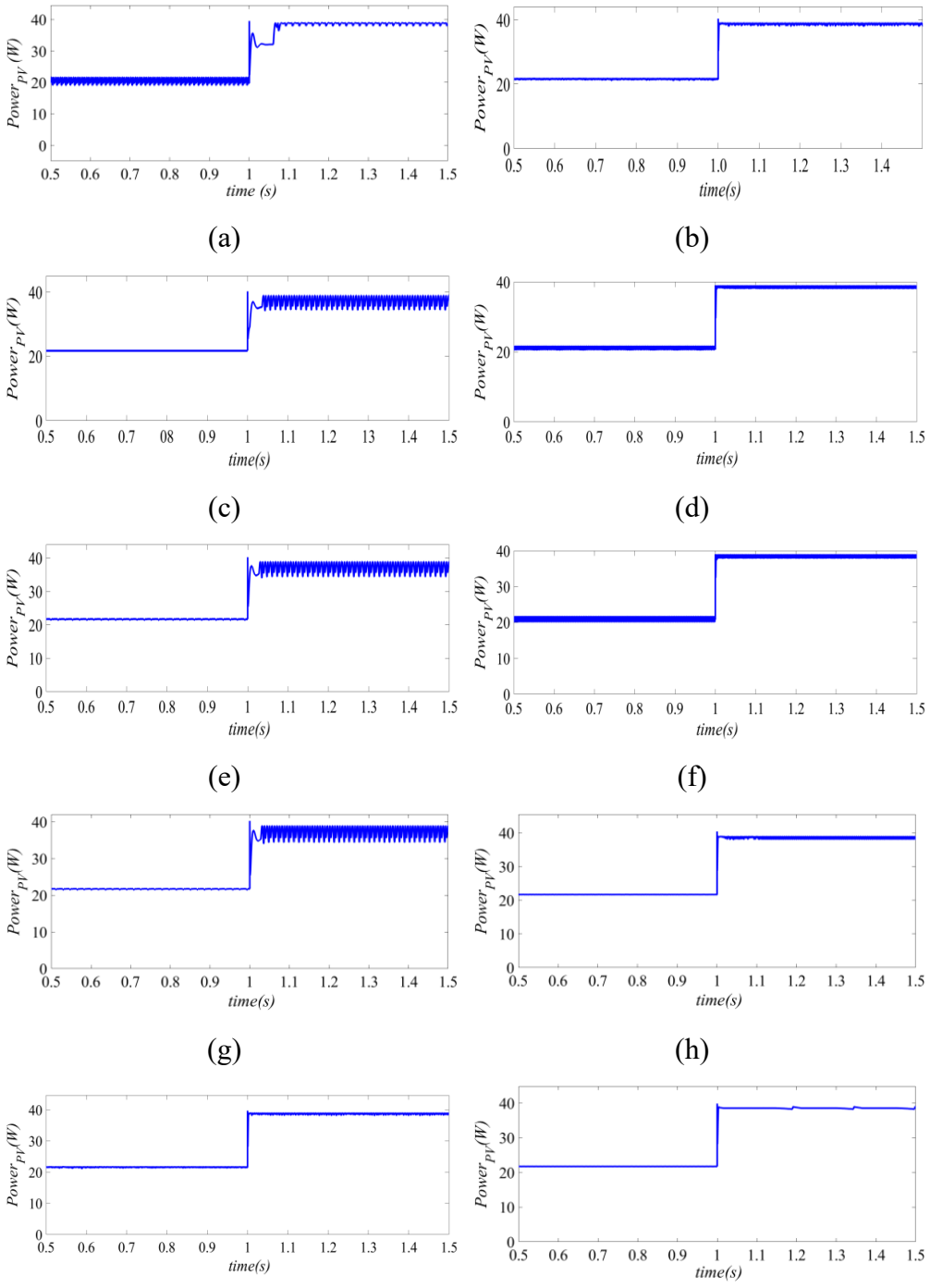


Fig. 4.19. Power response for a) P&O, b) Adaptive P&O, c) INC, d) Adaptive INC, e) INR, f) Adaptive INR, g) drift-free P&O, h) multisampling P&O, i) proposed an adaptive voltage perturbation-based (j) proposed dual perturbation based MPPT algorithms

The steady-state power response for conventional P&O, INC and INR techniques are depicted in Fig. 4.19 (a), (c) & (e). When compared to other techniques, P&O algorithm shows better performance (0.030 s response time and 97.51% efficiency) but steady-state oscillations are comparatively high (2.28% at low irradiance and 2.15 at high irradiance). Similarly, steady-state voltage response of adaptive versions of P&O, INC & INR techniques are illustrated in Fig. 4.19 (b), (d) & (f). The adaptive P&O technique shows better performance as compared to other techniques (0.028 s response time and 97.35% efficiency and low steady-state oscillations i.e., 2.12% at low irradiance and 2.02 at high irradiance). As seen in Fig. 4.19 (g), the drift-free P&O MPPT algorithm's voltage response exhibits low steady-state oscillations, a response time of 0.022s, and a maximum tracking efficiency of 96.95%. Fig. 4.19 (h) displays the multisampling MPPT algorithm's voltage response. In addition, Fig. 4.19 (i) shows an MPPT method that is based on adaptive voltage perturbation The proposed method achieves the maximum tracking efficiency of 98.95%, response time of 0.012s and very low steady-state oscillations (i.e., quantitatively 0.95% and 1.01% at low and high irradiance levels respectively). An efficiency level of 98.95% in tracking is attained by the proposed approach. Fig. 4.19 (j) shows the dual perturbation based MPPT algorithm which shows the lowest steady-state oscillations (i.e. 0.93% at 270W/m^2 and 0.99% at 480W/m^2), 0.002 s response time and 99.01% tracking efficiency.

D) Comparative Analysis

The comparison analysis utilizes photovoltaic factors such as control technique, drift occurrence, parameter tuning, operational region, tracking speed, steady-state oscillations, stability, complexity, cost, and tracking efficiency. The table of taxonomy is as shown in Table 4.3. The quantitative study is performed on the basis of response time and steady-state oscillations. The quantitative values are illustrated in Table 4.4. Similarly, pictorial view of

the same is depicted in Fig. 4.20, 4.21 & 4.22. The significant improvement of 1.44% is realized in tracking efficiency of the proposed adaptive voltage perturbation based MPPT algorithm.

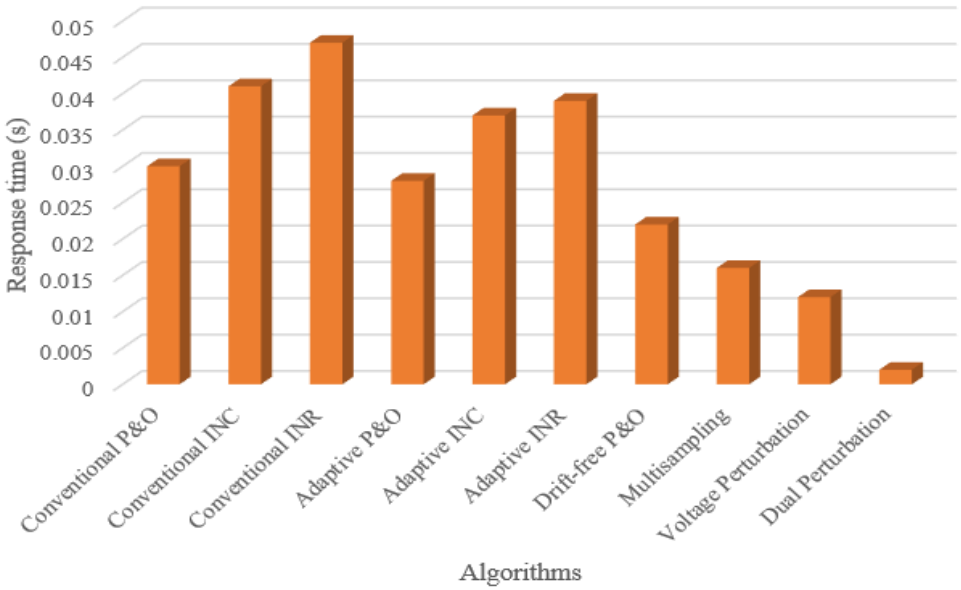


Fig. 4.20. Response time for various algorithms at step increase-in profile

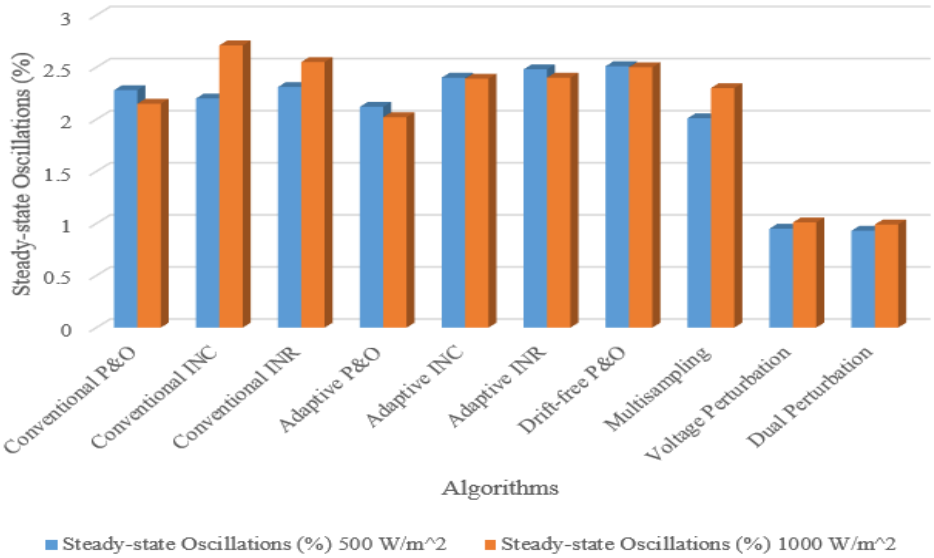


Fig. 4.21. Steady-state oscillations for various algorithms at step increase-in profile

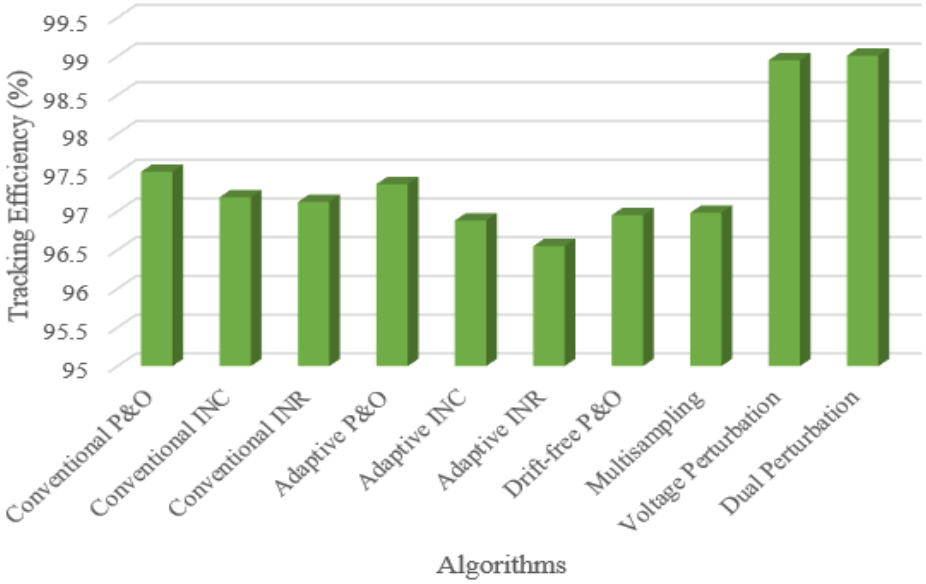


Fig. 4.22. Tracking Efficiency for various algorithms at step increase-in profile

Table 4.3. Table of taxonomy based on comparative analysis for step increase-in irradiance profile

Algorithms	Control Strategy	Drift Occurrence	Parameter Tuning	Operation region	Tracking speed	Steady-state Oscillations	Stability	Complexity	Cost	Tracking Efficiency
Conventional P&O	Power	✓	No	Both	VL	L	L	L	L	L
Conventional INC	Voltage	✓	No	Both	VL	L	VL	H	H	VL
Conventional INR	Current	✓	No	Both	VL	L	VL	H	H	VL
Adaptive P&O	Power	✓	No	Both	VL	L	L	L	L	L
Adaptive INC	Voltage	✓	No	Both	VL	H	VL	H	H	VL
Adaptive INR	Current	✓	No	Both	VL	H	VL	H	H	VL
Drift-free P&O	Power	×	Yes	Both	L	L	L	L	L	L
Multisampling	Power	×	Yes	Both	L	L	L	H	H	L
Modified P&O Voltage Perturbation	Voltage	×	Yes	Right	H	VL	H	L	L	H
Dual Perturbation	Dual	×	Yes	Both	H	VL	H	L	L	H

* VL: Very low, L: Low, H: High

Table 4.4. Performance parameters of algorithms at step increase-in irradiance profile

Algorithms	Response-time (s)	Steady-state Oscillations (%)		Tracking Efficiency (%)
		270 W/m^2	480 W/m^2	
Conventional P&O	0.030	2.28	2.15	97.51
Conventional INC	0.041	2.20	2.71	97.18
Conventional INR	0.047	2.31	2.55	97.12
Adaptive P&O	0.028	2.12	2.02	97.35
Adaptive INC	0.037	2.40	2.39	96.88
Adaptive INR	0.039	2.48	2.40	96.55
Drift-free P&O	0.022	2.51	2.50	96.95
Multisampling	0.016	2.01	2.30	96.98
Proposed Voltage Perturbation	0.012	0.95	1.01	98.95
Proposed Dual Perturbation	0.002	0.93	0.99	99.01

4.5.2. Step Decrease-in Irradiance profile Analysis

The evaluation of advanced adaptive P&O, INC, INR, and drift-free P&O MPPT algorithms is done in comparison to classic P&O, INC, and INR MPPT algorithms. A maximum power point tracking method based on voltage perturbations is proposed and assessed. The evaluations are conducted for the step drop in the irradiance profile illustrated in Fig. 4.23.

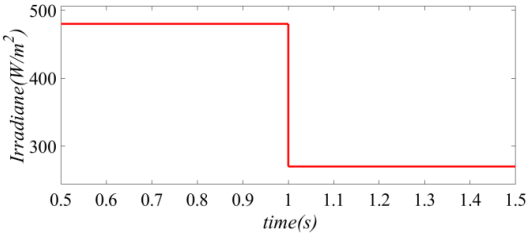


Fig. 4.23. Step decrease in irradiance profile

A) Voltage Analysis

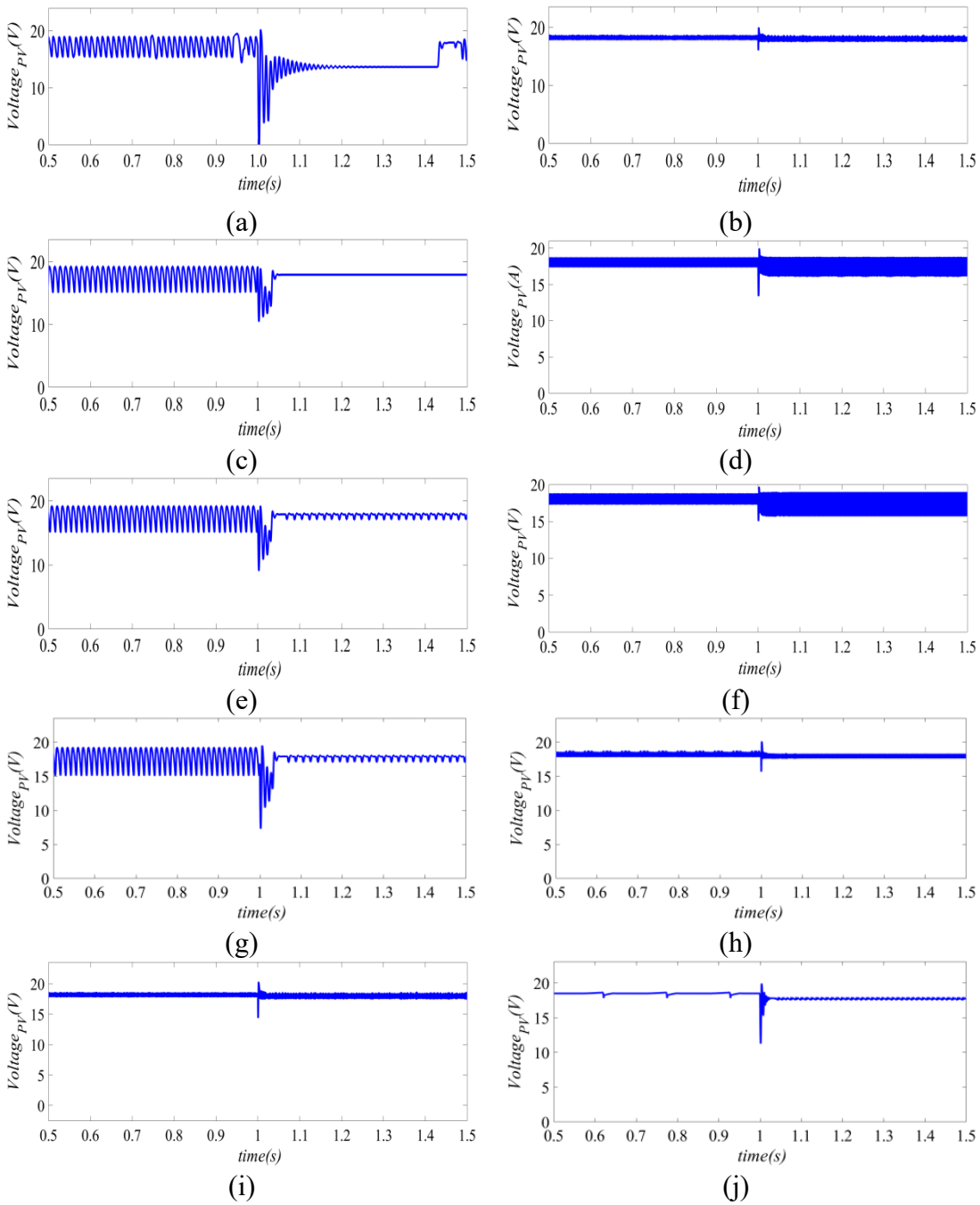


Fig. 4.24. Voltage response for a) P&O, b) Adaptive P&O, c) INC, d) Adaptive INC, e) INR, f) Adaptive INR, g) drift-free P&O, h) multisampling P&O, i) proposed an adaptive voltage perturbation-based (j) proposed dual perturbation based MPPT algorithms

Voltage analysis is defined in detail and performed on several algorithms in this sub-section. The proposed adaptive voltage perturbation-based MPPT method, along with conventional P&O, INC, and INR MPPT techniques, a state-of-the-art adaptive P&O, INC, and INR approach, and a drift-free P&O MPPT technique, are all implemented in terms of PV voltage. Here is a visual illustration of the same in Fig. 4.24. Fig 4.24 (a), (c), and (e) demonstrate steady-state voltage responses for P&O, INC, and INR techniques. Despite large stead-state oscillations (2.30% at low irradiance and 2.52% at high), P&O algorithm outperforms other approaches (0.030 s response time and 97.51% efficiency). The steady-state voltage responses of adaptive P&O, INC, and INR techniques are shown in Fig 4.24 (b), (d), and (f). Its response time of 0.028 s, success rate of 97.35%, and low steady-state oscillations (2.10% at low irradiance and 2.03% at high irradiance) make adaptive P&O better than other approaches. The voltage response of the drift-free P&O MPPT algorithm exhibits minimal steady-state oscillations, a response time of 0.022 s, and a maximum tracking efficiency of 96.95%, as shown in Fig. 4.24 (g). Fig. 4.24 (h) displays the multisampling MPPT algorithm's voltage response. Additionally, Fig. 4.24 (i) displays an adaptive voltage perturbation MPPT approach. The proposed tracking method achieves 98.81% efficiency. Fig. 4.24 (j) shows the dual perturbation based MPPT algorithm which shows the lowest steady-state oscillations (i.e. 0.93% at 270W/m^2 and 0.99% at 480W/m^2), 0.002 s response time and 99.01% tracking efficiency.

B) Current Analysis

This subsection covers current analysis procedures for various algorithms. PV current is used to implement conventional P&O, INC, and INR MPPT approaches, a state-of-the-art adaptive technique, drift-free P&O MPPT technique, and the suggested adaptive voltage perturbation-based MPPT algorithm.

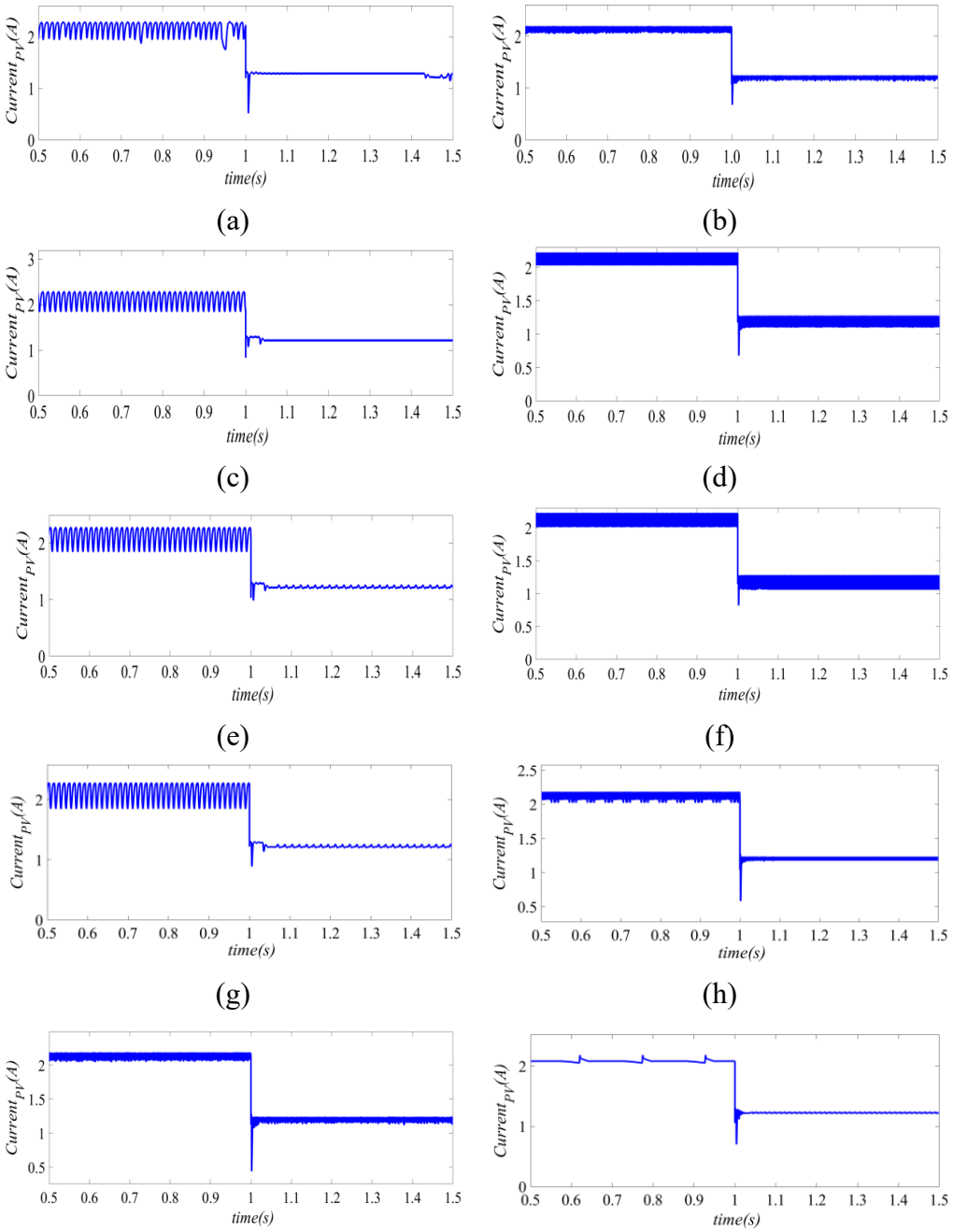


Fig. 4.25. Current response for a) P&O, b) Adaptive P&O, c) INC, d) Adaptive INC, e) INR & f) Adaptive INR, g) drift-free P&O, h) multisampling P&O, i) proposed an adaptive voltage perturbation-based (j) proposed dual perturbation based MPPT algorithms

Fig. 4.25 (a), (c), and (e) show traditional P&O, INC, and INR steady-state current responses. P&O algorithm outperforms others (0.030 s response time and 97.51%), however stead-state oscillations are high (2.30% at low irradiance and 2.52 at high). In Fig. 4.25 (b), (d), and (f), adaptive P&O, INC, and INR approaches show steady-state voltage response. The adaptive P&O technique outperforms others (0.028 s response time, 97.35%, and low steady-state oscillations, 2.10% at low irradiance and 2.03 at high). The drift-free P&O MPPT algorithm voltage response with a maximum efficiency of 96.95%, a reaction time of 0.022 s, and low steady-state oscillations is shown in Fig. 4.25 (g). Fig. 4.25 (h) displays the multisampling MPPT algorithm's voltage response. Additionally, Fig. 4.25 (i) displays an adaptive voltage perturbation MPPT approach. The proposed tracking method achieves 98.81% efficiency. Fig. 4.25 (j) shows the dual perturbation based MPPT algorithm which shows the lowest steady-state oscillations (i.e. 0.93% at 270W/m^2 and 0.99% at 480W/m^2), 0.002 s response time and 99.01% tracking efficiency.

C) Power Analysis

This subsection explains power analysis by utilizing various algorithms. PV power enables standard P&O, INC, and INR MPPT methods, a state-of-the-art adaptive technique, drift-free P&O MPPT, and the recommended adaptive voltage perturbation-based MPPT algorithm. Fig. 4.26 shows it. Traditional P&O, INC, and INR steady-state power responses are shown in Fig. 4.26 (a), (c), and (e). Despite large stead-state oscillations (2.30 at low irradiance and 2.52 at high), P&O algorithm surpasses others (0.030 s response time and 97.51% success rate). In Fig. 4.26 (b), (d), and (f), adaptive P&O, INC, and INR techniques exhibit steady-state voltage response. The adaptive P&O method is best (0.028 s response time, 97.35% efficiency, low steady-state oscillations, 2.10% at low irradiance, 2.03 at high).

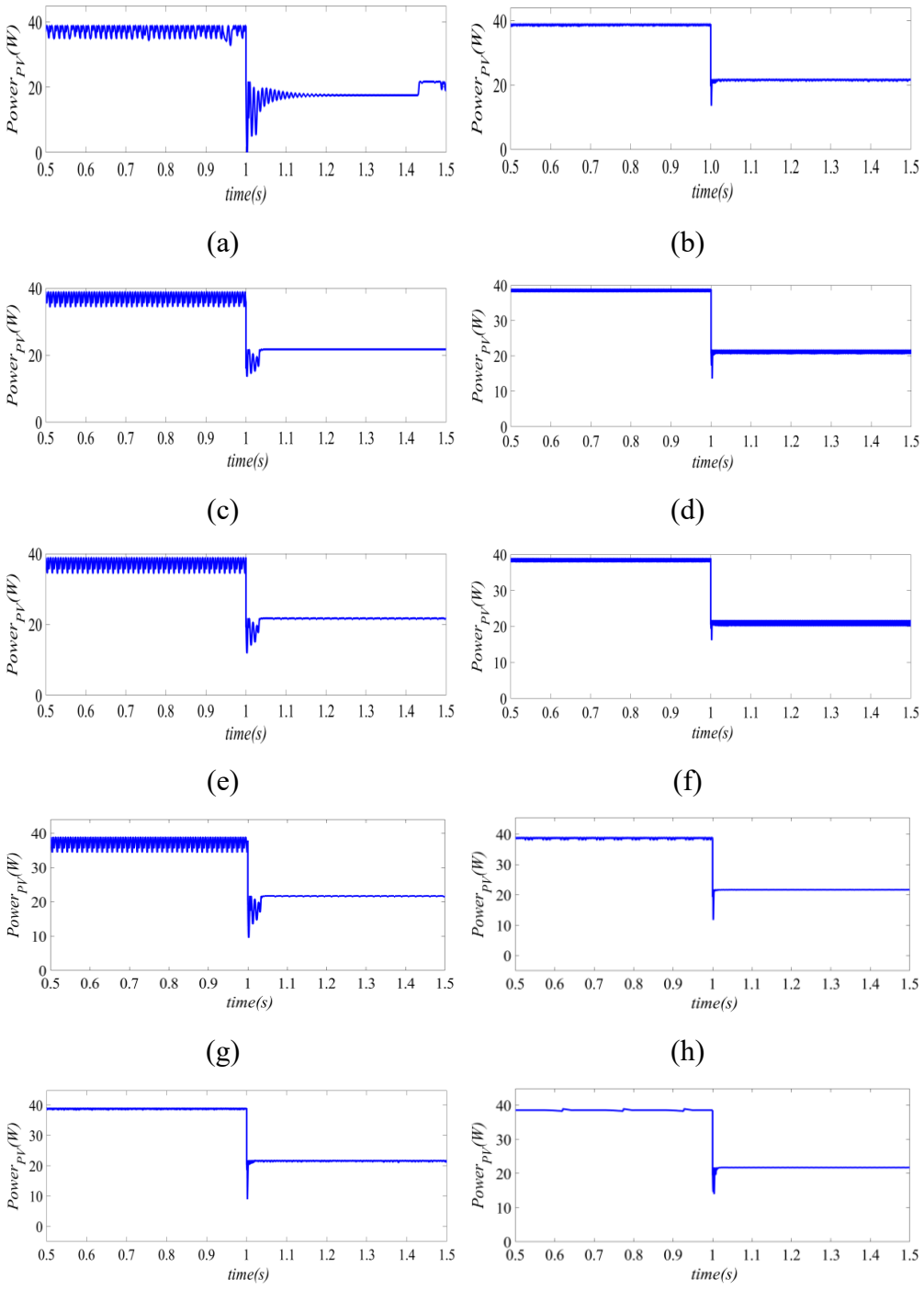


Fig. 4.26. Power response for a) P&O, b) Adaptive P&O, c) INC, d) Adaptive INC, e) INR, f) Adaptive INR, g) drift-free P&O, h) multisampling P&O, i) proposed an adaptive voltage perturbation-based (j) proposed dual perturbation based MPPT algorithms

Drift-free P&O MPPT algorithm voltage response with 96.95% efficiency, 0.022 s response time, and minimal steady-state oscillations is displayed in Fig. 4.26 (g). The voltage response of multisampling MPPT algorithm is shown in Fig. 4.26 (h). MPPT algorithm with adaptive voltage perturbation is shown in Fig. 4.26 (i). The method has a maximum tracking efficacy of 98.81%, response time of 0.012s, and very low steady-state oscillations (0.98% and 1.01% at high and low irradiance). An efficiency level of 98.95% in tracking is attained by the proposed approach. Fig. 4.26 (j) shows the dual perturbation based MPPT algorithm which shows the lowest steady-state oscillations (i.e. 0.93% at 270W/m^2 and 0.99% at 480W/m^2), 0.002s response time and 99.01% tracking efficiency.

D) Comparative Analysis

The following PV parameters are used in the comparative study: control method, drift occurrence, parameter tuning, operating region, tracking speed, steady-state oscillations, stability, complexity, cost, and tracking efficiency. Table 4.5 displays the taxonomy table for the same. Using response time and steady-state oscillations, the quantitative study is carried out.

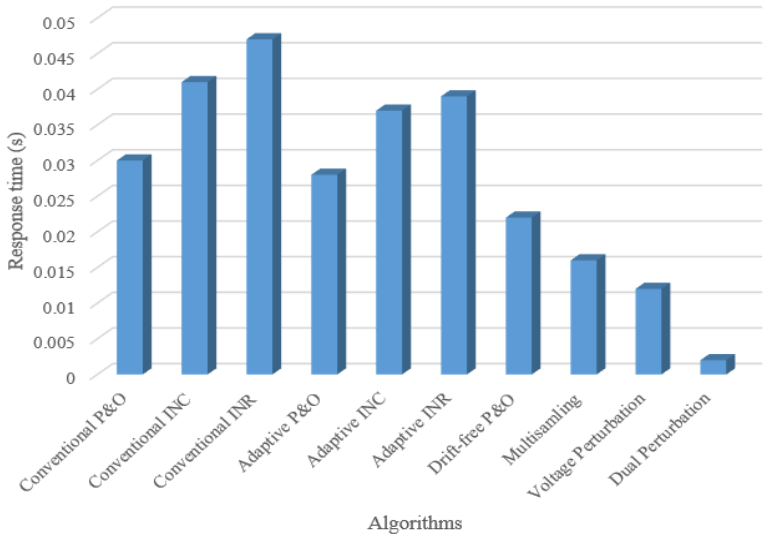


Fig. 4.27. Response time for various algorithms at step decrease-in profile

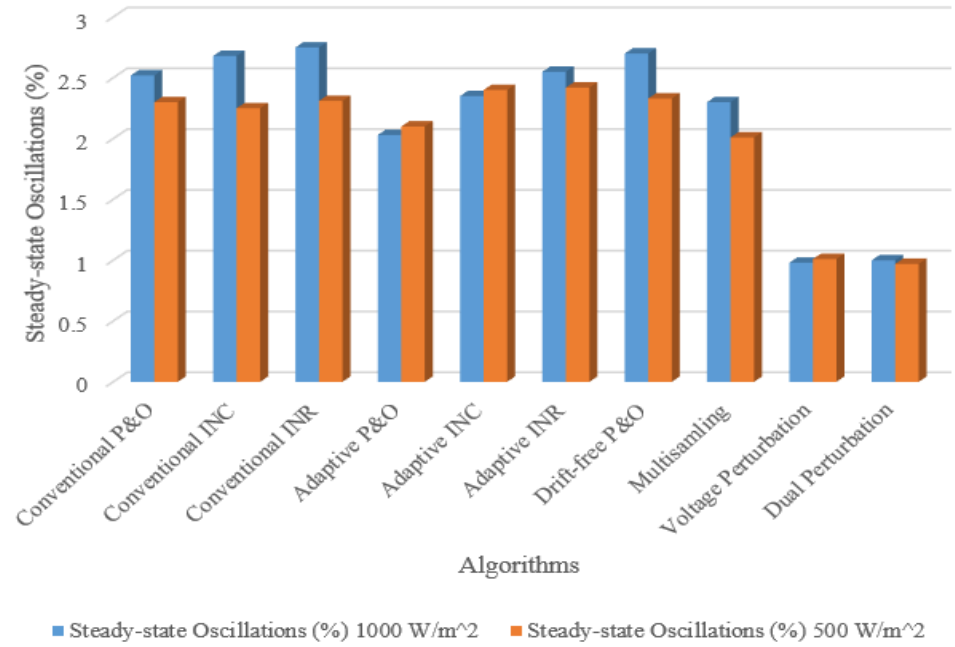


Fig. 4.28. Steady-state oscillations for various algorithms at step decrease-in profile

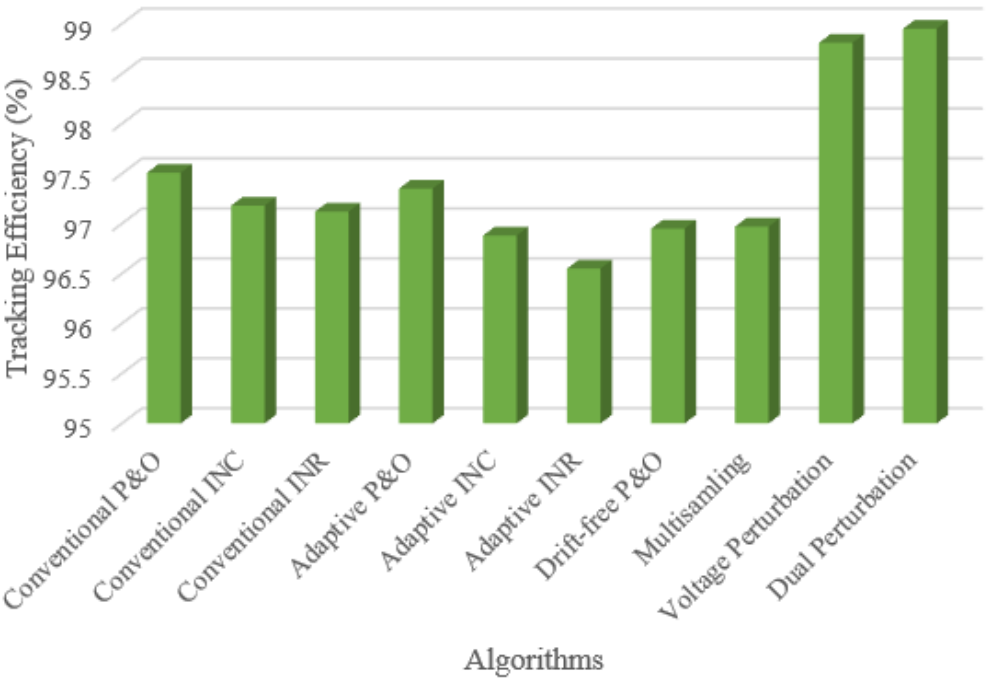


Fig. 4.29. Tracking Efficiency for various algorithms at step decrease-in profile

Table 4.5. Table of taxonomy based on comparative analysis for step decrease-in irradiance profile

Algorithms	Control Strategy	Drift Occurrence	Parameter Tuning	Operation region	Tracking speed	Steady-state Oscillations	Stability	Complexity	Cost	Tracking Efficiency
Conventional P&O	Power	✓	No	Both	VL	L	L	L	L	L
Conventional INC	Voltage	✓	No	Both	VL	L	VL	H	H	VL
Conventional INR	Current	✓	No	Both	VL	L	VL	H	H	VL
Adaptive P&O	Power	✓	No	Both	VL	L	L	L	L	L
Adaptive INC	Voltage	✓	No	Both	VL	H	VL	H	H	VL
Adaptive INR	Current	✓	No	Both	VL	H	VL	H	H	VL
Drift-free P&O	Power	×	Yes	Both	L	L	L	L	L	L
Multisampling	Power	×	Yes	Both	L	L	L	H	H	L
Proposed Voltage Perturbation	Voltage	×	Yes	Right	H	VL	H	L	L	H
Proposed Dual Perturbation	Dual	×	Yes	Both	H	VL	H	L	L	H

* VL: Very low, L: Low, H: High

Table 4.6. Performance parameters of algorithms step decrease-in irradiance profile

Algorithms	Response-time (s)	Steady-state Oscillations (%)		Tracking Efficiency (%)
		480 W/m²	270 W/m²	
Conventional P&O	0.030	2.52	2.30	97.51
Conventional INC	0.041	2.68	2.25	97.18
Conventional INR	0.047	2.75	2.31	97.12
Adaptive P&O	0.028	2.03	2.10	97.35
Adaptive INC	0.037	2.35	2.40	96.88
Adaptive INR	0.039	2.55	2.42	96.55
Drift-free P&O	0.022	2.70	2.33	96.95
Multisampling	0.016	2.30	2.01	96.97
Proposed Voltage Perturbation	0.012	1.01	0.98	98.81
Proposed Dual Perturbation	0.002	1.00	0.97	98.95

4.5.3. EN50530 Standard Irradiance Profile

A comparative study is carried out by considering conventional P&O, INC and INR MPPT algorithms and a state-of-art adaptive P&O, INC and INR and drift-free P&O MPPT algorithms. A voltage perturbation-based MPPT algorithm proposed here is also analyzed. The algorithms are also validated on the standard EN50530 irradiance pattern, as shown in Fig. 4.30. The proposed algorithm is analyzed using PV parameters like voltage, current and power with respect to time. Furthermore, the comparative study of the same is discussed in the fourth subsection. The performance comparison is based on parameters like response time, steady-state oscillations and tracking efficiency.

The tracking efficiency is determined using the formula specified in Eq. (4.27),

$$\text{Tracking Efficiency} = \frac{\text{Extracted Power}}{\text{Ideal Power}} = \frac{\int_0^T V_{PV} \times I_{PV}}{\int_0^T P_{MPP}} \qquad (4.27)$$

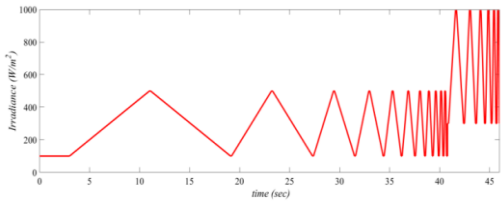


Fig. 4.30. Irradiance pattern of EN50530

A) Voltage Analysis

In this subsection, the detailed explanation of voltage analysis corresponds to various algorithms. Conventional P&O, INC and INR MPPT techniques and a state-of-art adaptive P&O, INC and INR techniques and drift-free P&O MPPT technique along with the proposed adaptive voltage perturbation-based MPPT algorithm, are realized in terms of PV voltage.

Fig. 4.31 (a), (c), and (e) display the transient voltage response for the traditional P&O, INC, and INR approaches, respectively. These algorithms have long reaction times, substantial drift, and steady-state oscillations. Although the INC technique exhibits less steady-state oscillations, the P&O algorithm performs better overall, with 93.25% tracking efficiency and 0.042s reaction time. Additionally, Fig. 4.31 (b), (d), and (f) show the adaptive versions of the P&O, INC, and INR approaches, respectively. These methods show a significant deviation as compared to conventional techniques. This is because these methods detect the substantial change in power and adjust step size accordingly to boost the convergence speed towards MPP. Among all of these, the adaptive P&O method shows better performance of 93.12% than other techniques. This comparative study also considered a state-of-the-art drift-free MPPT algorithm [26] to overcome the drift issue. This technique mainly covers drift issues and shows minimal deviation compared to conventional and adaptive methods, as illustrated in Fig. 4.31 (g).

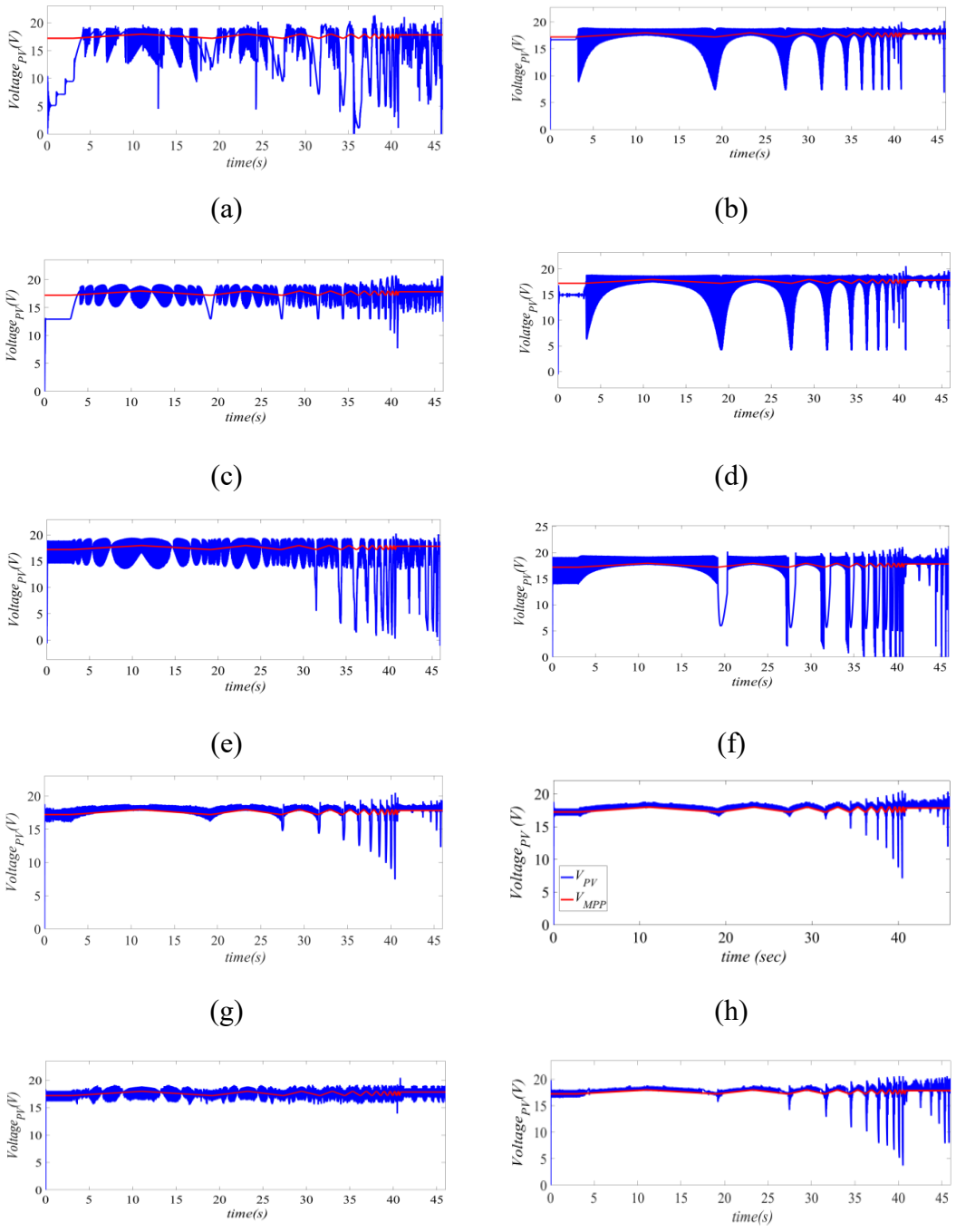


Fig. 4.31. Voltage response for a) P&O, b) Adaptive P&O, c) INC, d) Adaptive INC, e) INR, f) Adaptive INR, g) drift-free P&O, h) multisampling P&O, i) proposed an adaptive voltage perturbation-based (j) proposed dual perturbation based MPPT algorithms

The drift-free method shows the best performance as compared to traditional and adaptive techniques. The multisampling technique is also considered to cover up the drift issue as illustrated in Fig. 4.31 (h). Moreover, an adaptive voltage perturbation-based and dual perturbation based MPPT algorithms are proposed and designed in this study to overcome challenges like drift occurrence, deviation from 6MPP, slow response time and high steady-state oscillations. Fig. 4.31 (i) shows the transient voltage response of the proposed algorithm. The proposed method achieves 97.55% tracking efficiency, 12 ms response time and very low steady-state oscillations. While Fig. 4.31 (j) shows the transient voltage response of the proposed dual perturbation-based algorithm. The proposed method achieves 98.75% tracking efficiency, 12 ms response time and very low steady-state oscillations.

B) Current Analysis

In this subsection, a detailed explanation of the current analysis covers various algorithms. Conventional P&O, INC and INR MPPT techniques and a state-of-art adaptive P&O, INC and INR techniques and drift-free P&O MPPT technique, along with the proposed adaptive voltage perturbation-based MPPT algorithm, are realized in terms of PV current.

The transient current response for conventional P&O, INC and INR methods are shown in Fig. 4.32 (a), (c) and (e), respectively. These algorithms show high drift and steady-state oscillations and slow response time. Among all, the P&O algorithm shows better performance by 7.47%, but the INC method shows less steady-state oscillations as compared to P&O algorithm. Furthermore, Adaptive versions of P&O, INC and INR methods are depicted in Fig. 4.32 (b), (d) and (f), respectively. These methods show a large deviation as compared to conventional techniques.

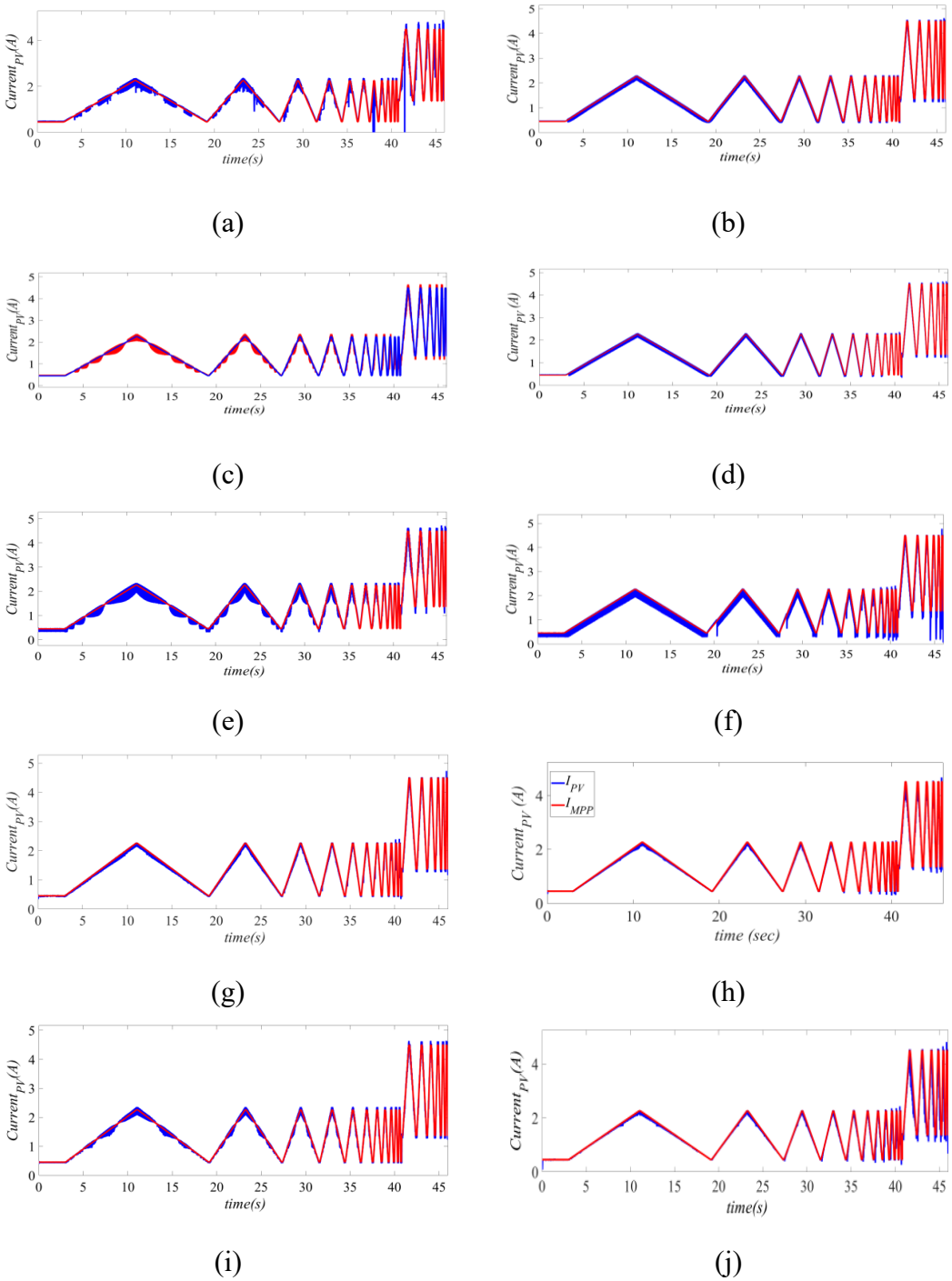


Fig. 4.32. Current response for a) P&O, b) Adaptive P&O, c) INC, d) Adaptive INC, e) INR & f) Adaptive INR, g) drift-free P&O, h) multisampling P&O, i) proposed an adaptive voltage perturbation-based (j) proposed dual perturbation based MPPT algorithms

This is because these methods detect the significant change in power and adjust step size accordingly to boost the convergence speed towards MPP. Among all of these, the adaptive P&O method shows significant improvement of 8.25% than other techniques. This comparative study also considered a state-of-the-art drift-free MPPT algorithm to overcome the drift issue. This technique mainly covers drift issues and shows minimal deviation compared to conventional and adaptive methods and shows the maximum tracking efficiency of 94.75%, as illustrated in Fig. 4.32 (g). The drift-free method shows the best performance as compared to traditional and adaptive techniques. The multisampling technique is also considered to cover up the drift issue as illustrated in Fig. 4.32 (h). This strategy demonstrates superior performance relative to traditional, adaptive, and drift-free P&O methods.

To address issues such drift incidence, divergence from MPP, sluggish reaction time, and excessive steady-state oscillations, an adaptive voltage perturbation-based MPPT algorithm is also suggested and created. The suggested algorithm's transient voltage response is displayed in Fig. 4.32 (i). The proposed method achieves 97.55% tracking efficiency, 12 ms response time and very low steady-state oscillations. While Fig. 4.32 (j) shows the transient voltage response of the proposed dual perturbation-based algorithm. The proposed method achieves 98.75% tracking efficiency, 2 ms response time and very low steady-state oscillations.

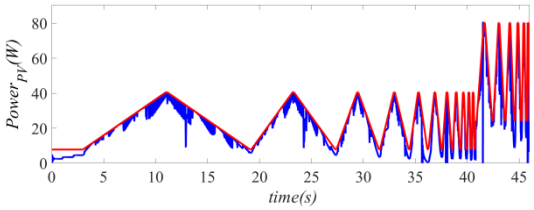
C) Power Analysis

This subsection presents a detailed power analysis of various MPPT algorithms. It includes conventional methods such as P&O, INC, and INR, as well as state-of-the-art adaptive variants of these techniques. Furthermore, the drift-free Perturb and Observe approach and the suggested adaptive voltage perturbation-based Maximum Power Point Tracking algorithm are evaluated for

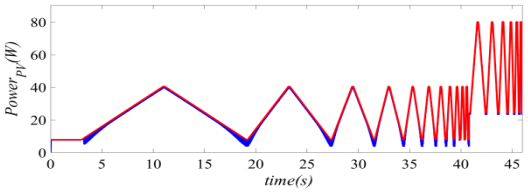
photovoltaic power performance. Fig. 4.33 presents a visual depiction of the comparison stud.

The drift-free Perturb and Observe method and the proposed adaptive voltage perturbation-based Maximum Power Point Tracking algorithm are assessed for solar power performance. Fig. 4.33 illustrates the comparative analysis. These algorithms show high drift and steady-state oscillations and slow response time. Among all, the P&O algorithm shows better performance by 7.47% as compared to other algorithms, but the INC method shows less steady-state oscillations. Furthermore, Adaptive versions of P&O, INC and INR algorithms are depicted in Fig. 4.33 (b), (d) and (f), respectively. These methods show a significant deviation as compared to conventional techniques. This is because these methods detect the substantial change in power and adjust step size accordingly to boost the convergence speed towards MPP. Among all of these, the adaptive P&O method shows better performance by 8.25% than other techniques. This comparative study also considered a state-of-the-art drift-free MPPT algorithm to overcome the drift issue. This technique mainly covers drift issues and shows less deviation than conventional and adaptive methods, as illustrated in Fig. 4.33 (g). The drift-free method shows 3.5% significant improvement as compared to traditional and adaptive techniques. The multisampling technique is also considered to cover up the drift issue as illustrated in Fig. 4.33 (h). This technique shows the best performance as compared to conventional, adaptive and drift-free P&O techniques.

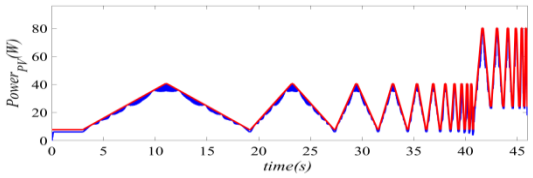
Moreover, an adaptive voltage perturbation-based MPPT algorithm is proposed and designed to overcome challenges like drift occurrence, deviation from MPP, slow response time and high steady-state oscillations. Fig. 4.33 (i) shows the transient voltage response of the proposed algorithm. The proposed method achieves 97.55% tracking efficiency, 12 ms response time and very low steady-state oscillations. While Fig. 4.33 (j) shows the transient voltage response of the proposed dual perturbation-based algorithm.


Power PV (W)
time(s)

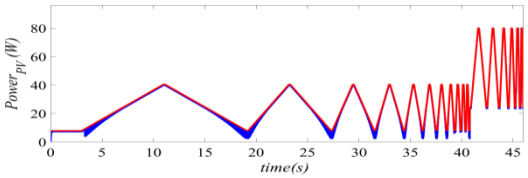
(a)


Power PV (W)
time(s)

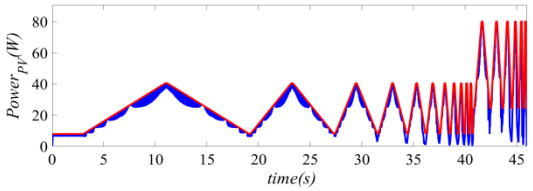
(b)


Power PV (W)
time(s)

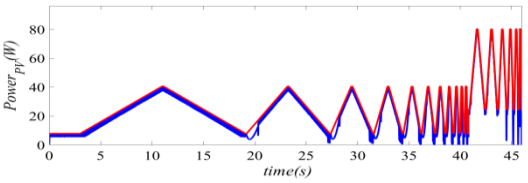
(c)


Power PV (W)
time(s)

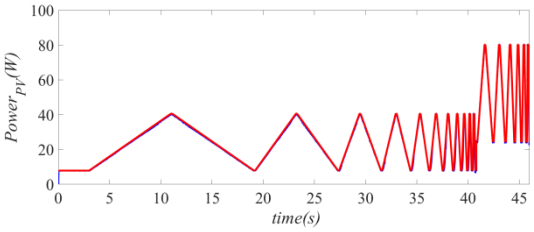
(d)


Power PV (W)
time(s)

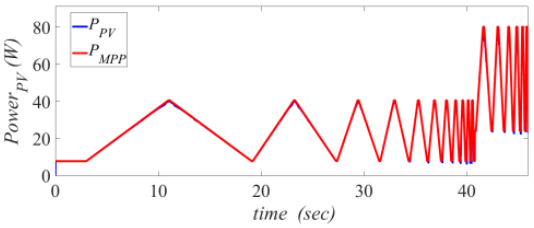
(e)


Power PV (W)
time(s)

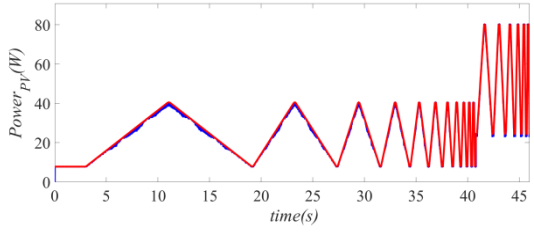
(f)


Power PV (W)
time(s)

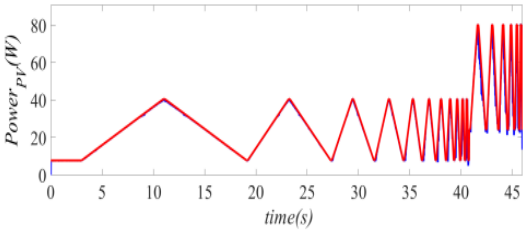
(g)


P PV
P MPP
Power PV (W)
time (sec)

(h)


Power PV (W)
time(s)

(i)


Power PV (W)
time(s)

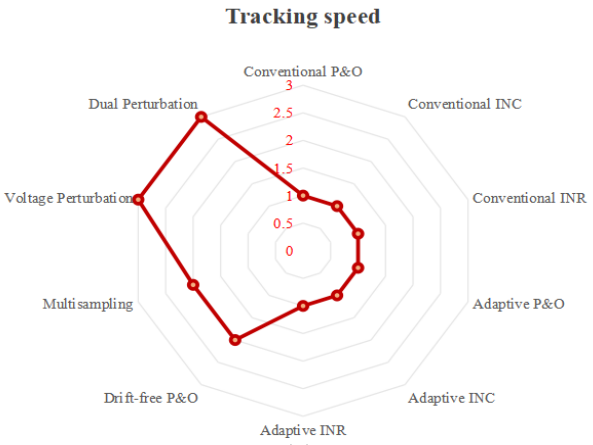
(j)

Fig. 4.33. Power response for a) P&O, b) Adaptive P&O, c) INC, d) Adaptive INC, e) INR, f) Adaptive INR, g) drift-free P&O, h) multisampling P&O, i) proposed an adaptive voltage perturbation-based (j) proposed dual perturbation based MPPT algorithms

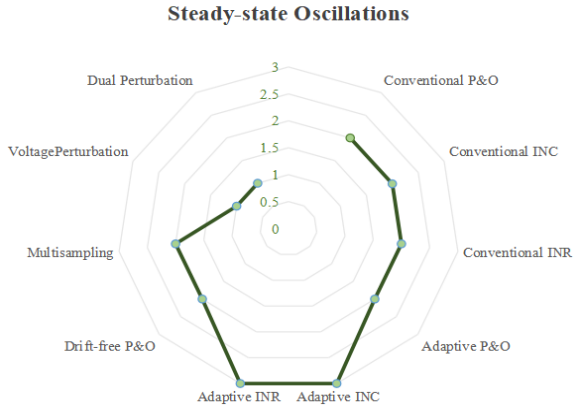
The proposed method achieves 98.75% tracking efficiency, 2 ms response time and very low steady-state oscillations.

D) Comparative Analysis

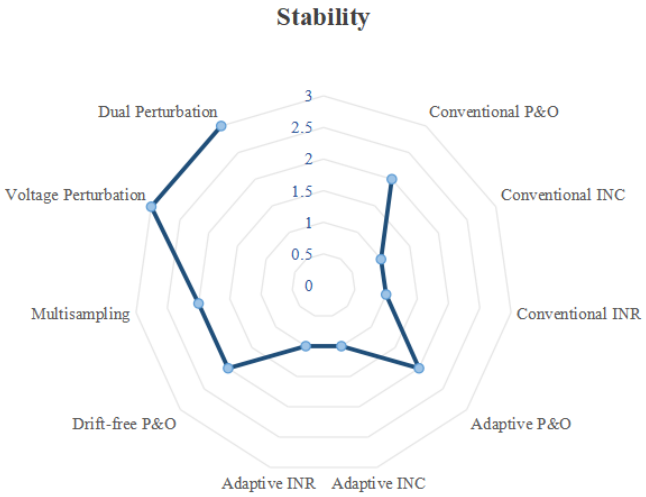
This subsection performs a comparative analysis of conventional P&O, INC and INR and the state-of-art adaptive versions of P&O, INC and INR and drift-free P&O, multisampling MPPT methods and proposed adaptive voltage perturbation-based and dual perturbation based MPPT algorithms. The comparative study is performed on various performance parameters like type of control strategy, drift occurrence, parameter tuning, region of operation, tracking speed, steady-state oscillations, stability, implementation complexity, and tracking efficiency as illustrated in Fig. 4.34 and Table 4.7. Moreover, a quantitative comparative study is performed using parameters like response time and tracking efficiency as shown in Fig. 4.35 and 4.36.



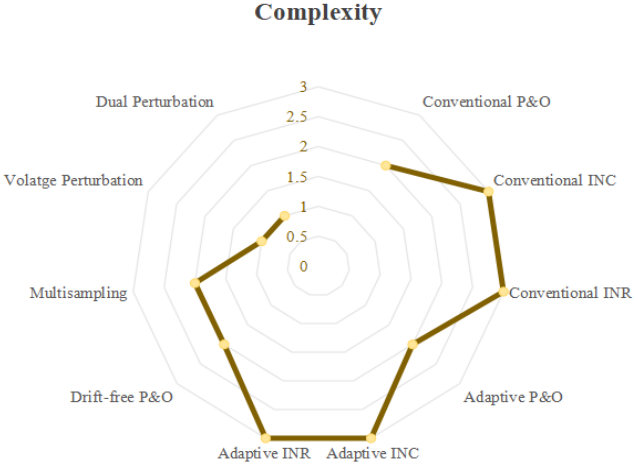
(a)


Steady-state Oscillations
Dual Perturbation
Conventional P&O
VoltagePerturbation
Conventional INC
Multisampling
Conventional INR
Drift-free P&O
Adaptive P&O
Adaptive INR
Adaptive INC
3
2.5
2
1.5
1
0.5
0

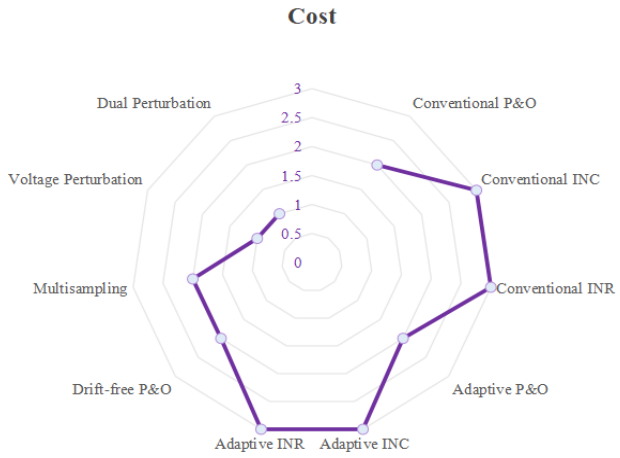
(b)


Stability
Dual Perturbation
Conventional P&O
Voltage Perturbation
Conventional INC
Multisampling
Conventional INR
Drift-free P&O
Adaptive P&O
Adaptive INR
Adaptive INC
3
2.5
2
1.5
1
0.5
0

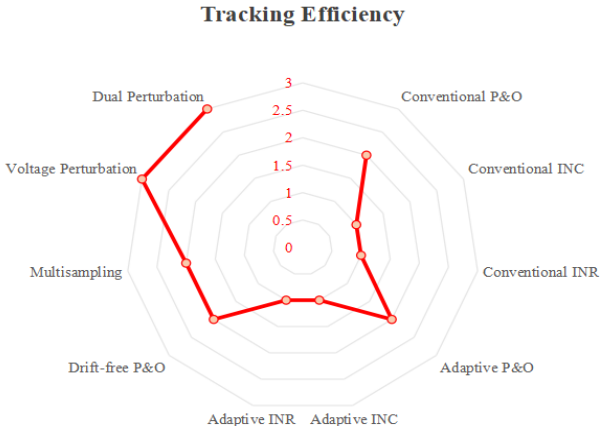
(c)


Complexity
Dual Perturbation
Conventional P&O
Volatge Perturbation
Conventional INC
Multisampling
Conventional INR
Drift-free P&O
Adaptive P&O
Adaptive INR
Adaptive INC
3
2.5
2
1.5
1
0.5
0

(d)



(e)



(f)

Fig. 4.34. Comparative behaviour of conventional, adaptive and proposed MPPT techniques on the basis of radial diagram behaviour for (a) Tracking Speed, (b) Oscillations, (c) Stability, (d) Complexity, (e) Cost and (f) Tracking Efficiency

The quantitative values for the same are illustrated in Table 4.8. The proposed method outperforms the conventional P&O, adaptive P&O and drift-free P&O, multisampling algorithms by a substantial margin of 4.3% and 4.43% as well as 2.8%, respectively. The proposed technique outperforms the other MPPT methods by providing 99.55% tracking efficiency and 0.012s response time. It not only avoids drift as it operates on the right region of the power curve

but also exhibit low steady-state oscillations, high speed of tracking, high stability, and low implementation complexity and excellent tracking efficiency.

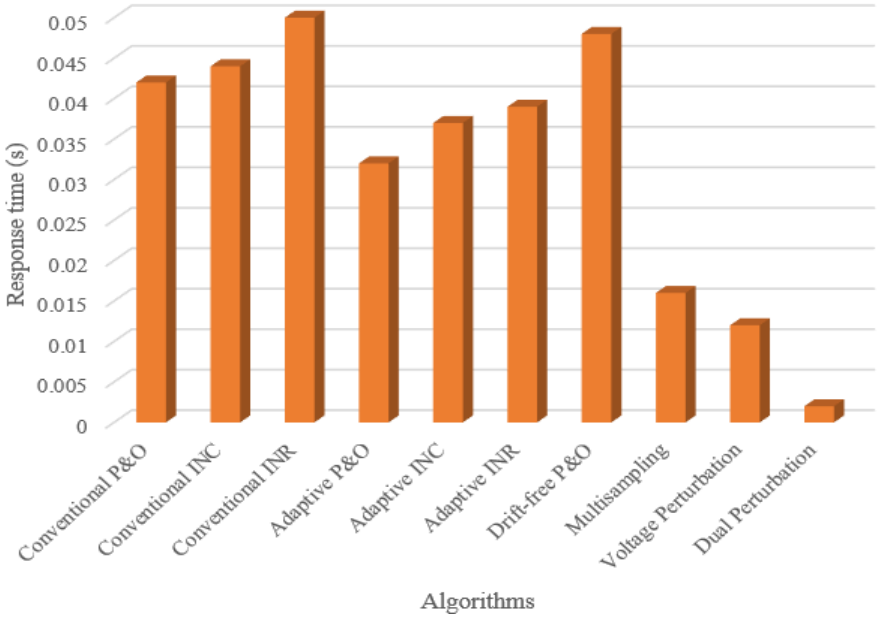


Fig. 4.35. Response time of various algorithms

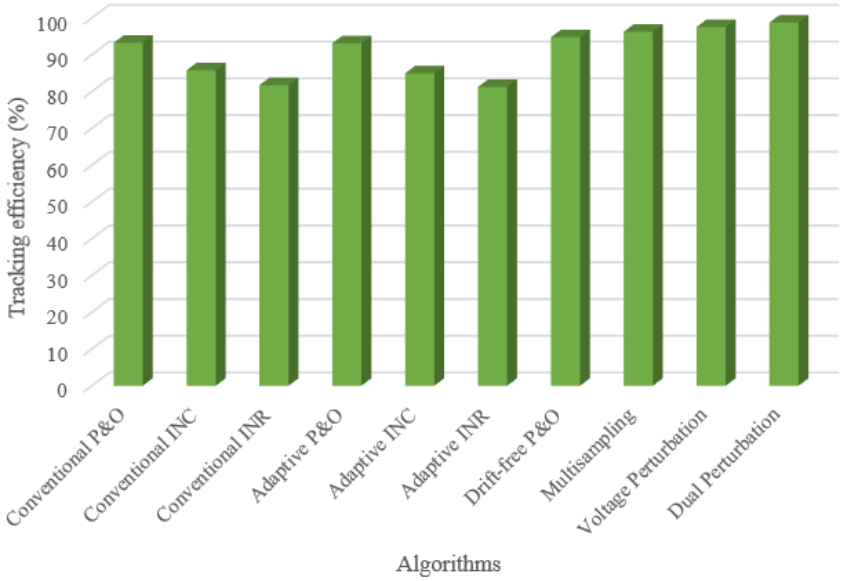


Fig. 4.36. Tracking Efficiency of various algorithms

Table 4.8. Performance parameters of algorithms at EN50530 irradiance profile

Algorithms	Response-time (s)	Tracking Efficiency (%)
Conventional P&O	0.042	93.25
Conventional INC	0.044	85.78
Conventional INR	0.050	81.75
Adaptive P&O	0.032	93.12
Adaptive INC	0.037	84.95
Adaptive INR	0.039	81.25
Drift-free P&O	0.048	94.75
Multisampling	0.016	96.25
Proposed Voltage Perturbation	0.012	97.55
Proposed Dual Perturbation	0.002	98.75

Table 4.7. Table of taxonomy based on comparative analysis for EN50530 irradiance profile

Algorithms	Control Strategy	Drift Occurrence	Parameter Tuning	Operation region	Tracking speed	Steady-state Oscillations	Stability	Complexity	Cost	Tracking Efficiency
Conventional P&O	Power	✓	No	Both	VL	L	L	L	L	L
Conventional INC	Voltage	✓	No	Both	VL	L	VL	H	H	VL
Conventional INR	Current	✓	No	Both	VL	L	VL	H	H	VL
Adaptive P&O	Power	✓	No	Both	VL	L	L	L	L	L
Adaptive INC	Voltage	✓	No	Both	VL	H	VL	H	H	VL
Adaptive INR	Current	✓	No	Both	VL	H	VL	H	H	VL
Drift-free P&O	Power	×	Yes	Both	L	L	L	L	L	L
Multisampling	Power	×	Yes	Both	L	L	L	H	H	L
Proposed Voltage Perturbation	Voltage	×	Yes	Right	H	VL	H	L	L	H
Proposed Dual Perturbation	Dual	×	Yes	Both	H	VL	H	L	L	H

*H: High, L: Low, VL: Very low

4.6. Summary

To achieve 1st objective i.e., formulation and implementation of drift-free MPPT algorithm under rapid change in irradiance, various MPPT techniques like conventional P&O, INC & INR, adaptive P&O, INC & INR, state-of-art multisampling, drift-free P&O and modified P&O MPPT algorithms are simulated on MATLAB/Simulink. All these techniques are realized on step increase-in and decrease-in as well as standard EN50530 irradiance patterns. In conclusion, this study presents a fast MPPT algorithm designed to mitigate the drift issue in PV systems during dynamic changes in irradiance changes. This study primarily aims to compare and contrast several algorithms, including the traditional and adaptive P&O, INC, and INR versions, the drift-free P&O, multisampling MPPT algorithms and proposed adaptive voltage perturbation-based and dual perturbation-based MPPT methods. All the algorithms are developed and put into operation on MTALB/Simulink. The analysis is performed on step increase-in, step decrease-in and EN50530 irradiance profiles.

The computational complexity of the proposed voltage perturbation and dual perturbation-based MPPT algorithms has been carefully evaluated to ensure their practical applicability in real-time PV grid-connected systems. The algorithms primarily rely on simple arithmetic operations such as voltage measurement, incremental perturbation, and decision logic, which significantly reduce the overall computational burden compared to advanced heuristic or optimization-based methods. This lightweight computational requirement makes them suitable for low-cost microcontrollers and DSP-based platforms commonly deployed in PV inverters. In terms of scalability, the algorithms can be extended to larger PV arrays or multi-string configurations without significant modifications, as the control strategy remains consistent across different system sizes. Furthermore, the dual perturbation technique enhances

tracking speed and accuracy under partial shading and fast irradiance variations without adding considerable complexity. Simulation and hardware results confirm that the algorithm maintains robustness even with increased PV capacity. Thus, the proposed approach offers a favourable balance between accuracy, speed, and computational efficiency, making it a scalable solution for large-scale standalone PV systems.

While the MPPT techniques provided a comprehensive analysis of conventional approaches to extracting the maximum available power from PV systems, their effectiveness is often limited under rapid environmental variations and grid interaction scenarios. To address these challenges, the focus now shifts towards the proposed FPPT techniques, which aim not only at maximizing power but also at ensuring stability, efficiency, and reliability in grid-connected operations. The following chapter presents the results and discussion of the FPPT strategies, highlighting their comparative performance.

CHAPTER 5

DESIGN AND ANALYSIS OF FLEXIBLE POWER POINT TRACKING ALGORITHM

This chapter marks a significant advancement in the design and analysis of flexible power point tracking (FPPT) algorithms. It emphasizes the simulation and implementation of various power-, current-, and voltage-based FPPT techniques, including the proposed FPPT algorithm.

5.1. Introduction

Keeping grid-connected photovoltaic (PV) systems operating efficiently and reliably in the face of changing environmental circumstances is of utmost importance. There are a lot of problems that make traditional MPPT approaches ineffective (Chellal et al., 2021b). The tendency to diverge from the Maximum Power Point with abrupt fluctuations in temperature or irradiance is a significant worry. Not only does this drift create substantial power losses, but it also destabilizes the grid connection, which in turn can result in voltage swings and lower the energy supply's overall reliability (Sarvi & Azadian, 2022). Improving the efficiency and reliability of PV systems that are connected to the grid depends on fixing these issues. Traditional MPPT approaches also have the serious flaw of naturally oscillating around the MPP (Mei et al., 2010b). These oscillations happen because the system is unable to stabilize at the optimal point because of the back-and-forth movement caused by the constant perturbations used to find the MPP (Yetayew & Workineh, 2021). The continual power fluctuations and mechanical stress that this behavior causes can reduce the operating lifespan of system components (Sreedhar & Jagadeesh, 2016). Additionally, the amount of useful energy sent into the grid is reduced due to the constant oscillations, which undermine the efficiency of the power conversion process (Mousa et al., 2021b). If we want an energy extraction

method that is steadier and more efficient, we must overcome this issue. To fix these issues, the non-drifting flexible power point tracking (FPPT) method incorporates sophisticated control systems that keep the system from veering off course and keep it firmly positioned at the MPP, regardless of how the surrounding environment changes (Pandey et al., 2008). The non-drifting FPPT approach guarantees a more consistent and dependable power output from the PV system by decreasing oscillatory behavior and eliminating drift (Nusrat et al., 2024). Both the efficiency of energy conversion and the longevity of the system components are improved by this increased stability (Cavalcanti et al., 2005). In addition, the non-drifting method helps with grid integration by making the power supply more stable and predictable, which is important for keeping the grid stable and keeping up with the needs of current energy networks (Hussein et al., 1995). It is critical for grid-connected PV systems to operate efficiently and consistently regardless of changes in the grid or environmental conditions (Boscaino et al., 2024). When dealing with low voltage ride-through (LVRT) and frequency ride-through (FRT) conditions, traditional FPPT systems frequently suffer from serious flaws that reduce their efficiency (F. Zhang et al., 2013). In the event of voltage dips or sags, which are common during grid disruptions, conventional FPPT algorithms could fail to sustain the MPP, resulting in significant power loss and instability in the system (Kim et al., 2001).

We need more resilient and flexible solutions because these problems can damage the grid connection and the energy supply's dependability. To keep PV systems running and stable during times of transient voltage dips, low voltage ride-through is an essential component of contemporary grid-connected systems (F. Zhang et al., 2013). However, conventional FPPT approaches may take too long to adapt to these changes, leading to power conversion inefficiencies and drifting away from the MPP (Killi & Samanta, 2015). Because the PV system

is ill-equipped to handle voltage fluctuations, drift not only decreases the amount of energy fed into the grid but can also lead to more instability. Improving PV systems' ability to withstand grid disturbances and maintain efficient power output requires fixing this defect (Kollimalla & Mishra, 2014). A further difficulty arises in frequent ride-through scenarios, when the system is required to frequently tolerate brief voltage disruptions (Sai et al., 2024). Because of their erratic behavior and shorter reaction times, traditional FPPT approaches can make these frequent interruptions even more noticeable (Satif et al., 2018). Reduced operational lifespan and increased maintenance costs can be caused by power fluctuations and mechanical stress on system components (Hashim et al., 2023b). The goal of the non-drifting FPPT method is to keep the MPP constant regardless of how often the grid experiences disturbances by offering a quicker and more consistent reaction to voltage variations (Büyük & İnci, 2023b). As a result, the PV system is more efficient and stable, which helps with grid integration and makes the energy supply more reliable (Tawiah-Mensah et al., 2022).

Several researchers have put forward FPPT control solutions in the past few years, which involve tweaking hill-climbing algorithms to increase convergence speed and decrease stead-state power oscillations. This allows them to follow the CPP of PV systems. A modified power-based FPPT algorithm with multi-mode operation (i.e., the ability to track CPP on both the left and right side of MPP) was proposed by the authors in (Büyük & İnci, 2023b). Although the suggested technique can faithfully monitor CPP, it will be rendered useless in the event of an abrupt shift in irradiance. Using a model predictive controller to monitor FPP while it is under battery load, the authors of (Lin & Liao, 2024) suggested a dc-link voltage based FPPT regulation. While the algorithm is not extensively investigated, the primary goal is to control battery life. Binary search based FPPT control was first proposed in (Motahhir

et al., 2020). Iteratively lowering the search space to half of its previous value primarily enhances the speed of convergence. Algorithms are not tested under conditions of fast changes in temperature or irradiance. Tracking the FPP regardless of an increase or decrease in the power reference value under STC is made possible by the secant technique based FPPT control that was introduced in (Belkaid et al., 2017). Although the suggested method is quick and exhibits fewer steady-state oscillations, it becomes unstable when considering external factors. The authors of (Guanghua et al., 2024) suggested a control technique for active disturbance rejection FPPT that is based on errors for PV systems to generate constant power. Although the technology outperforms the traditional P&O approach, it still lacks quick parameter adjustment. An FPPT control scheme based on hill climbing was suggested in (Ali & Petrov, 2024) for use in partial shading situations. However, the technique cannot lessen oscillations that occur in a stable state. Under constant temperature and variable irradiation, the authors of (Gupta et al., 2014) suggested a fuzzy logic and least mean square (LMS) control system for CPG. However, the method's complexity makes it expensive from an application standpoint. A GFPPT control for use in partially shaded environments was suggested in (Guenounou et al., 2021). Although the results fall short of expectations, the primary goal is to achieve CPP more quickly in the event of an abrupt change in irradiance. A technique for controlling virtual synchronous generators (VSGs) was suggested in (Vadi et al., 2021) as an FPPT algorithm. It has not been yet, but it may be utilized to keep the grid stable during intermittency. To deal with fluctuating irradiance, the authors of (Karmouni et al., 2022) suggested an MPPT/FPPT control based on a dc-link model. The researchers also created an algorithm called FS-MPC, which stands for finite-set model predictive control, to help grid-connected PV systems manage reactive and active power exchange correctly (Haghighat et al., 2023). A hill climbing and particle swarm optimization (HC&PSO) method is

suggested for use in the creation of the FPPT algorithm in (Oufettoul et al., 2023) under partial shade conditions (PSC). It has also been validated and tested. To keep the reserve power point at FPP when grid-connected PV systems experience disturbances, a dynamic reverse power point tracking was developed in (Tur & Bayindir, 2019). This tracking can offer current information on the available maximum power point. They presented a model-based (MB) FPPT method for PV arrays in (Tella et al., 2024).

5.2. System Description and Mathematical Modelling

This section introduces the detail description of grid-connected photovoltaic (PV) system. For grid-connected PV systems, the integration of the photovoltaic array with the utility grid requires careful consideration of inverter modeling, synchronization, and compliance with regional grid codes. The inverter not only converts DC to AC but also ensures proper synchronization of voltage, frequency, and phase with the grid to maintain system stability. Advanced synchronization techniques, such as phase-locked loops (PLL), are widely adopted to achieve seamless grid integration. Furthermore, grid codes mandate specific requirements for power quality, fault ride-through capability, harmonic distortion limits, and reactive power support, which must be incorporated into the inverter control strategy. In the context of Maximum Power Point Tracking (MPPT) and emerging Fast Power Point Tracking (FPPT) algorithms, the inverter must dynamically respond to rapid irradiance fluctuations while still meeting grid standards. Accurate inverter modeling allows for evaluating these control strategies under realistic operating conditions, ensuring reliable power delivery. Compliance with grid codes is particularly vital to avoid disconnections during grid disturbances and to support grid resilience. Thus, synchronization techniques, MPPT/FPPT performance, and inverter control strategies must be studied collectively for the

design of efficient and grid-compliant PV systems. The designed PV system for this work is illustrated in Fig 5.1. The P-V curve of the same is depicted in Fig. 5.2. To design this grid- connected PV systems various components like PV array, boost converter, PV inverter, inductor-capacitor-inductor (LCL) filter and micro-grid are utilized. The PV array consists of a single string comprising 9 PV panels connected in series to deliver the desired output power. Detailed specifications of the PV panels are provided in Table 5.1. The array's output is monitored using current and voltage sensors, which feed data to the MPPT controller. A boost converter, a critical component in the PV system's circuit design, is integrated to ensure efficient power conversion and management. The boost converter manages the voltage levels to suit the needs of the load or energy storage system, allowing the PV system to function at its MPP regardless of the irradiance circumstances (Bhattacharyya et al., 2020). In Table 2.2 you can see the detailed specification of the boost-converter.

Furthermore, the extracted power is passed through the PV inverter to convert the DC-supply into three phase AC-supply. To design this PV inverter, 6 MOSFETs have been used having phase shift of 180 degree each (Hua & Zhan, 2021). A LCL (inductor-capacitor-inductor) filter is installed between the PV inverter and the grid to suppress switching frequency harmonics generated by the grid-connected inverter (Kavya & Jayalalitha, 2022c). The requirement of grid depends on the grid-codes. Grid codes are essential for the effective functioning of grid-connected photovoltaic systems. The conditions for connecting installations to high- and extra-high-voltage grids, as well as distribution and low-voltage networks, are regulated by grid regulations (Chellakhi et al., 2022). In addition, system services, grid growth, and general grid operation are covered in the code. Grid- tied PV systems stand for the system linked to both solar panels and the main grid (S. Sharma et al., 2023). It

means that such a system can draw power from either panels or grid (Kahani et al., 2022).

5.2.1. Mathematical Model of grid-connected PV system

The formulation is executed in the stationary reference frame (SRF). (Liu et al., 2024). The conversion from the three-phase system into SRF is mentioned in Eq. (5.1)

$$v_{\alpha\beta} = \begin{bmatrix} v_\alpha \\ v_\beta \end{bmatrix} = \sqrt{\frac{2}{3}} \begin{bmatrix} 1 & -1/2 & -1/2 \\ 0 & \sqrt{3}/2 & -\sqrt{3}/2 \end{bmatrix} \begin{bmatrix} v_a \\ v_b \\ v_c \end{bmatrix} \quad (5.1)$$

Where, are the v_α, v_β voltages in the SRF and v_a, v_b, v_c are the grid voltages in the natural reference frame. As the system is three-phase three-wire, the phased currents will not contain zero sequences. The voltage and current are expressed in Eq. (5.2) to (5.7),

$$v_a = V^+ \cos(\omega t + \varphi^+) + V^- \cos(\omega t + \varphi^-) \quad (5.2)$$

$$v_b = V^+ \cos\left(\omega t - \frac{2\pi}{3} + \varphi^+\right) + V^- \cos\left(\omega t + \frac{2\pi}{3} + \varphi^-\right) \quad (5.3)$$

$$v_c = V^+ \cos\left(\omega t + \frac{2\pi}{3} + \varphi^+\right) + V^- \cos\left(\omega t - \frac{2\pi}{3} + \varphi^-\right) \quad (5.4)$$

$$i_a = I^+ \cos(\omega t + \delta^+) + I^- \cos(\omega t + \delta^-) \quad (5.5)$$

$$i_b = I^+ \cos\left(\omega t - \frac{2\pi}{3} + \delta^+\right) + I^- \cos\left(\omega t + \frac{2\pi}{3} + \delta^-\right) \quad (5.6)$$

$$i_c = I^+ \cos\left(\omega t + \frac{2\pi}{3} + \delta^+\right) + I^- \cos\left(\omega t - \frac{2\pi}{3} + \delta^-\right) \quad (5.7)$$

Where, V^+, V^-,$I^+$and I^- are the amplitudes of the positive sequence (PS) and negative sequence (NS) of the grid voltage and current and φ^+, φ^-, $\delta^+$and

δ^{-} are the phase angles of the same. The apparent power (S) is expressed in Eq. (5.8) as:

$$S = v \,.\, i^{*} \;=\; P + jQ \qquad (5.8)$$

In this context, v and i represent the voltage and current vectors in the synchronous reference frame (SRF), whereas P and Q denote active and reactive power, respectively. Under typical conditions, the grid voltage and loads are balanced, resulting in the absence of oscillatory components in both the active and reactive power, while the injected current remains entirely sinusoidal.

However, under conditions of intermittency or unbalance, the negative sequence (NS) components in both current and voltage must also be taken into account. Consequently, the apparent power (S) can be redefined as shown in Eq. (5.9).

$$S = v_{\alpha\beta} \,.\, i^{*}_{\alpha\beta} \;=\; \left(v^{+}_{\alpha\beta} + v^{-}_{\alpha\beta}\right).\left(i^{+}_{\alpha\beta} + i^{-}_{\alpha\beta}\right)^{*} = v^{+}_{\alpha\beta} \,.\, i^{+}_{\alpha\beta} * \; + v^{+}_{\alpha\beta} \,.\, i^{-*}_{\alpha\beta} + v^{-}_{\alpha\beta} \,.\, i^{+*}_{\alpha\beta} + v^{-}_{\alpha\beta} \,.\, i^{-*}_{\alpha\beta} \qquad (5.9)$$

In which $v^{+}_{\alpha\beta}$ and $v^{-}_{\alpha\beta}$ are derived from

$$v^{+}_{\alpha\beta} = \frac{1}{2}\begin{bmatrix} 1 & -q \\ q & 1 \end{bmatrix} v_{\alpha\beta} \text{ and } v^{-}_{\alpha\beta} = \frac{1}{2}\begin{bmatrix} 1 & q \\ -q & 1 \end{bmatrix} v_{\alpha\beta} \qquad (5.10)$$

Where, $q = e^{-j\pi/2}$ is a 90°-lagging phase-shifting operator applied to the time domain. Similarly, are obtained in Eq. (5.9). Equation (5.10) has four components in the formulation of perceived power. In the subsequent equations (Eq. (5.11) to (5.19)), the terms are denoted as active and reactive components P_n and Q_n, where n ranges from 1 to 4.

$$v_{\alpha\beta}^{+} \cdot i_{\alpha\beta}^{+} * = \left(v_{\alpha}^{+} + jv_{\beta}^{+}\right).\left(i_{\alpha}^{+} + ji_{\beta}^{+}\right)^{*} = v_{\alpha}^{+}i_{\alpha}^{+} + v_{\beta}^{+}i_{\beta}^{+} + j\left(v_{\beta}^{+}i_{\alpha}^{+} - v_{\alpha}^{+}i_{\beta}^{+}\right) \quad (5.11)$$

$$P_1 = v_{\alpha}^{+}i_{\alpha}^{+} + v_{\beta}^{+}i_{\beta}^{+} \quad (5.12)$$

$$Q_1 = v_{\beta}^{+}i_{\alpha}^{+} - v_{\alpha}^{+}i_{\beta}^{+} \quad (5.13)$$

$$P_2 = v_{\alpha}^{+}i_{\alpha}^{-} + v_{\beta}^{+}i_{\beta}^{-} \quad (5.14)$$

$$Q_2 = v_{\beta}^{+}i_{\alpha}^{-} - v_{\alpha}^{+}i_{\beta}^{-} \quad (5.15)$$

$$P_3 = v_{\alpha}^{-}i_{\alpha}^{+} - v_{\beta}^{-}i_{\beta}^{+} \quad (5.16)$$

$$Q_3 = v_{\beta}^{-}i_{\alpha}^{+} - v_{\alpha}^{-}i_{\beta}^{+} \quad (5.17)$$

$$P_4 = v_{\alpha}^{-}i_{\alpha}^{-} + v_{\beta}^{-}i_{\beta}^{-} \quad (5.18)$$

$$Q_4 = v_{\beta}^{-}i_{\alpha}^{-} - v_{\alpha}^{-}i_{\beta}^{-} \quad (5.19)$$

The product of two terms with the same sequence results in constant components of active and reactive power, as illustrated in Eqs. (5.12)- (5.13), and (5.18)- (5.19). In contrast, the oscillating components arise from the multiplication of terms with inverse sequences, as shown in Eqs. (5.14)- 5.17). The steady and fluctuating components of both active and reactive power are specified in Eqs. (5.20) - (5.25).

$$P = P_0 + \breve{P} \quad (5.20)$$

$$P_0 = P_1 + P_4 \quad (5.21)$$

$$\breve{P} = P_2 + P_3 \quad (5.22)$$

$$Q = Q_0 + \tilde{Q} \qquad (5.23)$$

$$Q_0 = Q_1 + Q_4 \qquad (5.24)$$

$$\tilde{Q} = Q_2 + Q_3 \qquad (5.25)$$

Where P and Q are the active and reactive power of the PV systems and P_0, Q_0, $\tilde{P}$, $\tilde{Q}$ are the constant and oscillating portions of active and reactive power respectively.

In balanced voltage sag faults, negative sequence components are nonexistent in both voltage and current, leading to the absence of oscillatory components in active and reactive power. Nonetheless, under unbalanced fault situations, non-symmetrical components manifest in both voltages and currents. As obtained from Equations (5.20) to (5.25), the active and reactive power consist of a constant component, denoted as P_0 and Q_0, respectively, along with two oscillating components, represented by $\tilde{P}$ and $\tilde{Q}$. In photovoltaic (PV) power systems, the DC-link typically receives the entire active power generated by the PV modules.

In balanced voltage sag faults, negative sequence components are absent in both voltage and current, resulting in the lack of oscillatory components in active and reactive power. However, in unbalanced fault conditions, non-symmetrical components appear in both voltages and currents. As derived from Equations (5.20) to (5.25). This means that appropriate control is required to synchronize the power flow from the PV source to the grid by controlling the dc link voltage (Utrilla et al., 2024). Therefore, the dc-link voltage will unavoidably oscillate at the same frequency if the injected active power exhibits double grid frequency fluctuations (Joshi et al., 2024). The capacitive dc-link's life cycle is negatively impacted by double grid frequency oscillations of the

voltage (Boscaino et al., 2024). An innovative technique to lessen these oscillations is suggested in the following section.

In order to eliminate active power oscillations, Eq. (5.22) has to be zero. In Eq. (5.21) and Eq. (5.24), P_0 and Q_0 are equal to the average active power (P_{ref} which is the output of the dc-link regulator) and reactive power (Q_{ref} which is calculated during grid faults) references. The control algorithm continually computes these values, as detailed in Section III-B. The main control aim is to mitigate oscillatory components in active power while allowing reactive power to fluctuate at double the grid frequency. Hence, $\breve{Q}$ is considered equal to$2\left(v_\beta^+ i_\alpha^- - v_\alpha^+ i_\beta^-\right)$.

Furthermore, Eq. 5.25 can be re-expressed as:

$$\breve{Q} = v_\beta^+ i_\alpha^- - v_\alpha^+ i_\beta^- + v_\beta^- i_\alpha^+ - v_\alpha^- i_\beta^+ = 2\left(v_\beta^+ i_\alpha^- - v_\alpha^+ i_\beta^-\right) \tag{5.26}$$

$$v_\beta^+ i_\alpha^- - v_\alpha^+ i_\beta^- - v_\beta^- i_\alpha^+ + v_\alpha^- i_\beta^+ = 0 \tag{5.27}$$

Moreover, Eq. (5.22), (5.23), (5.25) and (5.28) are shown as.

$$\begin{bmatrix} v_\alpha^+ & v_\beta^+ & v_\alpha^- & v_\beta^- \\ v_\alpha^- & v_\beta^- & v_\alpha^+ & v_\beta^+ \\ v_\beta^+ & -v_\alpha^+ & v_\beta^- & -v_\alpha^- \\ -v_\beta^- & v_\alpha^- & v_\beta^+ & -v_\alpha^+ \end{bmatrix} \begin{bmatrix} i_\alpha^+ \\ i_\beta^+ \\ i_\alpha^- \\ i_\beta^- \end{bmatrix} = \begin{bmatrix} P_{ref} \\ 0 \\ Q_{ref} \\ 0 \end{bmatrix} \tag{5.28}$$

Formulation of sinusoidal currents to deliver a certain amount of power to the grid. The mathematical relation for the same is mentioned below:

$$i_\alpha^+ = \frac{v_\alpha^+}{V_p - V_n} P_{ref} - \frac{v_{\alpha\perp}^+}{V_p + V_n} Q_{ref} \tag{5.29}$$

$$i_\alpha^- = \frac{v_\alpha^-}{V_p - V_n} P_{ref} - \frac{v_{\alpha\perp}^-}{V_p + V_n} Q_{ref} \tag{5.30}$$

$$i_{\beta}^{+} = \frac{v_{\beta}^{+}}{V_p - V_n} P_{ref} - \frac{v_{\beta\perp}^{+}}{V_p + V_n} Q_{ref} \qquad (5.31)$$

$$i_{\beta}^{-} = \frac{v_{\beta}^{-}}{V_p - V_n} P_{ref} - \frac{v_{\beta\perp}^{-}}{V_p + V_n} Q_{ref} \qquad (5.32)$$

$$\begin{bmatrix} V_{\alpha\perp} \\ V_{\beta\perp} \end{bmatrix} = \begin{bmatrix} 0 & -1 \\ 1 & 0 \end{bmatrix} \begin{bmatrix} V_{\alpha} \\ V_{\beta} \end{bmatrix} \qquad (5.33)$$

Where, $v_{\alpha\perp}$ and $v_{\beta\perp}$ are orthogonal voltages (90° -lead) of SRF voltage vector.

$$i_{\alpha P} = \frac{v_{\alpha}^{+} - v_{\alpha}^{-}}{\left(v_{\alpha}^{+2} + v_{\beta}^{+2}\right) + k_{\beta P}\left(v_{\alpha}^{-2} + v_{\beta}^{-2}\right)} P_{ref} \qquad (5.34)$$

$$i_{\beta P} = \frac{v_{\beta}^{+} - v_{\beta}^{-}}{\left(v_{\alpha}^{+2} + v_{\beta}^{+2}\right) + k_{\beta P}\left(v_{\alpha}^{-2} + v_{\beta}^{-2}\right)} P_{ref} \qquad (5.35)$$

$$i_{\alpha Q} = \frac{v_{\alpha\perp}^{+} - v_{\alpha\perp}^{-}}{\left(v_{\alpha\perp}^{+2} + v_{\beta\perp}^{+2}\right) + k_{\alpha Q}\left(v_{\alpha\perp}^{-2} + v_{\beta\perp}^{-2}\right)} Q_{ref} \qquad (5.36)$$

$$i_{\beta Q} = \frac{v_{\beta\perp}^{+} - v_{\beta\perp}^{-}}{\left(v_{\alpha\perp}^{+2} + v_{\beta\perp}^{+2}\right) + k_{\beta Q}\left(v_{\alpha\perp}^{-2} + v_{\beta\perp}^{-2}\right)} Q_{ref} \qquad (5.37)$$

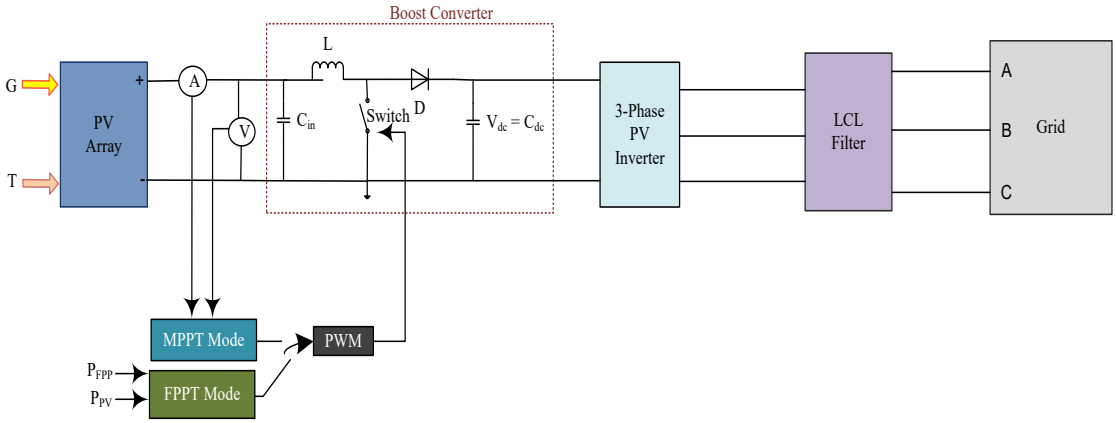


Fig. 5.1. Schematic Diagram of the FPPT algorithm.

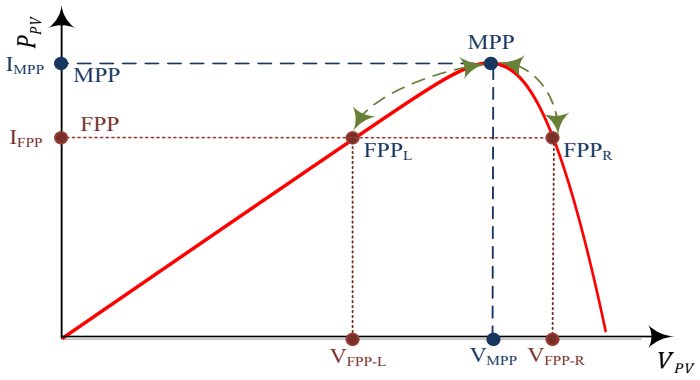


Fig. 5.2. P-V curve for constant power generation (CPG)

Table 5.1. Specifications of PV module

PV Panel Parameters	Specifications
P_{max} (W)	220.99
N_{cell}	60
V_{oc} (V)	36.6
I_{sc} (A)	8.2
V_{MPP} (V)	28.7
I_{MPP} (A)	7.7

Table 5.2. Specifications of Boost Converter

Components	Specifications
Capacitor C_{in} (µF)	99.95
Inductor L (mH)	15.39
Switch	1N5817
Diode D	IRFP460
Capacitor C_{out} (mF)	30.26
Switching Frequency (kHz)	20

5.3. FPPT Techniques

This section contains the detailed explanation of existing FPPT techniques. The power and current based FPPT techniques are taken in

consideration to carry out comparative study. The basic structure of current based and power based FPPT method is depicted in Fig. 5.3 & 5.4.

The current control based FPPT method works on current strategy. The PV voltage and current is used to evaluate power. The MPPT current and current limit are used as the input parameters of saturation block to measure the current limit. The reference current and PV panel current are compared and fed to PI controller. PI controller is used to generate the PWM pulses based on these calculations. The control structure of the same is depicted in Fig. 5.3 (Pathak et al., 2024; Saberi et al., 2023).

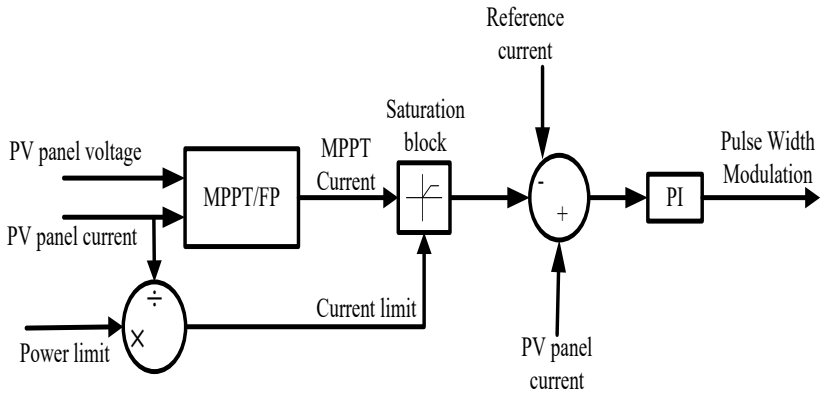


Fig. 5.3. Control structure of Current based FPPT method

The power based FPPT method is working on the power control strategy. By measuring current and voltage from PV panels MPPT/FP mode is performed and MPPT current is evaluated. Because of current and voltage values power is calculated. The saturation block is used to calculate the reference power by utilizing MPPT power and power limit as input parameters in saturation block. Reference power is further compared with PV power and the resultant power is fed to PI control. The control structure of the same is presented in Fig. 5.4 (Kumar Nayak et al., 2023).

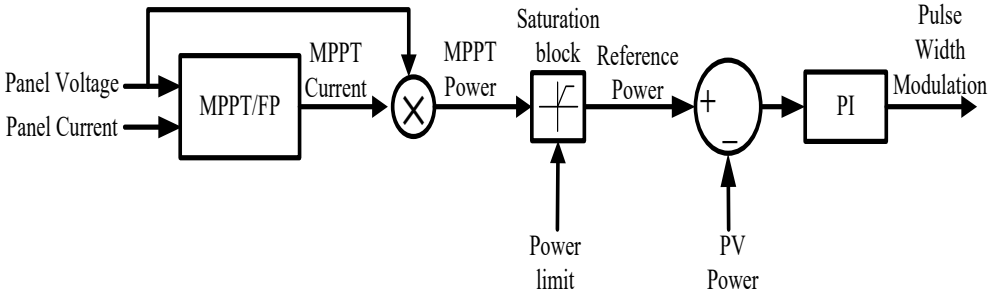


Fig. 5.4. Control structure of Power based FPPT method

5.4. Proposed Algorithm

This section contains the detailed explanation of proposed flexible power point tracking (FPPT) algorithm. Under normal operating conditions PV systems operates at maximum power point tracking (MPPT). MPPT is used to extract maximum power from the PV panels and its works on maximum transfer theorem. But at the time of disturbance in grid there is a need to stabilize the grid-connected PV systems which can be achieved by moving towards flexible power point tracking (FPPT).

The proposed technique is majorly focused on the dual perturbation FPPT control strategy. The algorithm is designed and simulated on MATLAB/Simulink.

When $\frac{dP}{dV} > 0$ then current control strategy will be used to track flexible power point (FPP) and when $\frac{dP}{dV} < 0$ then voltage control strategy will be used to achieve FPP. In other words, it can be concluded that on the left side of the trail FPP is reached based on voltage, and current is used to calculate FPP on the right side of the trail. The pictorial representation of the same is illustrated in current vs voltage (I-V) curve and power vs voltage (P-V) curve (Fig. 5.5).

Moreover, the flowchart of the same is depicted in Fig. 5.6.

Grid codes are mentioned in Eq. (5.38)

$$\begin{Bmatrix} Q_{ref} = 0, & if\ V_{pu} > 0.9 \\ Q_{ref} = S \times 1.5 \times (0.9 - V_{pu}), & if\ 0.2 < V_{pu} > 0.9 \\ Q_{ref} = 1.05 \times S, & if\ V_{pu} > 0.2 \end{Bmatrix} \quad (5.38)$$

So, V_{pu} is evaluated using Eq. mentioned below:

$$V_{pu} = \frac{\sqrt{v_{\alpha}^2 + v_{\beta}^2}}{V_b} \quad (5.39)$$

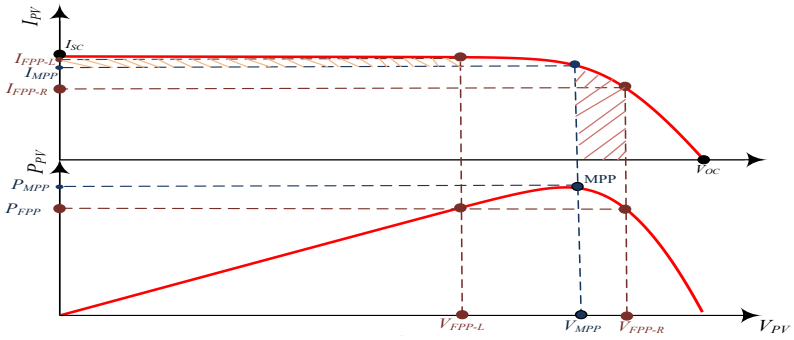


Fig. 5.5. Current vs Voltage (I-V) and Power vs Voltage (P-V) curve at maximum power point (MPP) and flexible power point (FPP)

Moreover, the flowchart of the proposed dual perturbation based FPPT algorithm is presented in Fig. 5.6. The current (I_{PV}), voltage (V_{PV}) are measured from the PV panel and using these values PV power (P_{PV}) will be calculated. Firstly mode of operation will be selected. If it is MPPT mode then proposed MPPT algorithm will operate (illustrated in Fig. 5.8.). If the mode of operation is CPG, then measurement of voltage (V_{ref}) and current (I_{ref}) perturbation will be done. Further, change in voltage ($\Delta V_{PV} = V_{old1} - V_{old}$), change in power ($\Delta P_{PV} = P_{old1} - P_{old}$) and change in reference power ($\Delta P_{ref} = P_{refold1} - P_{refold}$) will be calculated. Then it will test the condition that if $\frac{dP}{dV} > 0$ is true then current will be incremented else voltage will increment. To perform this dual perturbation a switch is used which will decide whether

voltage control will work or current control will work. The schematic diagram of the same is shown in Fig. 5.7.

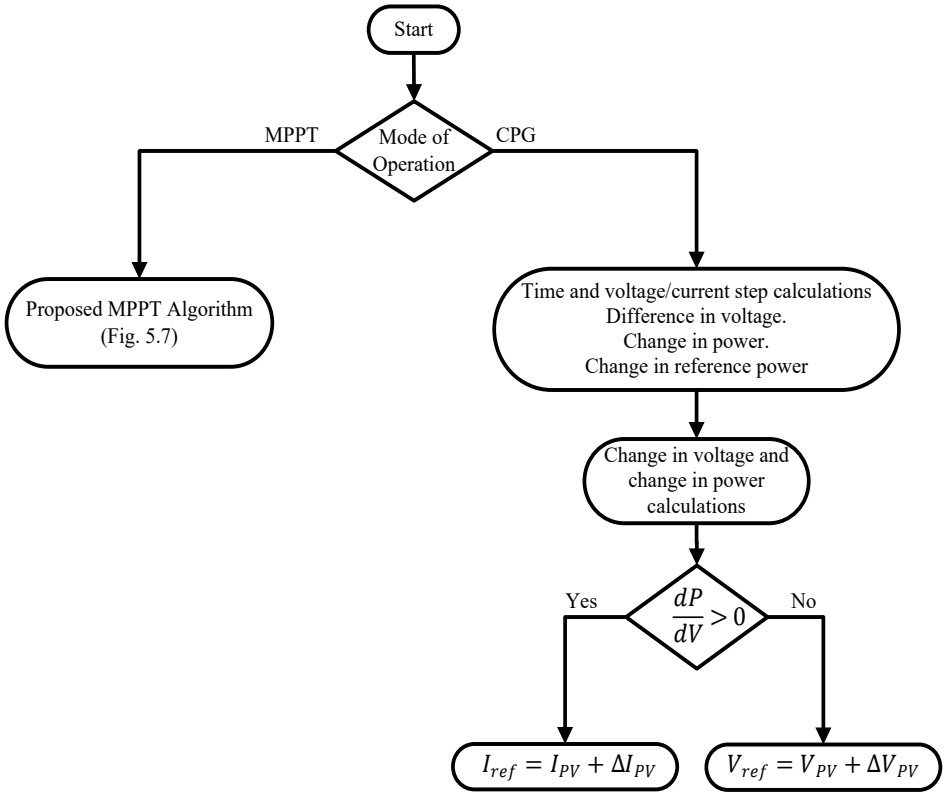


Fig. 5.6. Flowchart of proposed FPPT algorithm

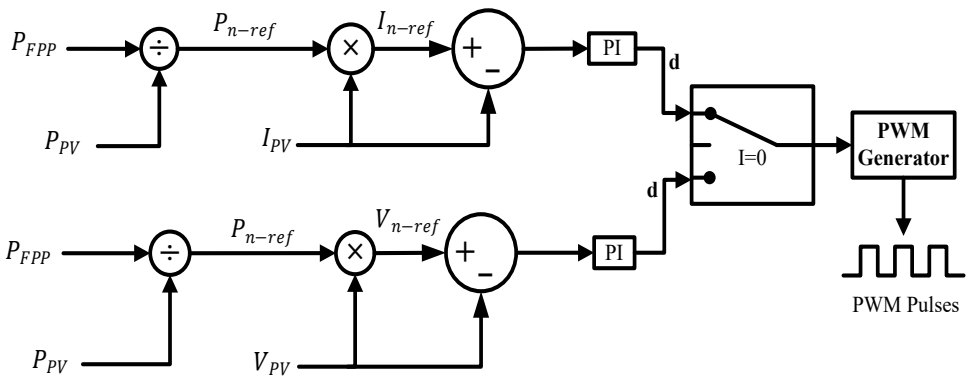


Fig. 5.7. Schematic Diagram of the FPPT algorithm.

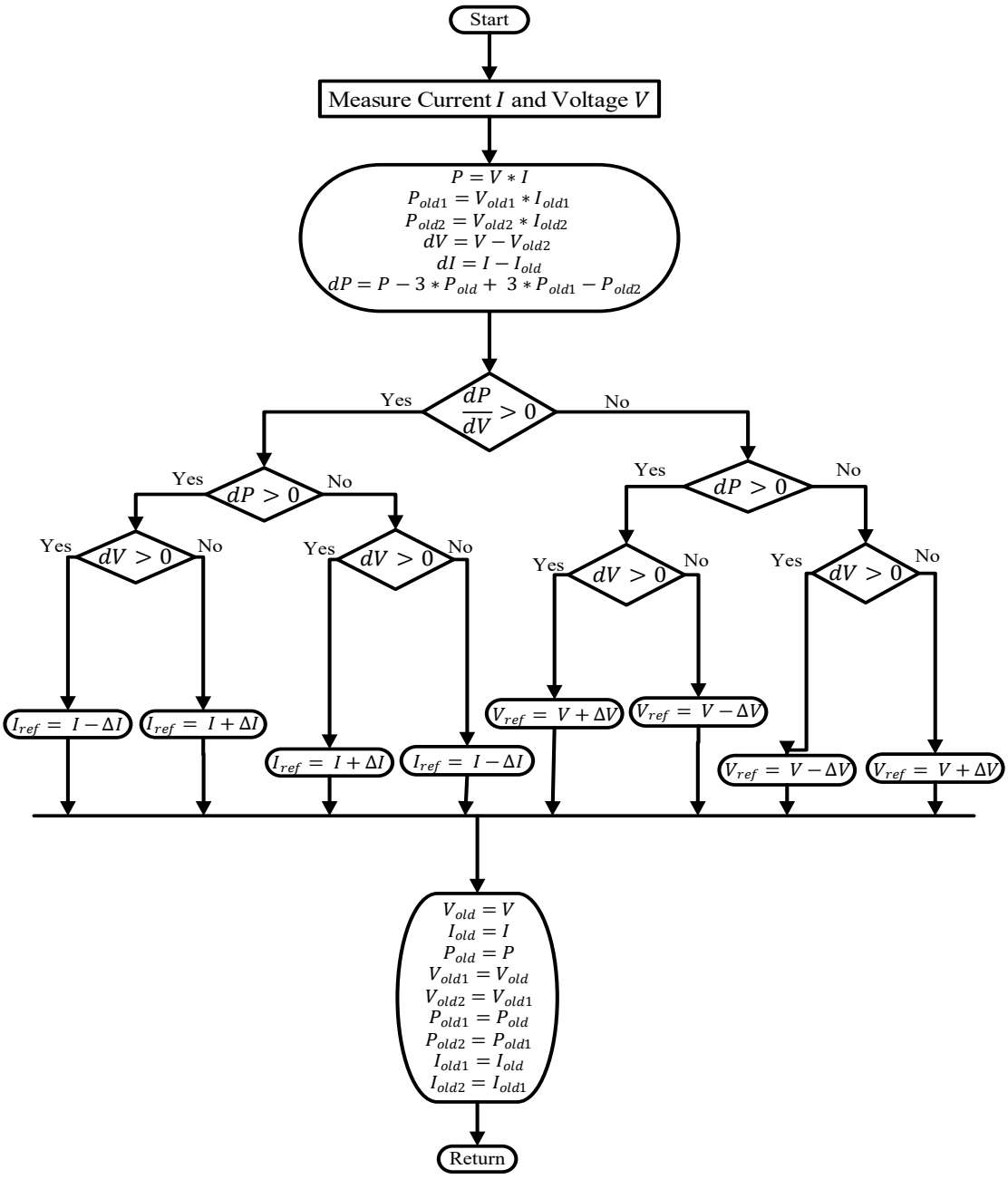


Fig. 5.8. Flowchart of proposed MPPT algorithm

5.5. Result and Discussion

Detailed results and discussion are provided in this section. A state-of-the-art power- and current-based FPPT method is implemented using

MATLAB/Simulink for 500 and 1000 W/m^2 irradiance patterns with rapid STC irradiance change, using current, voltage, and power curves to analyze the suggested method. For each analysis, response time, steady-state oscillations, and tracking efficiency are calculated. Different irradiance analysis is explained in the two subsections below. The voltage ride-through fault at 0.35s is considered. As seen in Fig. 5.9, this fault uses single-phase voltage dip.

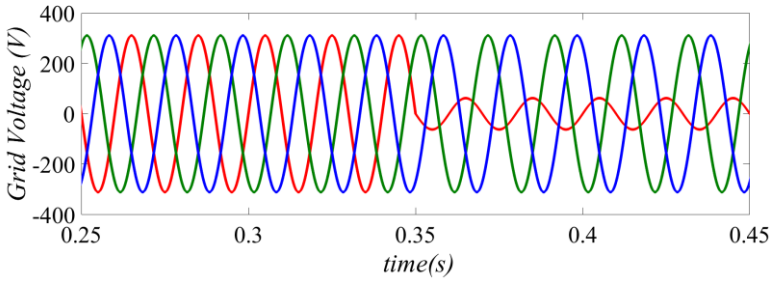


Fig. 5.9. Three-phase grid voltage

5.5.1. Irradiance - 1000 W/m^2

The state-of-the-art current and power-based FPPT algorithms and proposed algorithm are implemented under STC on 1000W/m^2 irradiance. Quantitative and pictorial results are shown. Fig. 5.10 shows how voltage, current, and power curves are used to provide graphical results. V-t, I-t, and P-t curves of current-based FPPT method are illustrated in Fig. 5.10 (a)-(c). Fig. 5.10 (d)-(f) shows power-based FPPT method V-t, I-t, and P-t curves. The dual perturbation-based FPPT algorithm's V-t, I-t, and P-t curves are shown in Fig. 5.10 (g)-(i). These quantitative data are shown in Table 5.3. The suggested FPPT algorithm has the highest tracking efficiency (99.76%), response time (15 ms), and minimum steady-state oscillations.

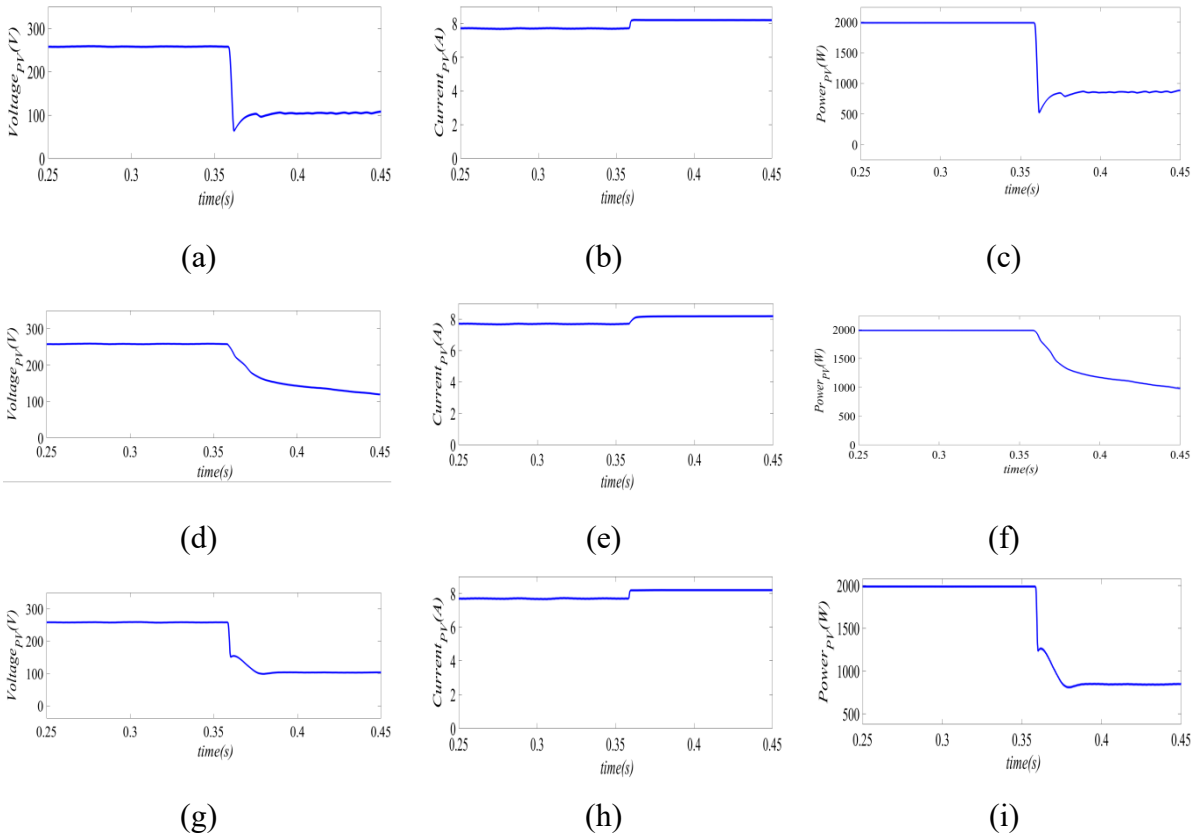


Fig. 5.10. a) Voltage, b) current and c) power vs time curve for current based FPPT algorithm, 10. d) Voltage, e) current and f) power vs time curve for power based FPPT algorithm, 10. g) Voltage, h) current and i) power vs time curve for proposed FPPT algorithm at 1000W/m^2.

Table 5.3. Performance Parameters of Algorithms 1000W/m^2

Algorithm	Response-time(ms)	Steady-state Oscillations	Tracking Efficiency (%)
Current based	28	1.06	98.41
Power based	41	1.02	97.13
Proposed	15	0.8	99.76

5.5.2. Irradiance - 500 W/m^2

In this subsection, the state-of-art current and power based FPPT algorithm and proposed FPPT algorithm is realized on 500W/m^2 irradiance condition under STC. The results are realized graphically and quantitatively. Graphical results are realized on the basis of voltage vs time (V-t), current vs time (I-t) and power vs time (P-t) curves which are illustrated in Fig. 5.11. The V-t, I-t and P-t curves of current based FPPT algorithm are shown in Fig. 5.11 (a)-(c) respectively. While V-t, I-t and P-t curves for power based FPPT algorithm are illustrated in Fig. 5.11 (d)-(f). Similarly, Fig. 5.11 (g)-(i) shows the V-t, I-t and P-t curves of proposed dual perturbation based FPPT algorithm. The quantitative results for same are depicted in Table 5.4. Among all, proposed FPPT algorithm show the maximum tracking efficiency of 99.87 %, response time of 3 ms and low steady-state oscillations.

Table 5.4. Performance Parameters of Algorithms for 500W/m^2

Algorithm	Response-time (ms)	Steady-state Oscillations	Tracking Efficiency
Current based	8	1.02	98.07
Power based	12	1.01	96.51
Proposed	3	0.6	99.87

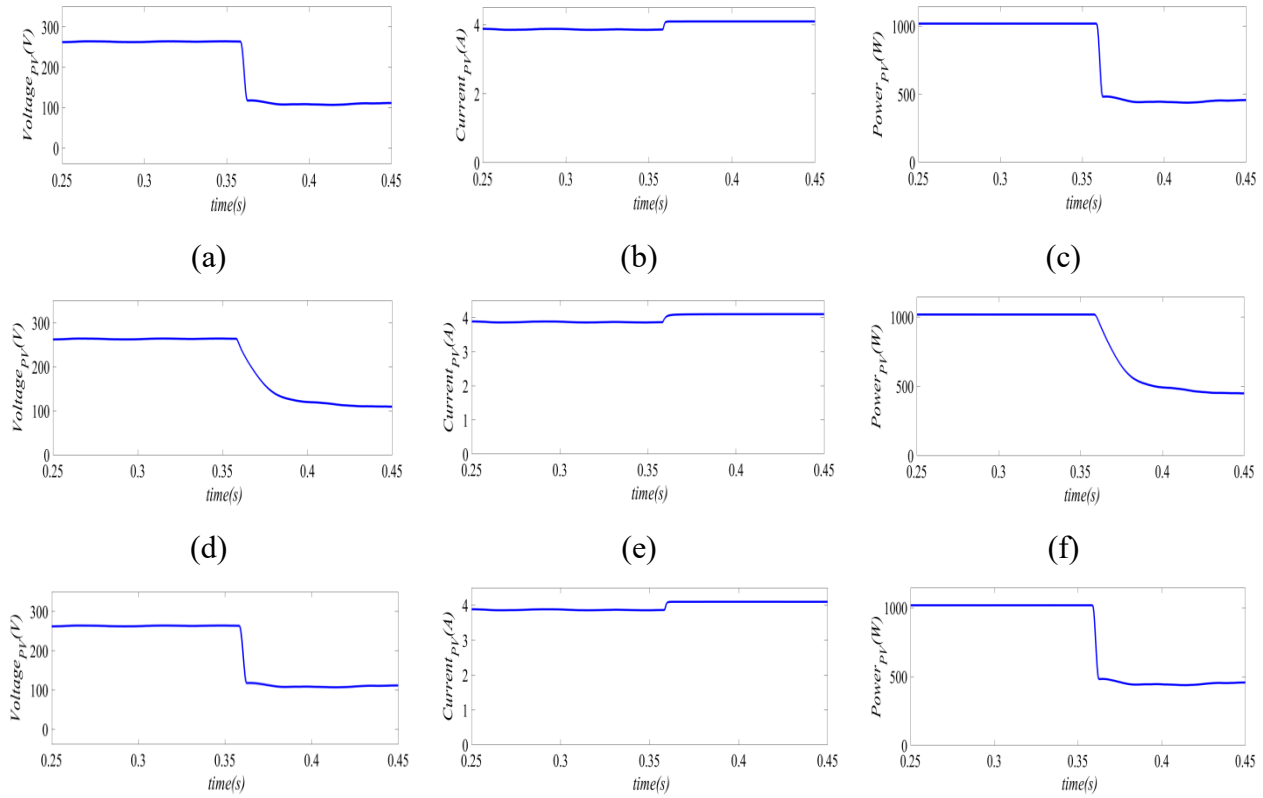


Fig. 5.11. a) Voltage, b) current and c) power vs time curve for current based FPPT algorithm, 11. d) Voltage, e) current and f) power vs time curve for power based FPPT algorithm, 11. g) Voltage, h) current and i) power vs time curve for proposed FPPT algorithm at 500 W/m^2.

5.5.3. Step Increase-in Irradiance Pattern

In this subsection, the state-of-art current and power based FPPT algorithm and proposed FPPT algorithm is realized on step increase-in irradiance condition under STC as depicted in Fig. 5.12. The results are realized graphically and quantitatively. Graphical results are realized on the basis of voltage vs time (V-t), current vs time (I-t) and power vs time (P-t) curves which are illustrated in Fig. 5.13. The V-t, I-t and P-t curves of current based FPPT algorithm are shown in Fig. 5.13 (a)-(c) respectively. While V-t, I-t and P-t curves for power based FPPT algorithm are illustrated in Fig. 5.13 (d)-(f). Similarly, Fig. 5.13 (g)-(i) shows the V-t, I-t and P-t curves of proposed dual perturbation based FPPT algorithm. In the beginning, 1000 W of power is produced, however when a fault occurs at 0.35 s, only 430 W of power is produced. With a 1s change in irradiance from 500W/m^2 to 1000W/m^2, 860 W is achieved at 1000W/m^2.

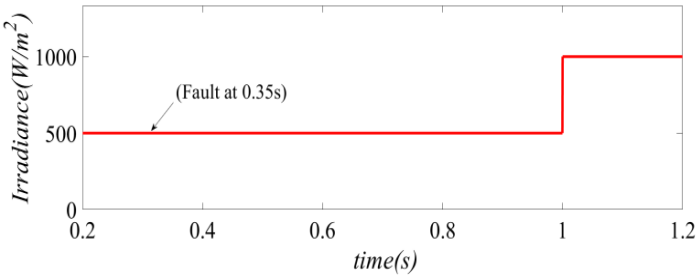


Fig. 5.12. Step increase-in irradiance pattern

Table 5.5. Performance Parameters for Step increase-in pattern

Algorithm	Response-time (ms)			Steady-state Oscillations	
	5000 W/m^2	At Fault	1000 W/m^2	500 W/m^2	1000 W/m^2
Current based	8	3	27	1.04	1.08
Power based	14	3	39	1.01	1.03
Proposed	4	2	11	0.8	0.91

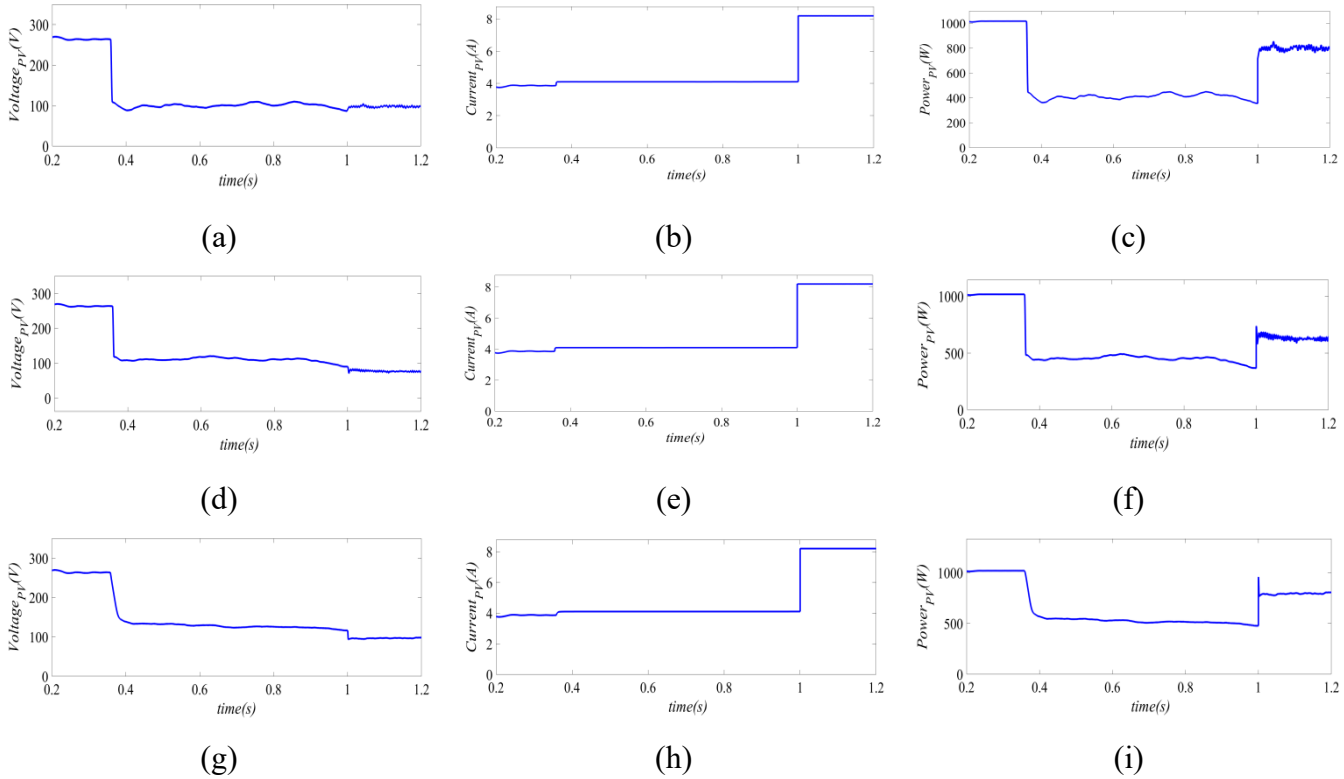


Fig. 5.13. a) Voltage, b) current and c) power vs time curve for current based FPPT algorithm, 13. d) Voltage, e) current and f) power vs time curve for power based FPPT algorithm, 13. g) Voltage, h) current and i) power vs time curve for proposed FPPT algorithm.

The quantitative results for same are depicted in Table 5.5. Among all, proposed FPPT algorithm show the maximum tracking efficiency of 99.75% and 99.55% achieved at 500W/m^2 and 1000W/m^2 irradiance profile respectively and very low steady-state oscillations (0.8% at 500W/m2 and 0.91% at 1000W/m^2).

5.5.4. Step Decrease-in Irradiance Pattern

In this subsection, the state-of-art current and power based FPPT algorithm and proposed FPPT algorithm is realized on step decrease-in irradiance condition under STC as depicted in Fig. 5.14. The results are realized graphically and quantitatively. Graphical results are realized on the basis of voltage vs time (V-t), current vs time (I-t) and power vs time (P-t) curves which are illustrated in Fig. 5.15. The V-t, I-t and P-t curves of current based FPPT algorithm are shown in Fig. 5.15 (a)-(c) respectively. While V-t, I-t and P-t curves for power based FPPT algorithm are illustrated in Fig. 5.15 (d)-(f). Similarly, Fig. 5.15 (g)-(i) shows the V-t, I-t and P-t curves of proposed dual perturbation based FPPT algorithm.

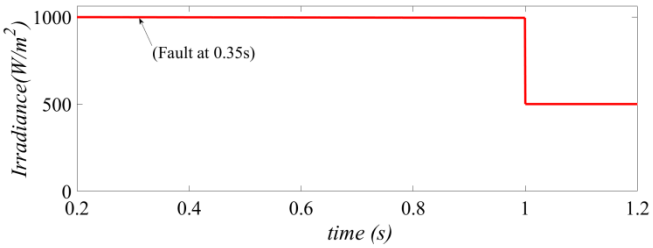


Fig. 5.14. Step decrease-in irradiance pattern

Table 5.6. Performance Parameters for Step increase-in pattern

Algorithm	Response-time (ms)			Steady-state Oscillations	
	1000 W/ m^2	At Fault	500 W/ m^2	1000 W/ m^2	500 W/ m^2
Current based	20	2	8	1.02	0.96
Power based	31	2	12	1.01	0.91
Proposed	7	1	4	0.78	0.61

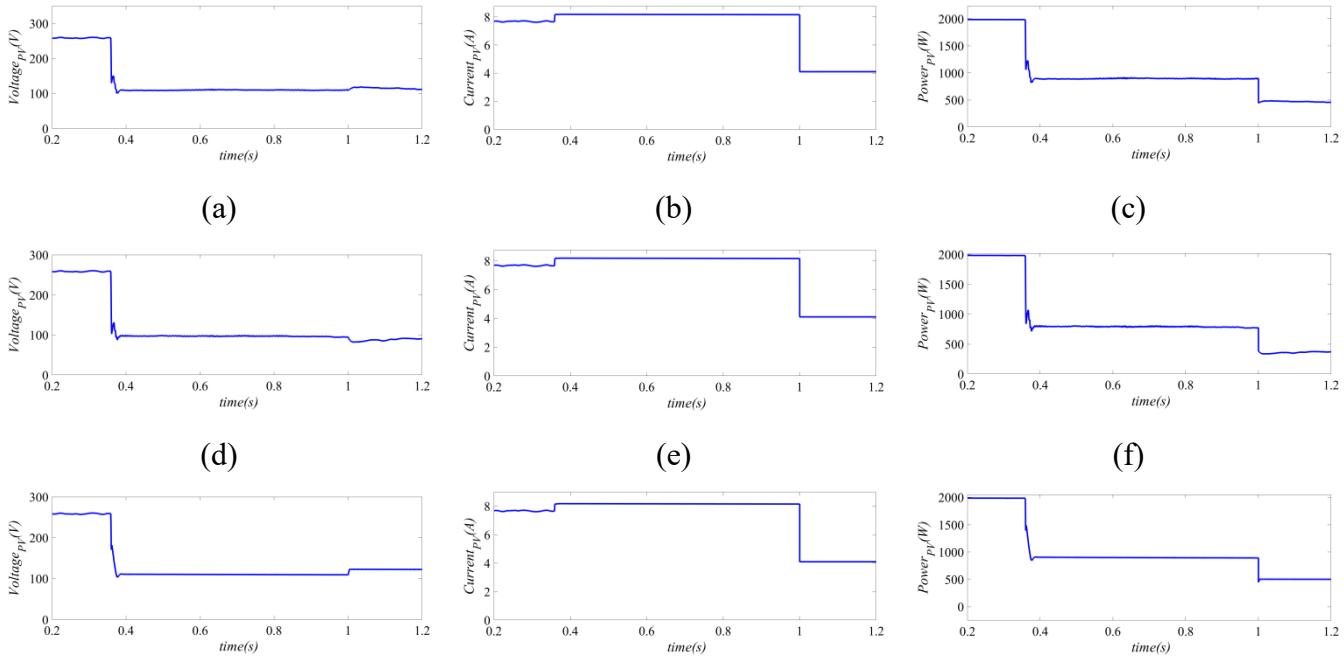


Fig. 5.15. a) Voltage, b) current and c) power vs time curve for current based FPPT algorithm, 15. d) Voltage, e) current and f) power vs time curve for power based FPPT algorithm, 15. g) Voltage, h) current and i) power vs time curve for proposed FPPT algorithm.

It has been realized that initially power 2000 W is achieved but when fault occurs at 0.35s 860W power is obtained. The irradiance is rapidly changed at 1s from 1000W/m2 to 500 W/m2 so 430 W is obtained at 1000W/m2. The quantitative results for same are depicted in Table 5.6. Among all, proposed FPPT algorithm shows the maximum tracking efficiency of 99.85% and 99.71% achieved at 500W/m2 and 1000W/m2 irradiance profile, respectively and very low steady-state oscillations such as 0.78% and 0.61 is achieved at 1000W/m2 and 500W/m2, respectively.

5.5.5. Comparative Analysis

A comparative analysis is performed on power-based, current-based, and the proposed dual perturbation-based FPPT algorithms to assess critical performance metrics including control strategy, operating region, drift occurrence, robustness, reactive power management, tracking speed, steady-state oscillations, implementation complexity, stability, dynamic response rate, cost, and tracking efficiency. The qualitative data is represented in Fig. 5.16 and Table 5.7 as table of taxonomy. Similarly, quantitative analysis is realized based on response time, steady-state oscillations and tracking efficiency which is illustrated in Fig. 5.17, 5.18 & 5.19 and Table 5.8. Among all, proposed dual perturbation based FPPT algorithms attains maximum efficiency of 99.87%, 3 ms response time and 0.6% steady-state oscillations.

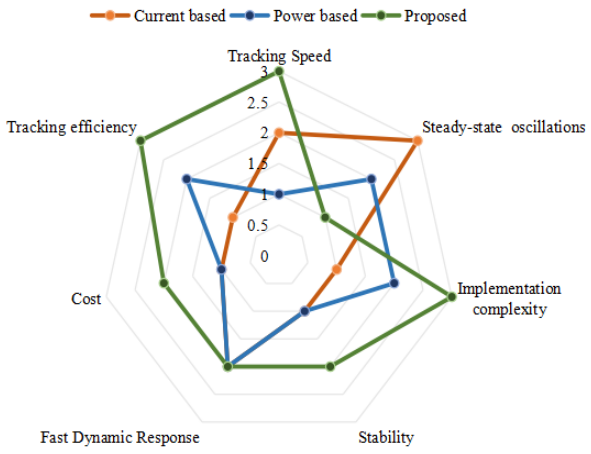


Fig. 5.16. Radial response behaviour for comparative study

A significant improvement of 0.09%, 0.46% and 3.36% is observed in response time, steady-state oscillations and tracking efficiency of proposed method when compared to power based FPPT method. While, with respect to current 0.05%, 0.42% and 1.8% improvement is realized in response time, steady-state oscillations and tracking efficiency.

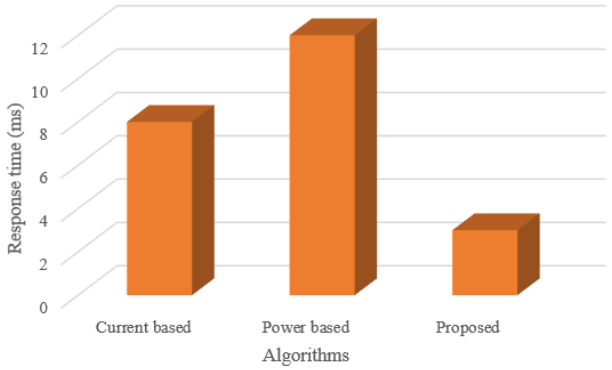


Fig. 5.17. Response time graph for various algorithms

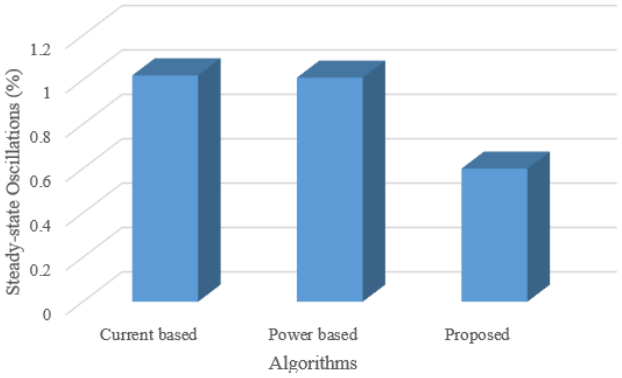


Fig. 5.18. Steady-state oscillations graph for various algorithms

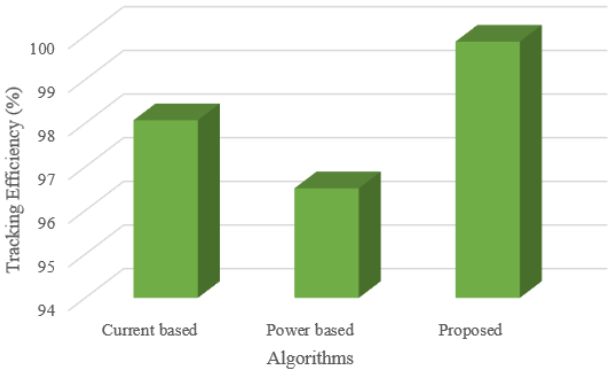


Fig. 5.19. Tracking efficiency graph for various algorithms

Table 5.7. Table of taxonomy based on comparative analysis

Algorithms	Control strategy	Operation Region	Drift occurrence	Robustness	Reactive Power	Tracking Speed	Steady-state oscillations	Implementation complexity	Stability	Fast Dynamic Response	Cost	Tracking efficiency
Current based	Power	Right	×	×	✓	M	H	L	L	M	L	L
Power based	Current	Right	×	×	✓	L	M	M	L	M	L	M
Proposed	Voltage and Current	Both	✓	✓	✓	H	L	H	M	L	M	H

* L: Low, M: Medium, H: High

Table 5.8. Performance Parameters of Algorithms

Algorithm	Response-time (ms)	Steady-state Oscillations	Tracking Efficiency
Current based	8	1.02	98.07
Power based	12	1.01	96.51
Proposed	3	0.6	99.87

5.6. Summary

This study focuses on the analysis of the non-drifting flexible power point tracking (FPPT) algorithm for grid-connected solar systems.

- In this work, a state-of-art current and power based FPPT algorithm and proposed dual perturbation based FPPT algorithm are designed and implemented on MTALB/Simulink.

- The algorithms are realized based on voltage vs time (V-t), current vs time (I-t) and power vs time (P-t) curves graphically for 100 W/m^2 and 500 W/m^2 irradiance conditions. Moreover, step increase in and step decrease in irradiance patterns are considered to perform the rapid change in irradiance analysis.

- Among all, the proposed dual perturbation based FPPT algorithm excels with the 3 ms response time, low steady-state oscillations and 99.87 % tracking efficiency as compared to other FPPT algorithms.

- Moreover, response time, steady-state oscillations and tracking efficiency is also realized to perform the quantitative analysis for the same. A significant improvement of 0.09%, 0.46% and 3.36% is observed in response time, steady-state oscillations and tracking efficiency of proposed method when compared to power based FPPT method. While, with respect

to current 0.05%, 0.42% and 1.8% improvement is realized in response time, steady-state oscillations and tracking efficiency.

- The computational complexity of the proposed dual perturbation-based FPPT algorithm is relatively low, as it primarily involves iterative voltage and power updates without requiring heavy mathematical operations or extensive data storage. The algorithm executes simple perturbation and comparison steps in real time, making it suitable for implementation in low-cost digital controllers. In terms of scalability, the proposed method can be effectively extended to larger grid-connected PV systems, as its modular structure allows independent optimization at the string or module level. The dual perturbation approach ensures faster convergence and reduced oscillations, which remain consistent even with the increasing size of the PV array. Additionally, the reduced computational overhead makes the method practical for large-scale systems where multiple MPPT units operate in parallel. However, communication and synchronization among distributed controllers in large installations may introduce latency, which can be mitigated with efficient coordination schemes. Overall, the algorithm maintains a balance between accuracy, speed, and hardware feasibility, ensuring adaptability for both small and utility-scale PV systems.

- The proposed work can be further carried forward for PV inverters and micro-grids.

The proposed FPPT techniques were first analyzed through simulation and their effectiveness in enhancing tracking speed and accuracy was demonstrated. It's difficult to validate the FPPT techniques on realistic environment. So, in the further chapter, the proposed MPPT techniques were

implemented on an experimental setup under varying irradiance and temperature conditions. The experimental results confirmed the reliability and robustness of the techniques in extracting optimum power from the PV system while maintaining grid stability. This seamless transition from FPPT analysis to MPPT experimental validation ensures a comprehensive evaluation of the proposed methods and highlights their practical applicability in real-time grid-connected PV environments.

CHAPTER 6

HARDWARE IMPLEMENTATION OF PROPOSED DUAL PERTURBATION BASED MPPT ALGORITHM UNDER CONTROLLED LAB ENVIRONMENT

This chapter outlines the implementation and validation of MPPT algorithms on experimental test bench. The algorithms are validated under realistic lab environment using a hardware experimental set up.

6.1.Introduction

Photovoltaic (PV) arrays and other renewable energy systems rely on MPPT to optimize power production in response to changing environmental circumstances. Despite fluctuations in load, temperature, and irradiance, MPPT ensures the PV system operates at its optimal efficiency. To enhance dynamic performance, MPPT systems typically employ a Proportional-Integral-Derivative (PID) controller, which provides a robust mechanism for fine-tuning the operating point. The PID controller consistently tracks the MPPT by uninterruptedly regulating the voltage or current, thereby minimizing any tracking errors.

Several crucial components are usually included in the hardware setup for a MPPT system with a PID controller. These include the PV array, a DC-DC converter, a microcontroller or digital signal processor. As a component of the feedback loop, the PID controller processes sensor data to ascertain the required modifications to the DC-DC converter's duty cycle. Solar power applications and other renewable energy systems cannot function without this configuration, which guarantees efficient and dependable energy collection.

6.2.MPPT PID Controller

MPPT stands for Maximum Power Point Tracking. It is a technique used in solar power systems to ensure the solar panel operates at its maximum power output. Since the power output of a solar panel depends on factors like sunlight intensity and temperature, MPPT adjusts the operating voltage to match the point where the solar panel delivers maximum power.

6.2.1. Boost Section and Output

A. Boost Converter

The boost converter steps up the solar panel voltage to the higher level needed for battery charging or grid integration. It generally consists of:

B. Solar Panel

Provides low DC voltage.

C. MPPT Controller

Maintains solar panel performance at optimal power output by continuously adjusting operating conditions to match the MPP under varying environmental factors.

D. Boost Converter

Steps up the voltage.

E. Inductor

Used in the boost converter for energy storage.

F. Switching Element (100NF10 N CHANNEL MOSFET)

Controls energy flow in the boost converter.

G. Diode

Ensures proper current direction.

H. Capacitor

Smoothens output.

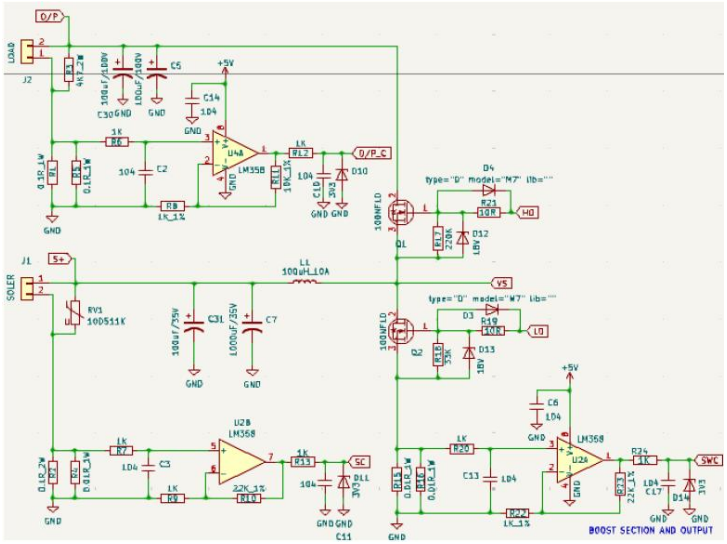


Fig. 6.1. Schematic diagram of boost converter and output

6.2.2. 1R2120 MOSFET Gate Driver IC

The 1R2120 is a MOSFET gate driver IC, designed to efficiently drive the gate of a MOSFET, particularly in high-speed switching applications. These types of ICs are crucial for controlling the operation of MOSFETs in numerous power electronics circuits, comprising DC-DC converters, motor drivers, and inverters.

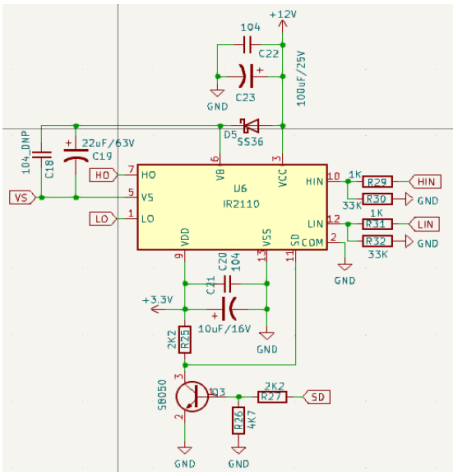


Fig. 6.2. Schematic diagram of MOSFET gate driver IC (1R2110)

6.2.3. MCU SECTION

A. Arm Cortex-M0+ Core

It operates at speeds up to 64 MHz, providing enough processing power to handle MPPT algorithms efficiently. The Cortex-M0+ core is energy-efficient, which is ideal for battery-powered or energy-sensitive applications like solar power systems.

B. Memory and Storage

32 KB Flash and 6 KB SRAM are available for storing the MPPT algorithm, configuration data, and control routines. Flash memory is sufficient for storing the MPPT firmware and any other application-specific code.

C. Analog-to-Digital Converters (ADC)

A 12-bit ADC with a sampling rate of up to 1 MSPS (million samples per second) is well-suited for measuring electrical performance (voltage and current) from the solar panel. High-resolution ADCs provide accurate

readings of voltage, essential for precise power calculation and MPP detection. MPPT algorithms like P&O or INC rely on accurate, real-time voltage and current data to effectively adjust the operating point.

D. PWM Output

The STM32G030K6T6 provides PWM outputs for driving the MOSFET gates in the DC-DC boost converter, which steps up the solar panel voltage to a usable level.

By adjusting the duty cycle of the PWM, the MCU can control the voltage and current going to the load or battery.

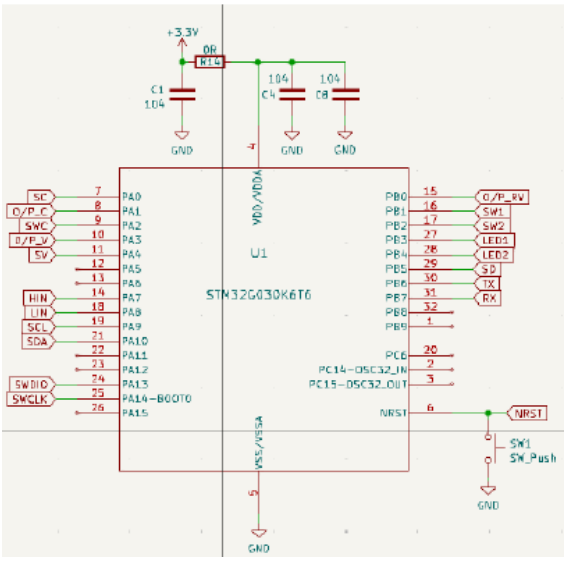


Fig. 6.3. Schematic diagram of MCU Section

6.2.4. SOLAR VOLTAGE SENSING

Solar Voltage Sensing refers to measuring the voltage output of a solar panel to monitor its performance and ensure efficient energy conversion. Using

47K and 4K7 resistors as a voltage divider reduces the input voltage, allowing safe voltage measurement for ADC reading.

6.2.5. OUTPUT VOLTAGE SENSING

Output Voltage Sensing in MPPT (Maximum Power Point Tracking) refers to measuring the electrical parameters (voltage at the output) of a solar panel or solar charge controller to optimize the power extraction. The LM358 Op-Amp is used to sense and amplify the output voltage from the solar panel in an MPPT system, providing a readable signal for the controller to adjust the operating point.

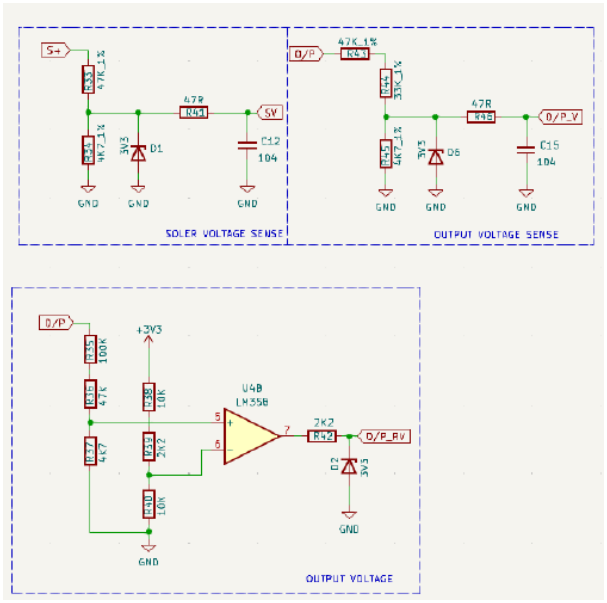


Fig. 6.4. Schematic diagram of Output Voltage Sensor

6.2.6. POWER SECTION

The 7805 Voltage regulator is a simple, widely used linear voltage regulator that converts a higher voltage (like 12V) down to a stable 5V output.

AMS1117 is a low dropout regulator that steps down the voltage from 5V to 3.3V.

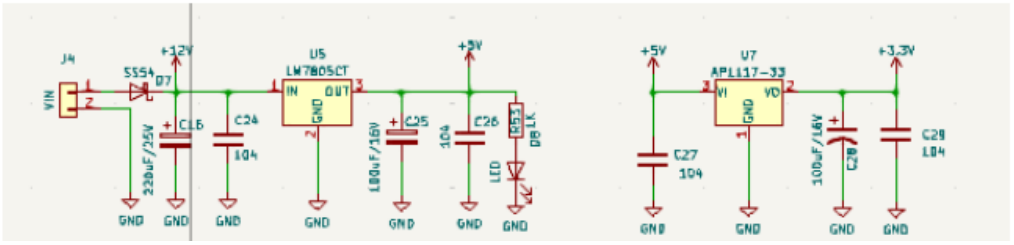


Fig. 6.5. Schematic diagram of Power Section

6.2.7. Universal Asynchronous Receiver-Transmitter (UART)

The STM32G030K6T6 generates PWM signals to control the MOSFET gates in the DC-DC boost converter, enabling voltage step-up from the solar panel to a usable level.

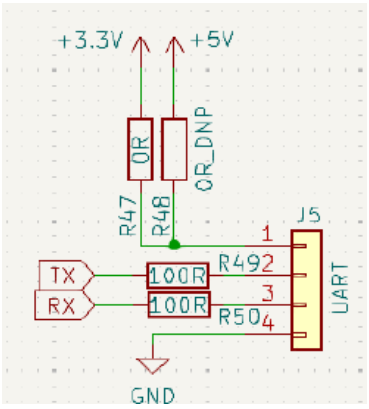


Fig. 6.6. Schematic diagram of UART

6.2.8. SWITCHES

A 10kΩ switch is used with a pull-up resistor to ensure a defined logic level when the switch is open, allowing the input to be pulled to a high voltage when not pressed.

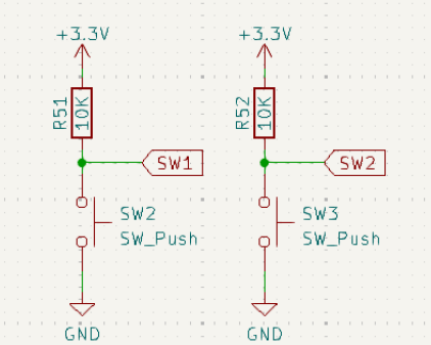


Fig. 6.7. Schematic diagram of Switches

6.2.9. LED'S

LED (Light Emitting Diode) is a semiconductor device that emits light when current flows through it. It is used for indication purposes.

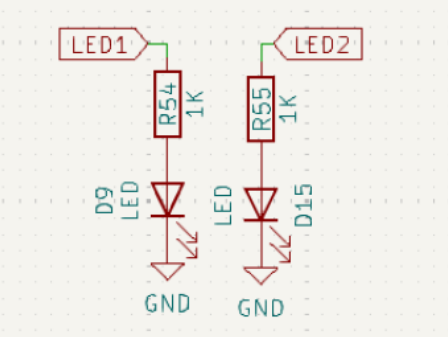


Fig. 6.8. Schematic diagram of LEDs

6.2.10. I2C

An OLED (Organic Light Emitting Diode) display using the I2C protocol allows easy integration of displays into microcontroller-based systems with minimal wiring. The OLED uses two wires for communication: SDA (Data) and SCL (Clock).

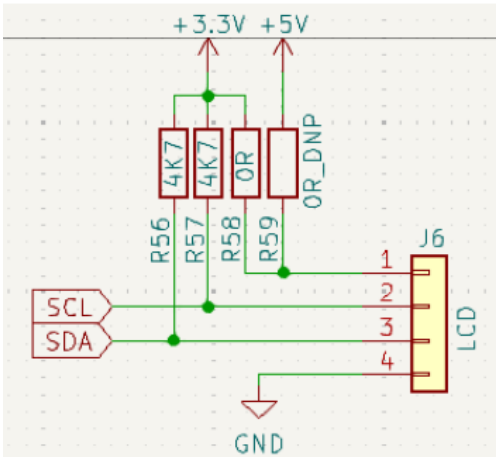


Fig. 6.9. Schematic diagram of I2C

The specification of the PV module and boost convertor are mentioned in table 6.1 & 6.2. To design this setup two PV panels has been used which are connected in parallel. The specification of the PV panel is mentioned in detail in table 6.1. The boost converter is designed using various components such as capacitors, inductor, switch and diode. The values of the same has been mentioned in table 6.2. The switching frequency is also mentioned. The switching frequency is 20KHz. The switching frequency depends on the desired output, input and power level, the components like capacitor and inductor and the switching losses associated with the switching device. As per all the components of boost convertor the switching frequency is 20KHz.

Table 6.1. Specifications of PV module

PV Panel Parameters	Specifications
P_{max} (W)	40.14
N_s	36
V_{oc} (V)	21.90
I_{sc} (A)	2.45
V_{MPP} (V)	17.40
I_{MPP} (A)	2.30

Table 6.2. Specifications of Boost Converter

Components	Specifications
Capacitor C_{in} (μF)	99.95
Inductor L (mH)	15.39
Switch	IGBT
Diode D	MOS-FET
Capacitor C_{out} (mF)	30.26
Switching Frequency (KHz)	20

Table 6.3. Specifications of PID Controller

Components	Specifications
Microcontroller (STM32G030K6T6)	ADC Ports (15) PWM Ports (8)
Current sensor	Using Shunt resistors
Voltage sensor	Using Voltage divider (47K)

6.3.Results and Discussion

This section explains about the results and discussion of experimental validation of proposed dual perturbation based MPPT algorithm in comparison with conventional P&O, adaptive P&O and drift-free P&O MPPT algorithms.

To make the PV array's total power bigger, two units are linked together in parallel. In Table 6.1, you can find information about the solar cells. The current and voltage readings are sent to the STM controller via voltage and current sensors whose specifications are given in Table 6.2. The PID controller have sixteen 16-bit ADC and DAC ports as well as six pulse width modulation ports, the latter of which is responsible for generating pulses in accordance with the duty cycle. Readings of the sensors' current and voltage are used to assess the PV system's power.

In contrast to the current sensor's 50 A maximum range, the voltage sensor is capable of measuring voltages up to 500 V. To transform the analogue signals detected by the voltage and current sensor into their digital equivalents, the RTS controller receives them through two separate ADC ports.

With the help of the PID device, the MPPT control method that was created in MATLAB/Simulink is checked in real time. To follow the MPP, the direction of the next disturbance is determined by the observed voltage and current values. The PID controller's pulse width modulation (PWM) port generates the pulses based on the duty cycle generated by the MPPT algorithm. These pulses are given to the MOSFET driver to drive the MOSFET switch which helps in impedance matching.

Using a programmable Ecosense PV emulator (IGE-PV4C400-001), the proposed approach was tested on a 40W monocrystalline PV module manufactured by Sri Sai Solar. The EN50530 irradiance profile is programmed on this PV emulator. Fixed, table, simulator, and programming modes are all available in PV emulator. We can check the MPPT control method we made in MATLAB/Simulink in real time with the help of the PID device. The hardware validation of the MPPT algorithms is accomplished using three experimental scenarios. The oscilloscope is used to record the waveforms in a csv file. To enhance the readability under dynamic change in irradiance, the csv file data is imported in MATLAB/Simulink environment to generate the plots. The complete experimental setup is shown in Fig. 6.10. The results are looked at at the input part of the boost converter because the main goal of the work is to look at how well the MPPT algorithms track, not how well they track across the output of the boost converter. The input side of the boost converter is used to test how well the MPPT methods work. To make a fast MPPT algorithm that

doesn't drift, the suggested MPPT algorithm is tested at the input of the dc-dc boost converter to see how well it works.

This makes sure that the MPPT algorithm's efficiency doesn't take into account the losses that happen in the boost converter.

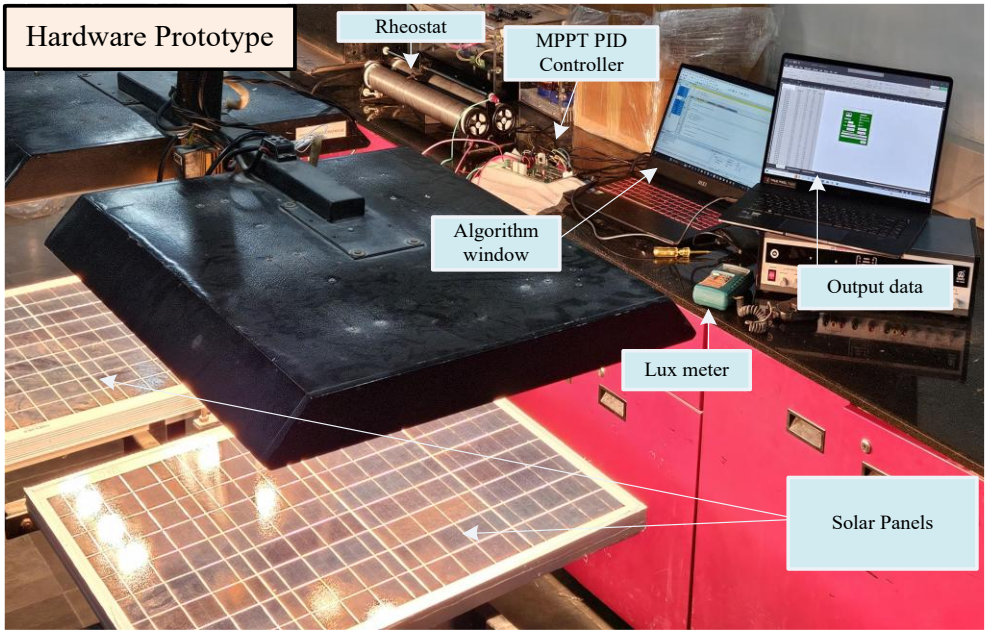


Fig. 6.10. Realistic view of Hardware Prototype

6.3.1. Irradiance at 270 W/m^2

The algorithms are realized at 270 W/m2 irradiance profile. The algorithms are analysed using PV parameters like current, voltage and power. The voltage vs time (V-t), current vs time (I-t) and power vs time (P-t) curve of the same is depicted in Fig. 6.11, 6.12 and 6.13 respectively.

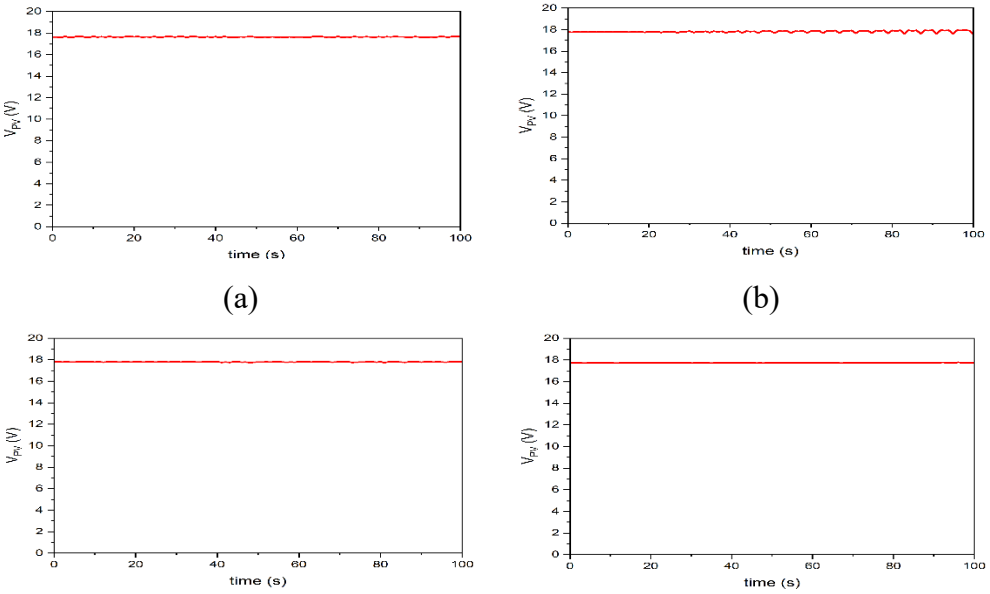


Fig. 6.11. Voltage response for a) P&O, b) Adaptive P&O, c) drift-free P&O and d) proposed dual perturbation based MPPT algorithms

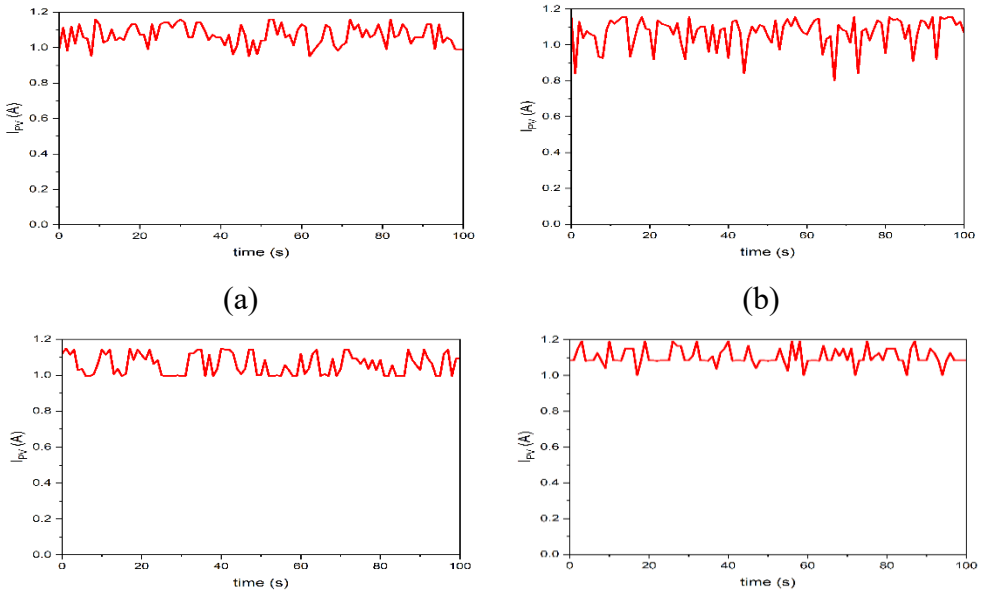


Fig. 6.12. Current response for a) P&O, b) Adaptive P&O, c) drift-free P&O and d) proposed dual perturbation based MPPT algorithms

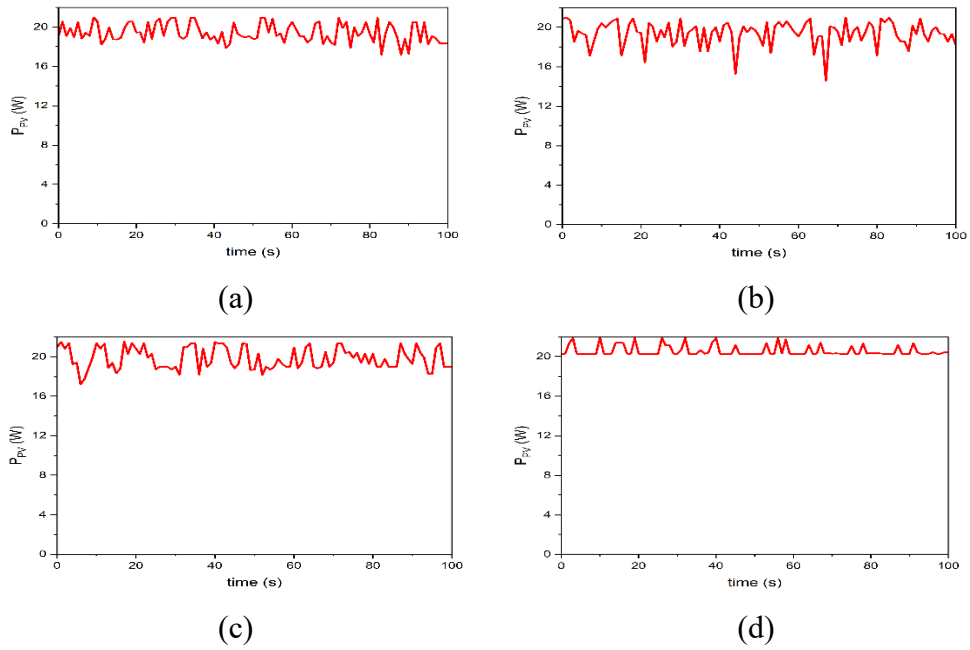


Fig. 6.13. Power response for a) P&O, b) Adaptive P&O, c) drift-free P&O and d) proposed dual perturbation based MPPT algorithms

6.3.2. Irradiance at 480 W/m^2

The algorithms are realized at 480 W/m^2 irradiance profile. The algorithms are analysed using PV parameters like current, voltage and power. The V-t, I-t and P-t curve of the same is depicted in fig. 6.14, 6.15 and 6.16 respectively.

The proposed MPPT algorithm has been thoroughly validated through experimental analysis conducted in a realistic laboratory environment. During the evaluation, the variation of voltage, current, and output power with respect to time was carefully observed and analyzed. The results clearly demonstrate that the proposed MPPT algorithm consistently achieves higher maximum power extraction compared to the conventional drift-free MPPT technique.

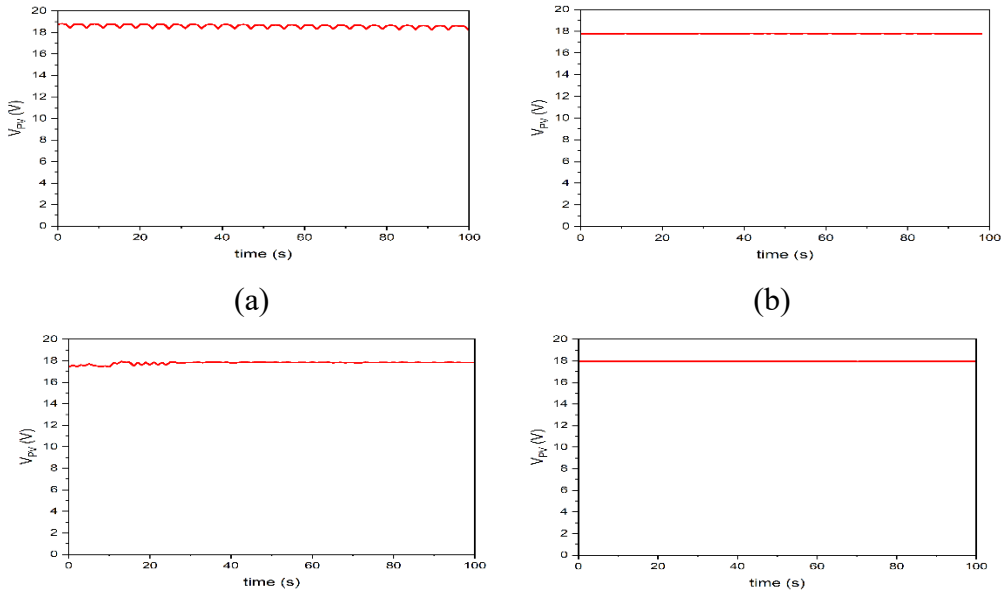


Fig. 6.14. Voltage response for a) P&O, b) Adaptive P&O, c) drift-free P&O and d) proposed dual perturbation based MPPT algorithms

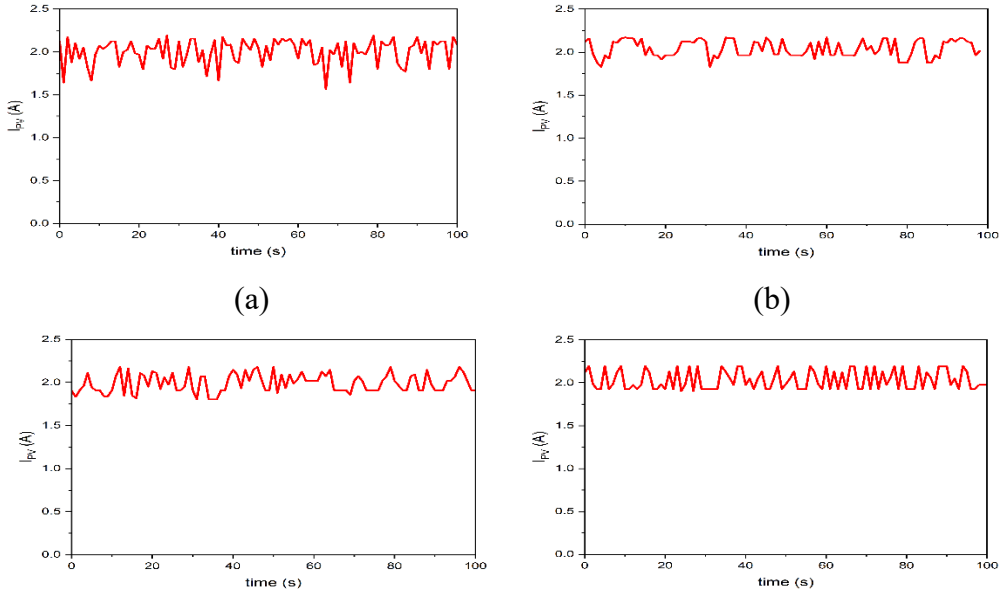


Fig. 6.15. Current response for a) P&O, b) Adaptive P&O, c) drift-free P&O and d) proposed dual perturbation based MPPT algorithms

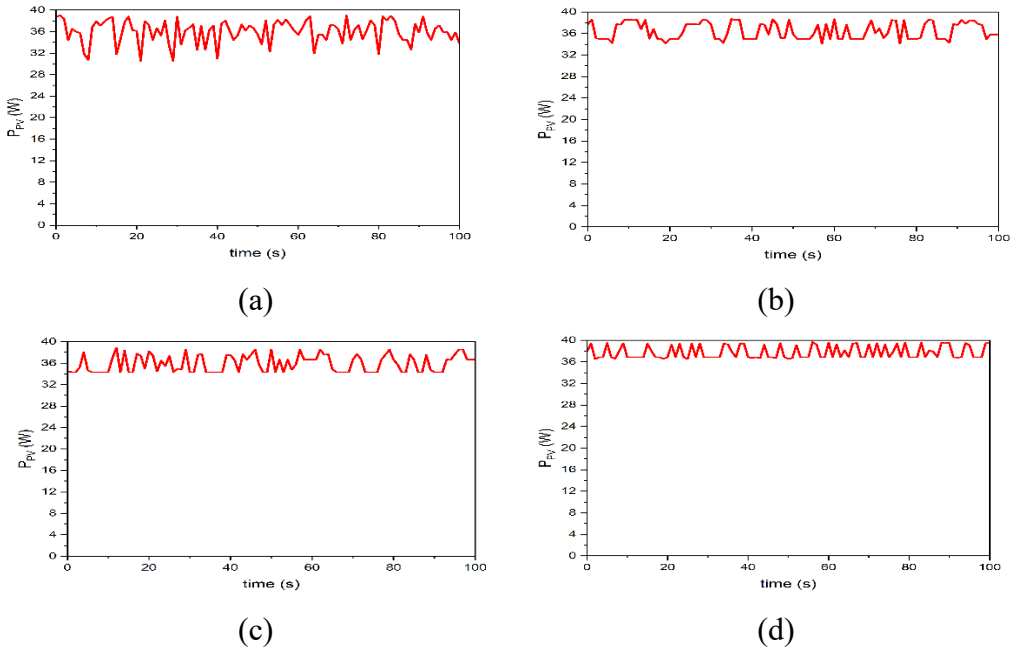


Fig. 6.16. Power response for a) P&O, b) Adaptive P&O, c) drift-free P&O and d) proposed dual perturbation based MPPT algorithms

This superior performance is primarily attributed to the higher voltage and current levels maintained by the proposed approach, which directly enhance the overall power output. Consequently, the proposed algorithm not only ensures more efficient power tracking but also outperforms other existing MPPT algorithms in terms of stability and effectiveness under practical operating conditions.

6.3.3. Step Increase-in Irradiance

The algorithms are realized at step increase-in irradiance profile. The algorithms are analysed using PV parameters like current, voltage and power. The V-t, I-t and P-t curve of the same is depicted in Fig. 6.17, 6.18 and 6.19 respectively.

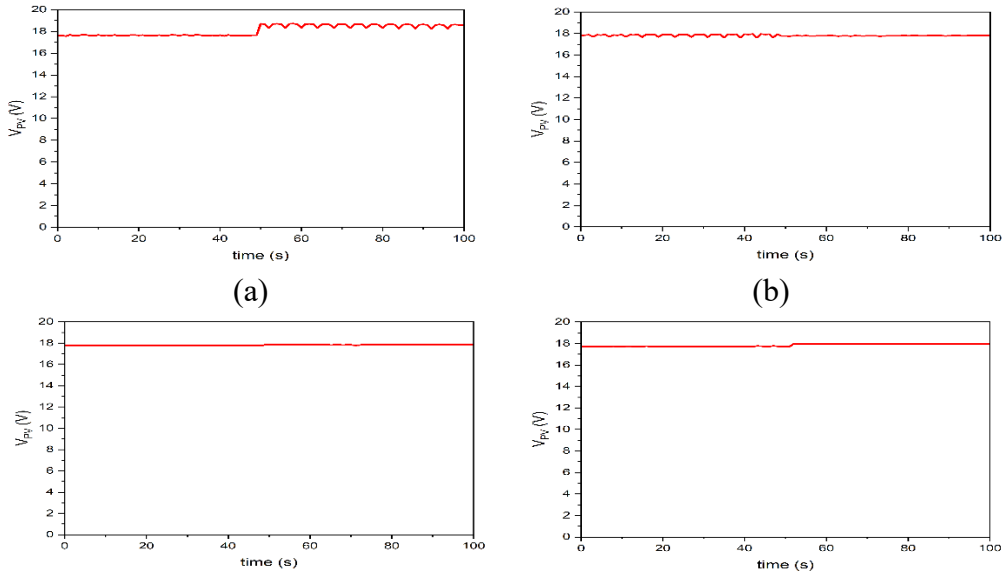


Fig. 6.17. Voltage response for a) P&O, b) Adaptive P&O, c) drift-free P&O and d) proposed dual perturbation based MPPT algorithms

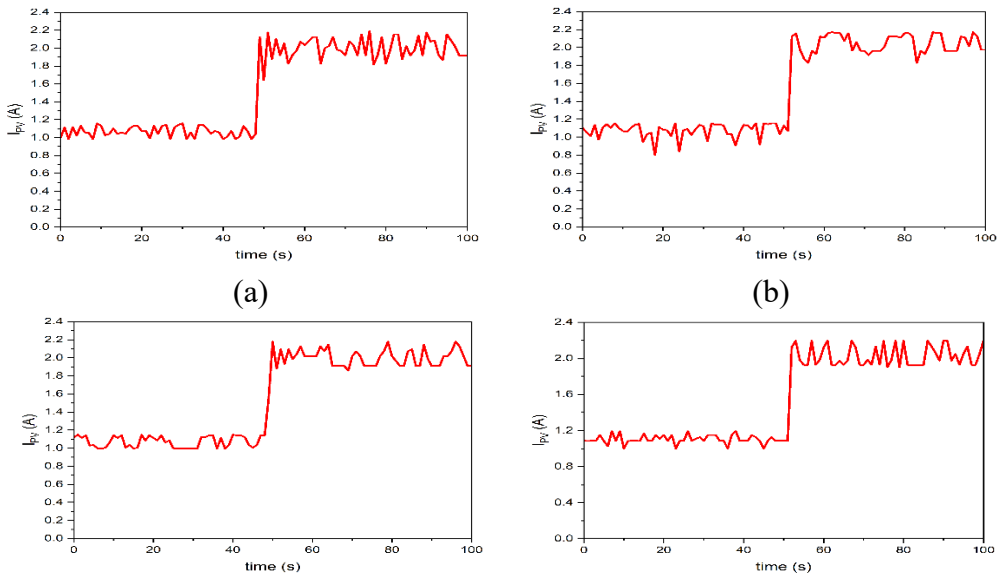


Fig. 6.18. Current response for a) P&O, b) Adaptive P&O, c) drift-free P&O and d) proposed dual perturbation based MPPT algorithms

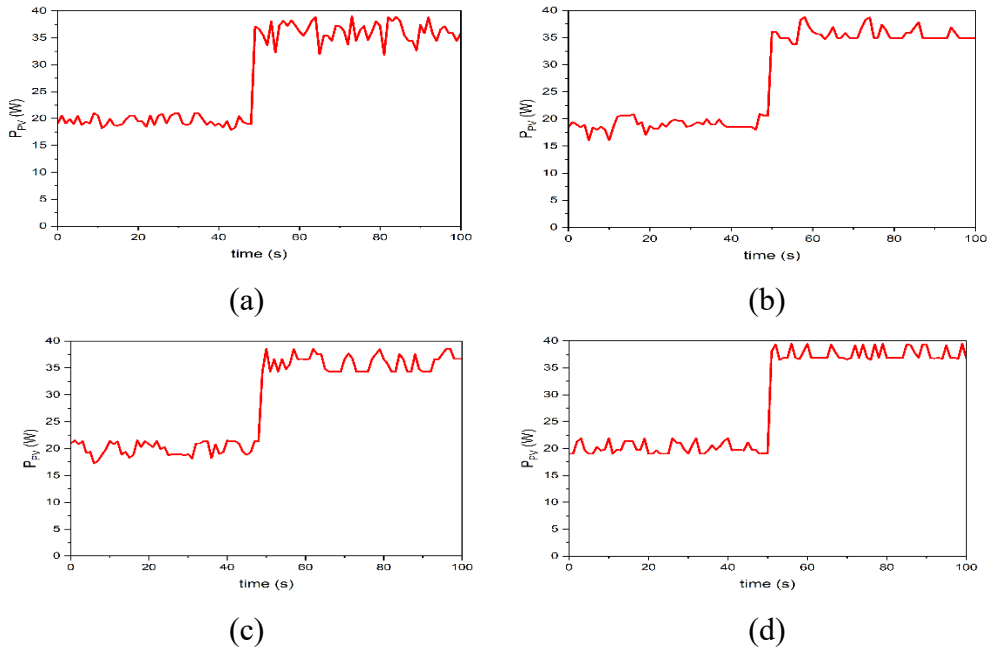


Fig. 6.19. Power response for a) P&O, b) Adaptive P&O, c) drift-free P&O and d) proposed dual perturbation based MPPT algorithms

6.3.4. Step Decrease-in Irradiance

The methods are carried out at a step drop in the irradiance profile. PV factors, such as current, voltage, and power, are used to analyze the methods. Fig. 6.20, 6.21, and 6.22 show the V-t, I-t, and P-t curves for the same thing.

The analysis is performed to validate the proposed MPPT algorithm on realistic lab environment. The voltage, power and current analysis is done with respect to time. In this case the maximum power is achieved in case of proposed MPPT algorithm to the drift-free MPPT algorithm because the voltage and current of the same is also high as compared to the other MPPT algorithms.

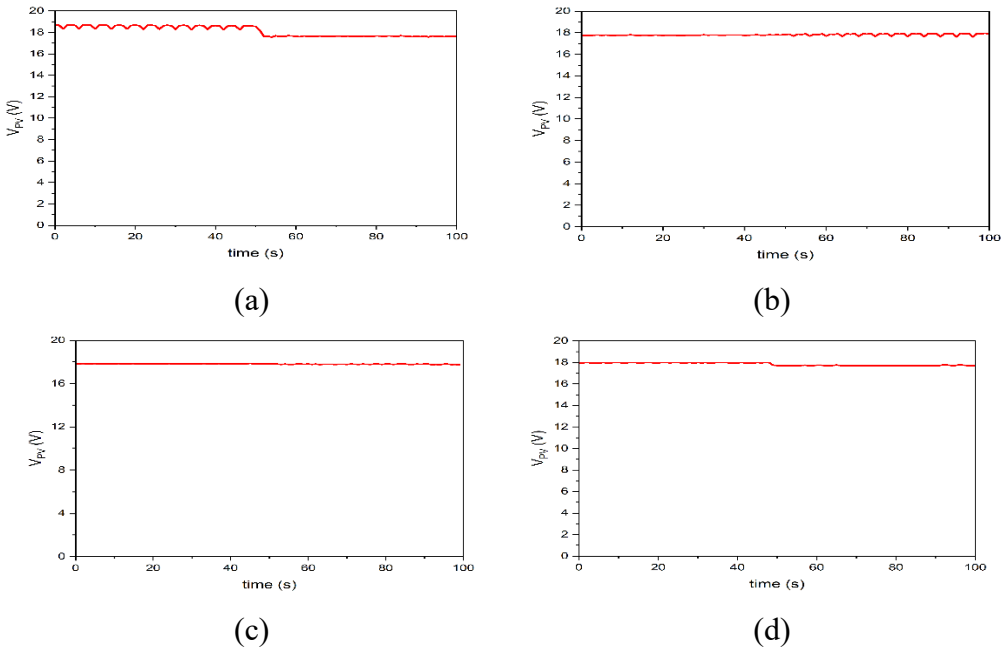


Fig. 6.20. Voltage response for a) P&O, b) Adaptive P&O, c) drift-free P&O and d) proposed dual perturbation based MPPT algorithms

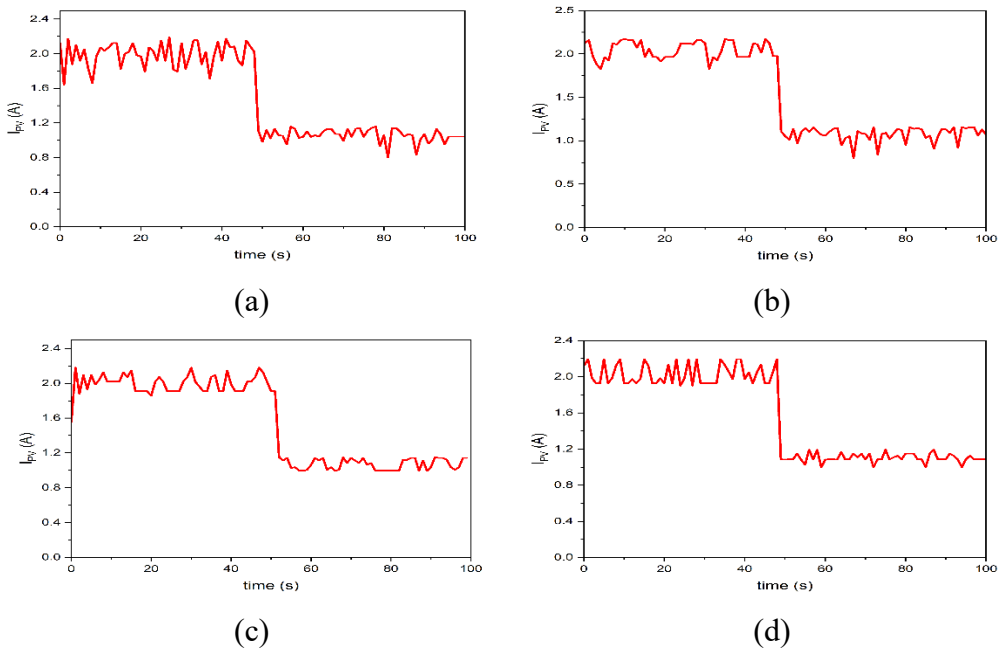


Fig. 6.21. Current response for a) P&O, b) Adaptive P&O, c) drift-free P&O and d) proposed dual perturbation based MPPT algorithms

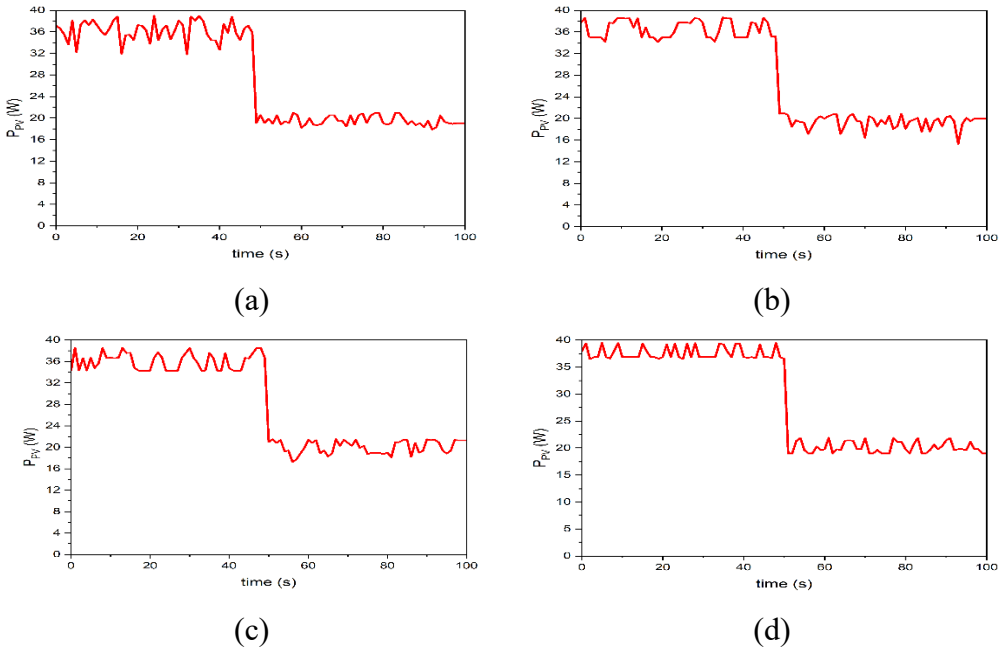


Fig. 6.22. Power response for a) P&O, b) Adaptive P&O, c) drift-free P&O and d) proposed dual perturbation based MPPT algorithms

6.3.5. Comparative Analysis

The algorithms are realized at G=270 W/m^2 and 480W/m^2 as well as step increase-in and step decrease-in irradiance profile. The comparative analysis is performed and the response time, steady-state oscillations and tracking efficiency graphs of the same are depicted in fig. 6.23, 6.24 and 6.25, respectively.

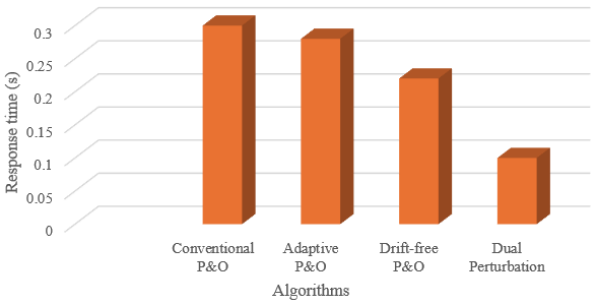


Fig. 6.23. Response time of MPPT algorithms

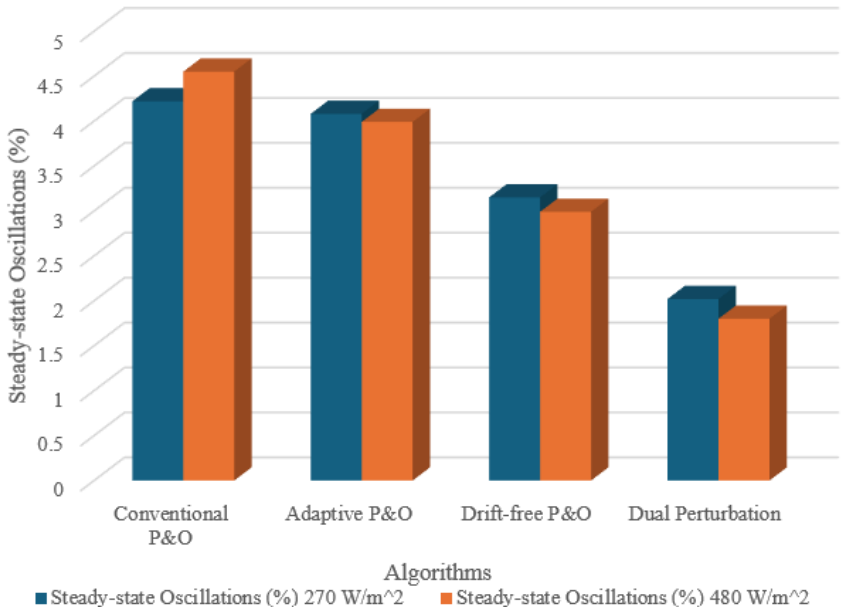


Fig. 6.24. Steady-state oscillations of MPPT algorithms

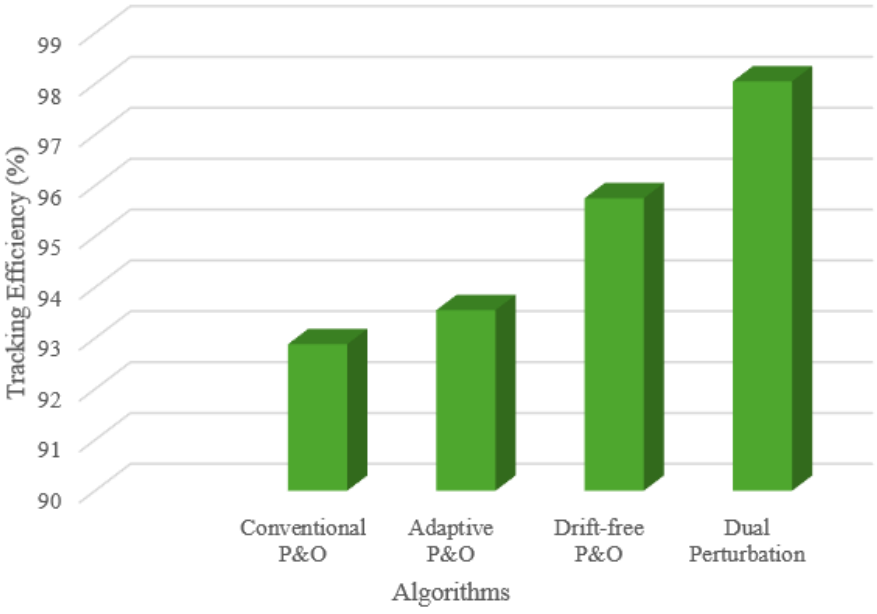


Fig. 6.25. Tracking efficiency of MPPT algorithms

Table 6.4. Performance parameters of algorithms

Algorithms	Response -time (s)	Steady-state Oscillations (%)		Tracking Efficiency (%)
		270 W/m^2	480 W/m^2	
Conventional P&O	0.30	4.22	4.55	92.88
Adaptive P&O	0.28	4.08	3.99	93.55
Drift-free P&O	0.22	3.15	2.99	95.75
Proposed Dual Perturbation	0.10	2.02	1.8	98.05

6.3.6. Statistical Analysis

A nonparametric test called the Wilcoxon signed rank test is used to look at the data for adaptive P&O and the suggested dual disturbance. What the test showed is shown in tables 6.4 and 6.5. It can be clearly seen from the obtained results that the proposed algorithm is showing better min, Q1, Median, Q3 and max of 2%, 2.6%, 1.1%, 2.4% and 1% respectively as compared to adaptive P&O MPPT algorithm. This analysis proves that the proposed dual perturbation based MPPT algorithm is better as compared to other MPPT algorithms.

Table 6.5. Descriptive Statistics

Algorithm	N	Min	Q1	Median	Q3	Max
Adaptive P&O	101	34.05801	34.97673	35.93354	37.7764	38.67656
Proposed Dual Perturbation	101	36.48176	36.84973	36.84973	39.31471	39.67647

Table 6.6. Test Statistics

Algorithm	W	Z	Asymp. Prob> |W|
Adaptive P&O	5151	8.74921	<0.0001
Proposed Dual Perturbation	5151	8.84891	<0.0001

6.4. Summary

This study experimentally validates the dual perturbation-based MPPT method by comparing it against conventional, adaptive, and drift-free P&O MPPT algorithms. Validation tracks the maximum power point (MPP) quickly and effectively while avoiding losses. MPPT algorithm efficiency is tested at the boost converter input to achieve this. Since the goal is to build a quick, drift-free MPPT algorithm, its efficiency is tested at the DC-DC boost converter input to avoid include boost converter losses.

Further, A detailed discussion on the performance outcomes is presented, followed by conclusions and future scopes in the coming chapter that highlight the significance of the proposed approach. Finally, the thesis outlines possible future research directions, emphasizing advancements in adaptive algorithms, real-time implementation, and integration with smart grid technologies.

CHAPTER 7
CONCLUSION AND FUTURE SCOPE

This thesis work presents the development and implementation of a drift-free MPPT algorithm designed to enhance efficiency under rapid irradiance variations. A comprehensive evaluation of existing and advanced MPPT techniques, including P&O, INC, incremental resistance (INR), multisampling MPPT, drift-free P&O, and the novel adaptive voltage perturbation-based and dual perturbation-based MPPT methods, was conducted using MATLAB/Simulink and experimental prototype. The performance of these algorithms was assessed during the step increase-decrease, and EN50530 standard irradiance profiles to compare their tracking efficiency, response time, and steady-state oscillations. A summary of the core contributions and results of this research is given below,

- The novel MPPT algorithm effectively addresses the drift issues inherent in conventional P&O methods by incorporating multiple measurements and adaptive control strategies. This ensures precise and stable tracking of the MPP, significantly improving PV system efficiency.

- Comparatively, the standard P&O algorithm exhibits a tracking response efficiency of 93.25% and a response time of 0.042 s, while adaptive MPPT methods such as adaptive P&O improve the efficiency to 93.12% with a response time of 0.032 s.

- The drift-free P&O MPPT technique, which eliminates drift, achieves a tracking efficiency of 94.75% but exhibits a longer response time of 0.048 s.

- Under step increase and step decrease irradiance profiles, the proposed algorithm achieves superior performance compared to existing MPPT

techniques, attaining a tracking efficiency of 98.75%, response time of 2 ms, and minimal steady-state oscillations.

- In the case of step increment irradiance, the novel method attains a highest tracking efficiency of 98.95%, a response time of 0.012 s, and low steady-state oscillations (0.95% at low and 1.01% at high irradiance levels).

- When subjected to a step decrease in irradiance, the proposed approach achieves 98.81% tracking efficiency, a response time of 0.012 s, and low steady-state oscillations (0.98% at low and 1.01% at high irradiance levels).

- The newly developed adaptive voltage perturbation-based MPPT method demonstrates the best overall performance, achieving a tracking response efficiency of 97.55% with a response time of 0.012 s.

To validate these findings, experimental testing was conducted to compare the proposed dual perturbation-based MPPT algorithm against traditional P&O, adaptive P&O, and drift-free P&O techniques. The experiments focused on tracking efficiency at the input side of a boost converter, ensuring that MPPT efficiency calculations excluded losses within the converter. Following outcomes deliberates the key experimental results as,

- The conventional P&O method exhibits a response time of 0.30 s, with steady-state oscillations of 4.22% at 270 W/m² and 4.55% at 480 W/m², achieving 92.88% tracking efficiency.

- The adaptive P&O method shows a response time of 0.28 s and steady-state oscillations of 4.08% at 270 W/m² and 3.99% at 480 W/m², with 93.55% tracking efficiency.

- The drift-free P&O method achieves a response time of 0.22 s, steady-state oscillations of 3.15% at 270 W/m² and 2.99% at 480 W/m², and 95.75% tracking efficiency.

- The proposed dual perturbation-based MPPT algorithm significantly outperforms these methods, with a response time of 0.10 s, steady-state oscillations of 2.02% at 270 W/m² and 1.80% at 480 W/m², and 98.05% tracking efficiency.

The results confirm the proposed algorithm's effectiveness in fast and accurate MPP tracking, proving its suitability for practical PV applications. The study further develops and validates a non-drifting FPPT algorithm for grid-connected PV systems. Key findings are summarized below:

- A state-of-the-art current and power-based FPPT algorithm, along with the proposed dual perturbation-based FPPT approach, was developed and implemented in MATLAB/Simulink.

- The performance of these algorithms was evaluated graphically through voltage-time (V-t), current-time (I-t), and power-time (P-t) characteristics under irradiance conditions of 100 W/m² and 500 W/m², as well as step increase and decrease profiles.

- The proposed dual perturbation-based FPPT algorithm delivers optimal performance, featuring a response time of 3 ms, minimal steady-state oscillations, and a tracking efficiency of 99.87%.

- Compared to the power-based FPPT method, the proposed approach exhibits a significant improvement of 0.09% in response time, 0.46% in steady-state oscillations, and 3.36% in tracking efficiency. Similarly, compared to the current-based FPPT method, improvements of 0.05%,

0.42%, and 1.8% were observed in response time, steady-state oscillations, and tracking efficiency, respectively.

Future Scope

Future research can focus on enhancing MPPT algorithms to improve accuracy and efficiency under highly dynamic conditions. The integration of artificial intelligence (AI) and machine learning techniques could allow for adaptive real-time optimization, ensuring maximum power extraction under fluctuating environmental conditions. Implementing hardware-based solutions with advanced microcontrollers or FPGAs can further improve real-time processing and reduce response times. The proposed fast, drift-free MPPT algorithm can be integrated into PV inverters to enhance energy efficiency and grid compatibility. Moreover, scalability for larger photovoltaic arrays and diverse environmental conditions remains a promising area for further exploration.

Furthermore, advancements in software and control strategies may contribute to more cost-effective and scalable solutions for solar energy systems. By integrating predictive analytics and self-learning algorithms, MPPT techniques can evolve to handle more complex irradiance patterns and partial shading conditions efficiently. Additionally, research can be extended to explore the application of flexible power point tracking in microgrid-connected PV systems to enhance grid stability and energy management.

In conclusion, the proposed dual perturbation-based MPPT and FPPT algorithms outperform conventional and state-of-the-art techniques, showing notable improvements in response time, steady-state oscillations, and tracking efficiency. The results of this research advance MPPT technology for

photovoltaic systems, laying the groundwork for more robust, adaptive, and efficient energy harvesting solutions in renewable energy applications.

In the future, the scope of this work can be extended by integrating IoT-enabled monitoring systems to ensure real-time data acquisition and remote control of grid-connected PV systems. The adoption of AI-based adaptive control strategies can further enhance both MPPT and FPPT by enabling predictive and self-learning algorithms. Additionally, incorporating real-time weather and irradiance data inputs can improve system responsiveness under rapidly changing environmental conditions. Such advancements will contribute to more reliable, efficient, and intelligent PV grid integration, aligning with the needs of modern smart grids.

REFERENCES

Ahmed, M., Harbi, I., Kennel, R., Rodriguez, J., & Abdelrahem, M. (2022). Model-based maximum power point tracking algorithm with constant power generation capability and fast DC-link dynamics for two-stage PV systems. *IEEE Access*, *10*, 48551–48568.

Alaas, Z., Elbarbary, Z. M. S., Rezvani, A., & Le, B. N. (2023). Analysis and enhancement of MPPT technique to increase accuracy and speed in photovoltaic systems under different conditions. *Optik*, *289*, 171208.

Albarracin, R., & Alonso, M. (2013). Photovoltaic reactive power limits. *2013 12th International Conference on Environment and Electrical Engineering*, 13–18.

Ali, N. K., & Petrov, T. (2024). Design and analysis of MPPT for PV system by perturb and observe algorithm. *E3S Web of Conferences*, *542*, 01010.

Belkaid, A., Colak, I., & Kayisli, K. (2017). Implementation of a modified P&O-MPPT algorithm adapted for varying solar radiation conditions. *Electrical Engineering*, *99*, 839–846.

Bhattacharyya, S., Samanta, S., & Mishra, S. (2020). Steady output and fast tracking MPPT (SOFT-MPPT) for P&O and InC algorithms. *IEEE Transactions on Sustainable Energy*, *12*(1), 293–302.

Boscaino, V., Ditta, V., Marsala, G., Panzavecchia, N., Tine, G., Cosentino, V., Cataliotti, A., & Di Cara, D. (2024). Grid-connected photovoltaic inverters: Grid codes, topologies and control techniques. *Renewable and Sustainable Energy Reviews*, *189*, 113903.

Büyük, M., & İnci, M. (2023a). Improved drift-free P&O MPPT method to enhance energy harvesting capability for dynamic operating conditions of fuel cells. *Energy*, *267*, 126543.

Büyük, M., & İnci, M. (2023b). Improved drift-free P&O MPPT method to enhance energy harvesting capability for dynamic operating conditions of fuel cells. *Energy*, *267*, 126543.

Cavalcanti, M. C., Oliveira, K. C., Azevedo, G. M., Moreira, D., & Neves, F. A. (2005). Maximum power point tracker techniques for photovoltaic systems. *Proc. Power Electronics and Intelligent Control for Energy Conservation PELINCEC'05*, 1–8.

Chellakhi, A., El Beid, S., & Abouelmahjoub, Y. (2022). An improved adaptable step-size P&O MPPT approach for standalone photovoltaic systems with battery station. *Simulation Modelling Practice and Theory*, *121*, 102655.

Chellal, M., Guimaraes, T. F., & Leite, V. (2021a). Experimental evaluation of mppt algorithms: A comparative study. *International Journal of Renewable Energy Research (IJRER)*, *11*(1), 486–494.

Chellal, M., Guimaraes, T. F., & Leite, V. (2021b). Experimental evaluation of mppt algorithms: A comparative study. *International Journal of Renewable Energy Research (IJRER)*, *11*(1), 486–494.

Chen, P.-C., Chen, P.-Y., Liu, Y.-H., Chen, J.-H., & Luo, Y.-F. (2015). A comparative study on maximum power point tracking techniques for photovoltaic generation systems operating under fast changing environments. *Solar Energy*, *119*, 261–276.

Escobar, G., Pettersson, S., Ho, C. N. M., & Rico-Camacho, R. (2017). Multisampling maximum power point tracker (MS-MPPT) to compensate irradiance and temperature changes. *IEEE Transactions on Sustainable Energy*, *8*(3), 1096–1105.

Gomez-Merchan, R., Vazquez, S., Alcaide, A. M., Tafti, H. D., Leon, J. I., Pou, J., Rojas, C. A., Kouro, S., & Franquelo, L. G. (2020). Binary search based flexible power point tracking algorithm for photovoltaic systems. *IEEE Transactions on Industrial Electronics*, *68*(7), 5909–5920.

Guanghua, L., Siddiqui, F. A., Aman, M. M., Shah, S. H. H., Ali, A., Soomar, A. M., & Shaikh, S. (2024). Improved maximum power point tracking algorithms by using numerical analysis techniques for photovoltaic systems. *Results in Engineering*, *21*, 101740.

Guenounou, O., Belkaid, A., Colak, I., Dahhou, B., & Chabour, F. (2021). Optimization of fuzzy logic controller based maximum power point tracking using hierarchical genetic algorithms. *2021 9th International Conference on Smart Grid (IcSmartGrid)*, 207–211.

Gupta, A., Kumar, P., Pachauri, R., & Chauhan, Y. K. (2014). Effect of environmental conditions on single and double diode PV system: comparative study. *International Journal of Renewable Energy Research*, *4*(4), 849–858.

Haghighat, M., Niroomand, M., Tafti, H. D., Townsend, C. D., & Fernando, T. (2023). A review of state-of-the-art flexible power point tracking algorithms in photovoltaic systems for grid support: Classification and application. *Journal of Modern Power Systems and Clean Energy*.

Hashim, N., Jamhari, M. K. A. M., & Baharom, R. (2023a). Adaptive Drift-Free Hill Climbing Maximum Power Point Tracking for PV Systems. *2023 7th International Conference on Information Technology (InCIT)*, 226–231.

Hashim, N., Jamhari, M. K. A. M., & Baharom, R. (2023b). Adaptive Drift-Free Hill Climbing Maximum Power Point Tracking for PV Systems. *2023 7th International Conference on Information Technology (InCIT)*, 226–231.

Hashimoto, J., Ustun, T. S., & Otani, K. (2017). Smart inverter functionality testing for battery energy storage systems. *Smart Grid and Renewable Energy*, *8*(11), 337–350.

Honsberg, C. B., & Bowden, S. G. (2019). Photovoltaics education website. *PV Education*.

Hou, G., Ke, Y., & Huang, C. (2021). A flexible constant power generation scheme for photovoltaic system by error-based active disturbance rejection control and perturb & observe. *Energy*, *237*, 121646.

Hua, C.-C., & Zhan, Y.-J. (2021). A hybrid maximum power point tracking method without oscillations in steady-state for photovoltaic energy systems. *Energies*, *14*(18), 5590.

Husain, A. A. F., Hasan, W. Z. W., Shafie, S., Hamidon, M. N., & Pandey, S. S. (2018). A review of transparent solar photovoltaic technologies. *Renewable and Sustainable Energy Reviews*, *94*, 779–791.

Hussein, K. H., Muta, I., Hoshino, T., & Osakada, M. (1995). Maximum photovoltaic power tracking: an algorithm for rapidly changing atmospheric conditions. *IEE Proceedings-Generation, Transmission and Distribution*, *142*(1), 59–64.

Jately, V., & Arora, S. (2017). Development of a dual-tracking technique for extracting maximum power from PV systems under rapidly changing environmental conditions. *Energy*, *133*, 557–571.

Joshi, J., Jately, V., Kala, P., Sharma, A., Lim, W. H., & Azzopardi, B. (2024). Control strategy for current limitation and maximum capacity utilization of grid connected PV inverter under unbalanced grid conditions. *Scientific Reports*, *14*(1), 10118.

Kahani, R., Jamil, M., & Iqbal, M. T. (2022). An improved perturb and observed maximum power point tracking algorithm for photovoltaic power systems. *Journal of Modern Power Systems and Clean Energy*, *11*(4), 1165–1175.

Karmouni, H., Chouiekh, M., Motahhir, S., Dagal, I., Oufettoul, H., Qjidaa, H., & Sayyouri, M. (2022). A novel MPPT algorithm based on Aquila optimizer under PSC and implementation using raspberry. *2022 11th International Conference on Renewable Energy Research and Application (ICRERA)*, 446–451.

Kavya, M., & Jayalalitha, S. (2021). A Novel Shift and Search (S&S) Algorithm for Tracking Maximum Power in PV Systems: An Approach to Increase Efficiency. *International Journal of Precision Engineering and Manufacturing-Green Technology*, *8*(6), 1699–1710.

Kavya, M., & Jayalalitha, S. (2022a). A novel coarse and fine control algorithm to improve maximum power point tracking (MPPT) efficiency in photovoltaic system. *ISA Transactions*, *121*, 180–190.

Kavya, M., & Jayalalitha, S. (2022b). A novel coarse and fine control algorithm to improve maximum power point tracking (MPPT) efficiency in photovoltaic system. *ISA Transactions*, *121*, 180–190.

Kavya, M., & Jayalalitha, S. (2022c). A novel coarse and fine control algorithm to improve maximum power point tracking (MPPT) efficiency in photovoltaic system. *ISA Transactions*, *121*, 180–190.

Kesilmiş, Z. (2022). A manhattan metric based perturb and observe maximum power point tracking algorithm for photovoltaic systems. *Energy Sources, Part A: Recovery, Utilization, and Environmental Effects*, *44*(1), 469–492.

Killi, M., & Samanta, S. (2015). Modified perturb and observe MPPT algorithm for drift avoidance in photovoltaic systems. *IEEE Transactions on Industrial Electronics*, *62*(9), 5549–5559.

Kim, T.-Y., Ahn, H.-G., Park, S. K., & Lee, Y.-K. (2001). A novel maximum power point tracking control for photovoltaic power system under rapidly changing solar radiation. *ISIE 2001. 2001 IEEE International Symposium on Industrial Electronics Proceedings (Cat. No. 01TH8570)*, *2*, 1011–1014.

Kollimalla, S. K., & Mishra, M. K. (2014). A novel adaptive P&O MPPT algorithm considering sudden changes in the irradiance. *IEEE Transactions on Energy Conversion*, *29*(3), 602–610.

Kumar, A., & Kumar, P. (2021). Power quality improvement for grid-connected PV system based on distribution static compensator with fuzzy logic controller and UVT/ADALINE-based least mean square controller. *Journal of Modern Power Systems and Clean Energy*, *9*(6), 1289–1299.

Kumar Nayak, J., Thalla, H., & Ghosh, A. (2023). Efficient maximum power point tracking algorithms for photovoltaic systems with reduced number of sensors. *Process Integration and Optimization for Sustainability*, *7*(1), 191–213.

Kumar, V., & Singh, M. (2020). Derated mode of power generation in PV system using modified perturb and observe MPPT algorithm. *Journal of Modern Power Systems and Clean Energy*, *9*(5), 1183–1192.

Kumaresan, A., Tafti, H. D., Kandasamy, N. K., Farivar, G. G., Pou, J., & Subbaiyan, T. (2021). Flexible power point tracking for solar photovoltaic systems using secant method. *IEEE Transactions on Power Electronics*, *36*(8), 9419–9429.

Leridon, H. (2020). World population outlook: Explosion or implosion? *Population Societies*, *573*(1), 1–4.

Lewis, N. S. (2016). Research opportunities to advance solar energy utilization. *Science*, *351*(6271), aad1920.

Li, X., Wen, H., Hu, Y., Du, Y., & Yang, Y. (2020). A comparative study on photovoltaic MPPT algorithms under EN50530 dynamic test procedure. *IEEE Transactions on Power Electronics*, *36*(4), 4153–4168.

Li, X., Wen, H., Hu, Y., & Jiang, L. (2019). Drift-free current sensorless MPPT algorithm in photovoltaic systems. *Solar Energy*, *177*, 118–126.

Lin, S., & Liao, W. (2024). Research on photovoltaic dynamic MPPT algorithm based on adaptive PSO optimization. *Journal of Computational Methods in Sciences and Engineering*, *24*(1), 595–609.

Liu, T., Wan, X., Peng, Q., Zeng, X., Li, Y., & Meng, J. (2024). Dual-mode fast frequency control of PV systems with inertia emulation from DC-link capacitor considering voltage restoration. *CSEE Journal of Power and Energy Systems*.

Manjunath, M. G., Vyjayanthi, C., & Modi, C. N. (2021). Adaptive step size based drift-free P&O algorithm with power optimiser and load protection for maximum power extraction from PV panels in stand-alone applications. *IET Renewable Power Generation*, *15*(6), 1270–1285.

Mei, Q., Shan, M., Liu, L., & Guerrero, J. M. (2010a). A novel improved variable step-size incremental-resistance MPPT method for PV systems. *IEEE Transactions on Industrial Electronics*, *58*(6), 2427–2434.

Mei, Q., Shan, M., Liu, L., & Guerrero, J. M. (2010b). A novel improved variable step-size incremental-resistance MPPT method for PV systems. *IEEE Transactions on Industrial Electronics*, *58*(6), 2427–2434.

Mirhosseini, M., Pou, J., & Agelidis, V. G. (2014). Single-and two-stage inverter-based grid-connected photovoltaic power plants with ride-through capability under grid faults. *IEEE Transactions on Sustainable Energy*, *6*(3), 1150–1159.

Motahhir, S., El Hammoumi, A., & El Ghzizal, A. (2020). The most used MPPT algorithms: Review and the suitable low-cost embedded board for each algorithm. *Journal of Cleaner Production*, *246*, 118983.

Mousa, H. H. H., Youssef, A.-R., & Mohamed, E. E. M. (2021a). State of the art perturb and observe MPPT algorithms based wind energy conversion systems: A technology review. *International Journal of Electrical Power & Energy Systems*, *126*, 106598.

Mousa, H. H. H., Youssef, A.-R., & Mohamed, E. E. M. (2021b). State of the art perturb and observe MPPT algorithms based wind energy conversion systems: A technology review. *International Journal of Electrical Power & Energy Systems*, *126*, 106598.

Narang, A., Tafti, H. D., Townsend, C. D., Farivar, G., Pou, J., Konstantinou, G., & Vazquez, S. (2019). An algorithm for fast flexible power point tracking in photovoltaic power plants. *IECON 2019-45th Annual Conference of the IEEE Industrial Electronics Society*, *1*, 4387–4392.

Nayak, P. K., Mahesh, S., Snaith, H. J., & Cahen, D. (2019). Photovoltaic solar cell technologies: analysing the state of the art. *Nature Reviews Materials*, *4*(4), 269–285.

Nusrat, M., Mekhilef, S., Mubin, M., Ahmed, S., Seyedmahmoudian, M., Stojcevski, A., & Alshammari, O. (2024). Advancements in flexible power point tracking and power control strategies for photovoltaic power plants: A comprehensive review. *Energy Reports*, *12*, 237–250.

Oufettoul, H., Motahhir, S., Abdelmoula, I. A., Aniba, G., Issa, W., & Mahir, O. (2023). Optimum MPPT technique for reconfiguring the photovoltaic array under partial shading failure. *2023 12th International Conference on Renewable Energy Research and Applications (ICRERA)*, 331–338.

Pandey, A., Dasgupta, N., & Mukerjee, A. K. (2008). High-performance algorithms for drift avoidance and fast tracking in solar MPPT system. *IEEE Transactions on Energy Conversion*, *23*(2), 681–689.

Parlevliet, D., & Moheimani, N. R. (2014). Efficient conversion of solar energy to biomass and electricity. *Aquatic Biosystems*, *10*(1), 4.

Pathak, D., Katyal, A., & Gaur, P. (2024). An Enhanced Drift-Free Perturb and Observe Maximum Power Point Tracking Method Using Hybrid Metaheuristic Algorithm for a Solar Photovoltaic Power System. *Iranian Journal of Science and Technology, Transactions of Electrical Engineering*, *48*(2), 759–779.

Peng, B.-R., Ho, K.-C., & Liu, Y.-H. (2017). A novel and fast MPPT method suitable for both fast changing and partially shaded conditions. *IEEE Transactions on Industrial Electronics*, *65*(4), 3240–3251.

Pilakkat, D., & Kanthalakshmi, S. (2018). Drift free variable step size perturb and observe MPPT algorithm for photovoltaic systems under rapidly increasing insolation. *Electronics*, *22*(1), 19–26.

Podder, A. K., Roy, N. K., & Pota, H. R. (2019). MPPT methods for solar PV systems: a critical review based on tracking nature. *IET Renewable Power Generation*, *13*(10), 1615–1632.

Qiu, L., Ono, L. K., & Qi, Y. (2018). Advances and challenges to the commercialization of organic–inorganic halide perovskite solar cell technology. *Materials Today Energy*, *7*, 169–189.

Riquelme-Dominguez, J. M., & Martinez, S. (2020). Comparison of different photovoltaic perturb and observe algorithms for drift avoidance in fluctuating irradiance conditions. *2020 IEEE International Conference on Environment and Electrical Engineering and 2020 IEEE Industrial and Commercial Power Systems Europe (EEEIC/I&CPS Europe)*, 1–5.

Saberi, A., Niroomand, M., & Dehkordi, B. M. (2023). An Improved P&O Based MPPT for PV Systems with Reduced Steady-State Oscillation. *International Journal of Energy Research*, *2023*(1), 4694583.

Sai, B. S. V., Mohanty, R., Mohanty, S., Chatterjee, D., Dhanamjayulu, C., Chinthaginjala, R., Kotb, H., & Elrashidi, A. (2024). An efficient MPPT techniques for inter-harmonic reduction in grid connected hybrid wind and solar energy systems. *Heliyon*, *10*(5).

Sangwongwanich, A., Yang, Y., & Blaabjerg, F. (2015). High-performance constant power generation in grid-connected PV systems. *IEEE Transactions on Power Electronics*, *31*(3), 1822–1825.

Sangwongwanich, A., Yang, Y., & Blaabjerg, F. (2017). A sensorless power reserve control strategy for two-stage grid-connected PV systems. *IEEE Transactions on Power Electronics*, *32*(11), 8559–8569.

Sangwongwanich, A., Yang, Y., Blaabjerg, F., & Sera, D. (2017). Delta power control strategy for multistring grid-connected PV inverters. *IEEE Transactions on Industry Applications*, *53*(4), 3862–3870.

Sangwongwanich, A., Yang, Y., Blaabjerg, F., & Wang, H. (2017). Benchmarking of constant power generation strategies for single-phase grid-connected photovoltaic systems. *IEEE Transactions on Industry Applications*, *54*(1), 447–457.

Sarang, S. A., Raza, M. A., Panhwar, M., Khan, M., Abbas, G., Touti, E., Altamimi, A., & Wijaya, A. A. (2024). Maximizing solar power generation through conventional and digital MPPT techniques: a comparative analysis. *Scientific Reports*, *14*(1), 8944.

Saremi, M., Pourfarzad, H., & Nemati, M. (2020). Design of a fuzzy current-sensor less maximum power point tracking algorithm for photovoltaic systems. *IET Renewable Power Generation*, *14*(18), 3724–3731.

Sarvi, M., & Azadian, A. (2022). A comprehensive review and classified comparison of MPPT algorithms in PV systems. *Energy Systems*, *13*(2), 281–320.

Satif, A., Hlou, L., & Elgouri, R. (2018). An improved perturb and observe maximum power point tracking algorithm for photovoltaic systems. *2018 Renewable Energies, Power Systems & Green Inclusive Economy (REPS-GIE)*, 1–6.

Shaikh, A. M., Shaikh, M. F., Shaikh, S. A., Krichen, M., Rahimoon, R. A., & Qadir, A. (2023). Comparative analysis of different MPPT techniques using boost converter for photovoltaic systems under dynamic shading conditions. *Sustainable Energy Technologies and Assessments*, *57*, 103259.

Sharma, S., Jately, V., Kuchhal, P., Kala, P., & Azzopardi, B. (2023). A comprehensive review of flexible power-point-tracking algorithms for grid-connected photovoltaic systems. *Energies*, *16*(15), 5679.

Sharma, V., Haque, M. H., & Aziz, S. M. (2019). PV generation and load profile data of net zero energy homes in South Australia. *Data in Brief*, *25*, 104235.

Sholapur, S., Mohan, K. R., & Narsimhegowda, T. R. (2014). Boost converter topology for pv system with perturb and observe mppt algorithm. *IOSR Journal of Electrical and Electronics Engineering (IOSR-JEEE)*, *9*(4), 50–56.

Sreedhar, S., & Jagadeesh, D. (2016). A review on optimization algorithms for MPPT in solar PV system under partially shaded conditions. *IOSR J. Electr. Electron. Eng*, 23–32.

Tafti, H. D., Maswood, A. I., Konstantinou, G., Pou, J., & Blaabjerg, F. (2017). A general constant power generation algorithm for photovoltaic systems. *IEEE Transactions on Power Electronics*, *33*(5), 4088–4101.

Tafti, H. D., Maswood, A. I., Pou, J., Konstantinou, G., & Agelidis, V. G. (2016). An algorithm for reduction of extracted power from photovoltaic strings in grid-tied photovoltaic power plants during voltage sags. *IECON 2016-42nd Annual Conference of the IEEE Industrial Electronics Society*, 3018–3023.

Tafti, H. D., Sangwongwanich, A., Yang, Y., Konstantinou, G., Pou, J., & Blaabjerg, F. (2018). A general algorithm for flexible active power control of photovoltaic systems. *2018 IEEE Applied Power Electronics Conference and Exposition (APEC)*, 1115–1121.

Tafti, H. D., Sangwongwanich, A., Yang, Y., Pou, J., Konstantinou, G., & Blaabjerg, F. (2018). An adaptive control scheme for flexible power point tracking in photovoltaic systems. *IEEE Transactions on Power Electronics*, *34*(6), 5451–5463.

Tafti, H. D., Townsend, C. D., Konstantinou, G., & Pou, J. (2018). A multi-mode flexible power point tracking algorithm for photovoltaic power plants. *IEEE Transactions on Power Electronics*, *34*(6), 5038–5042.

Tafti, H. D., Wang, Q., Townsend, C. D., Pou, J., & Konstantinou, G. (2022). Global flexible power point tracking in photovoltaic systems under partial shading conditions. *IEEE Transactions on Power Electronics*, *37*(9), 11332–11341.

Talha, M., Raihan, S. R. S., Abd Rahim, N., Akhtar, M. N., Butt, O. M., & Hussain, M. M. (2022). Multi-functional PV inverter with low voltage ride-through and constant power output. *IEEE Access*, *10*, 29567–29588.

Tawiah-Mensah, P. N., Addison, J., Dei Oppong, S., & Effah, F. B. (2022). An improved Perturb and Observe Maximum Power Point Tracking Algorithm

with the capability of drift avoidance in PV systems. *2022 IEEE PES/IAS PowerAfrica*, 1–5.

Tella, V. C., Agili, B., & He, M. (2024). Advanced MPPT control algorithms: A comparative analysis of conventional and intelligent techniques with challenges. *European Journal of Electrical Engineering and Computer Science*, *8*(4), 6–20.

Tur, M. R., & Bayindir, R. (2019). Project surveys for determining and defining key performance indicators in the development of smart grids in energy systems. *International Journal of Smart Grid*, *3*(2), 103–107.

Tyukhov, I. (n.d.). *SOLAR ENERGY CONVERSION IN NANOSTRUCTURED INTERFACES*.

Utrilla, C., Tafti, H. D., Kumaresan, A., Buire, J., Debusschere, V., Pou, J., & Hadjsaid, N. (2024). A simplified model of flexible power point tracking algorithms in double-stage photovoltaic systems. *Mathematics and Computers in Simulation*, *224*, 20–33.

Vadi, S., Gurbuz, F. B., Sagiroglu, S., & Bayindir, R. (2021). Optimization of pi based buck-boost converter by particle swarm optimization algorithm. *2021 9th International Conference on Smart Grid (IcSmartGrid)*, 295–301.

Xie, Z., & Wu, Z. (2022). A flexible power point tracking algorithm for photovoltaic system under partial shading condition. *Sustainable Energy Technologies and Assessments*, *49*, 101747.

Yadav, I., Maurya, S. K., & Gupta, G. K. (2020). A literature review on industrially accepted MPPT techniques for solar PV system. *International*

Journal of Electrical and Computer Engineering (IJECE), *10*(2), 2117–2127.

Yan, H. W., Narang, A., Tafti, H. D., Farivar, G. G., & Pou, J. (2020). Reduced battery usage in a hybrid battery and photovoltaic stand-alone DC microgrid with flexible power point tracking. *2020 IEEE Energy Conversion Congress and Exposition (ECCE)*, 3894–3899.

Yetayew, T. T., & Workineh, T. G. (2021). A Comprehensive Review and Evaluation of Classical MPPT Techniques for a Photovoltaic System. *Advances of Science and Technology: 8th EAI International Conference, ICAST 2020, Bahir Dar, Ethiopia, October 2-4, 2020, Proceedings, Part I 8*, 259–272.

Zhang, B., Zhao, P., & Zhao, J. (2022). Research on control strategy of two-stage photovoltaic virtual synchronous generator with variable power point tracking. *Energy Reports*, *8*, 283–290.

Zhang, F., Thanapalan, K., Procter, A., Carr, S., & Maddy, J. (2013). Adaptive hybrid maximum power point tracking method for a photovoltaic system. *IEEE Transactions on Energy Conversion*, *28*(2), 353–360.

Zhang, X., Jia, J., Zheng, L., Yi, W., & Zhang, Z. (2023). Maximum power point tracking algorithms for wind power generation system: Review, comparison and analysis. *Energy Science & Engineering*, *11*(1), 430–444.

List of Publications

Name: Sakshi Sharma
ORCID: https://orcid.org/0009-0000-5813-531X

- S. Sharma, V. Jately, P. Kuchhal, P. Kala, & B. Azzopardi, "A comprehensive review of flexible power-point-tracking algorithms for grid-connected photovoltaic systems", Energies, 16(15), 5679, 2023, https://doi.org/10.3390/en16155679, (SCI, IF: 3.2).
- S. Sharma, K. Kumar, R. K. Pachauri, & P. Kuchhal, "Numerical simulations, design and modeling of methylammonium tin iodide halide-based single-junction perovskite solar cell", Electrical Engineering, 1-15, 2023, https://doi.org/10.1007/s00202-023-02166-x. (SCI, IF:1.6).
- Sakshi Sharma, Vibhu Jately and Piyush Kuchhal, "A Fast MPPT Algorithm for Drift Mitigation in PV System during Dynamic Change in Irradiance", International Journal of Renewable Energy Research (IJRER). (ESCI, IF: 2.9)
- Sakshi Sharma, Vibhu Jately and Piyush Kuchhal, Rupendra Kumar Pachauri "A Comprehensive study of adaptive MPPT algorithms for PV systems under rapid change in irradiance", Journal of Electrical Engineering & Technology. (SCI, IF: 1.6) (Under Review).
- Sakshi Sharma, Vibhu Jately and Piyush Kuchhal, "Dual Perturbation based Flexible Power Point Tracking Technique for Grid-Connected PV Systems", Scientific Reports. (SCI, IF: 3.8) (Communicated).

FUNDING ACKNOWLEDGEMENT

This Research was conducted with the financial support provided by UPES, Dehradun, India

Sakshi Sharma

OPTIMUM POWER POINT TRACKING TECHNIQUES FOR GRIDCONNECTED PHOTOVOLATIC SYSTEMS

Quick Submit

Quick Submit

University of Petroleum & Energy Studies

Document Details

Submission ID

trn:oid:::1:3272100418

Submission Date

Jun 9, 2025, 12:40 PM GMT+5:30

Download Date

Jun 9, 2025, 12:46 PM GMT+5:30

File Name

Thesis_finalized_Sakshi_for_plag_run.pdf

File Size

6.1 MB

158 Pages

29,541 Words

153,658 Characters

6% Overall Similarity

The combined total of all matches, including overlapping sources, for each database.

Filtered from the Report

- Bibliography
- Quoted Text
- Small Matches (less than 14 words)

Match Groups

41 Not Cited or Quoted 5%
Matches with neither in-text citation nor quotation marks

11 Missing Quotations 1%
Matches that are still very similar to source material

0 Missing Citation 0%
Matches that have quotation marks, but no in-text citation

0 Cited and Quoted 0%
Matches with in-text citation present, but no quotation marks

Top Sources

5% Internet sources
4% Publications
0% Submitted works (Student Papers)

Integrity Flags

2 Integrity Flags for Review

Replaced Characters
146 suspect characters on 26 pages
Letters are swapped with similar characters from another alphabet.

Hidden Text
47 suspect characters on 2 pages
Text is altered to blend into the white background of the document.

Our system's algorithms look deeply at a document for any inconsistencies that would set it apart from a normal submission. If we notice something strange, we flag it for you to review.

A Flag is not necessarily an indicator of a problem. However, we'd recommend you focus your attention there for further review.

Match Groups

- **41** Not Cited or Quoted 5%
  Matches with neither in-text citation nor quotation marks
- **11** Missing Quotations 1%
  Matches that are still very similar to source material
- **0** Missing Citation 0%
  Matches that have quotation marks, but no in-text citation
- **0** Cited and Quoted 0%
  Matches with in-text citation present, but no quotation marks

Top Sources

5% Internet sources
4% Publications
0% Submitted works (Student Papers)

Top Sources

The sources with the highest number of matches within the submission. Overlapping sources will not be displayed.

1	Internet	
www.mdpi.com		4%
2	Publication	
Ehsan Afshari, Gholam Reza Moradi, Ramin Rahimi, Babak Farhangi, Yongheng Y...		<1%
3	Internet	
vbn.aau.dk		<1%
4	Internet	
library.iyte.edu.tr		<1%
5	Internet	
1library.net		<1%
6	Internet	
www.hbni.ac.in		<1%
7	Internet	
www.econstor.eu		<1%
8	Internet	
docksci.com		<1%
9	Internet	
www.ijisae.org		<1%
10	Internet	
www.coursehero.com		<1%

11 Internet

www.reality.com <1%

12 Internet

media.suub.uni-bremen.de <1%

13 Internet

patents.justia.com <1%

14 Internet

www.iotpe.com <1%